1-9-2012

Scope and Mechanistic Study of the Coupling Reaction of α,β-Unsaturated Carbonyl Compounds with Alkenes: Uncovering Electronic Effects on Alkene Insertion vs Oxidative Coupling Pathways

Ki Hyeok Kwon
Marquette University

Do W. Lee
Marquette University, do.lee@marquette.edu

Chae S. Yi
Marquette University, chae.yi@marquette.edu

Accepted version. *Organometallics*, Vol. 31, No. 1 (January 9, 2012): 495-504. DOI.

Scope and Mechanistic Study of the Coupling Reaction of α, β-Unsaturated Carbonyl Compounds with Alkenes: Uncovering Electronic Effects on Alkene Insertion vs Oxidative Coupling Pathways

Li-Hyeok Kwon
Department of Chemistry, Marquette University, Milwaukee, WI
Do W. Lee
Department of Chemistry, Marquette University, Milwaukee, WI
Chae S. Yi
Department of Chemistry, Marquette University, Milwaukee, WI

Organometallics, Vol 31, No. 1 (January 9, 2012): pg. 495-504. DOI.

Abstract: The cationic ruthenium-hydride complex $[(C_6H_6)(PCy_3)(CO)RuH]^+BF_4^-$ (**1**) was found to be a highly effective catalyst for the intermolecular conjugate addition of simple alkenes to α,β-unsaturated carbonyl compounds to give (*Z*)-selective tetrasubstituted olefin products. The analogous coupling reaction of cinnamides with electron-deficient olefins led to the oxidative coupling of two olefinic C–H bonds in forming (*E*)-selective diene products. The intramolecular version of the coupling reaction efficiently produced indene and bicyclic fulvene derivatives. The empirical rate law for the coupling reaction of ethyl cinnamate with propene was determined as: rate = $k[\mathbf{1}]^1[\text{propene}]^0[\text{cinnamate}]^{-1}$. A negligible deuterium kinetic isotope effect (k_H/k_D = 1.1±0.1) was measured from both (*E*)-$C_6H_5CH{=}C(CH_3)CONHCH_3$ and (*E*)-$C_6H_5CD{=}C(CH_3)CONHCH_3$ with styrene. In contrast, a significant normal isotope effect (k_H/k_D = 1.7±0.1) was observed from the reaction of (*E*)-$C_6H_5CH{=}C(CH_3)CONHCH_3$ with styrene and styrene-d_{10}. A pronounced carbon isotope effect was measured from the coupling reaction of (*E*)-$C_6H_5CH{=}CHCO_2Et$ with propene (^{13}C(recovered)/^{13}C(virgin) at C_β = 1.019(6)), while a negligible carbon isotope effect (^{13}C(recovered)/^{13}C(virgin) at C_β = 0.999(4)) was obtained from the reaction of (*E*)-$C_6H_5CH{=}C(CH_3)CONHCH_3$ with styrene. Hammett plots from the correlation of *para*-substituted *p*-X-$C_6H_4CH{=}CHCO_2Et$ (X = OCH_3, CH_3, H, F, Cl, CO_2Me, CF_3) with propene and from the treatment of (*E*)-$C_6H_5CH{=}CHCO_2Et$ with a series of *para*-substituted styrenes *p*-Y-$C_6H_4CH{=}CH_2$ (Y = OCH_3, CH_3, H, F, Cl, CF_3) gave the positive slopes for both cases (ρ = +1.1±0.1 and +1.5±0.1, respectively). Eyring analysis of the coupling reaction led to the thermodynamic parameters, $\Delta H^\ddagger$ = 20±2 kcal mol^{-1} and $S^\ddagger$ = −42±5 e.u. Two separate mechanistic pathways for the coupling reaction have been proposed on the basis of these kinetic and spectroscopic studies.

Introduction

To stem growing environmental pollutions due to wasteful byproducts, chemical industries in recent years have been increasingly interested in replacing traditional synthetic methods with "green" catalytic methods that form desired products from readily available and renewable feedstocks.[1] One such prominent example is the Wittig-type carbonyl olefination methods, whose synthetic prowess has been immensely demonstrated over the years in both laboratory-scale and industrial processes, but pose debilitating problems especially for large-scale industrial applications because of the formation of byproducts resulted from the utilization of stoichiometric amount of ylides (or carbanion equivalents).[2] Considerable research efforts have been directed to develop transition metal-catalyzed olefination methods as a means to increase synthetic efficacy while reducing the formation of wasteful byproducts. Designing expeditious catalytic

Organometallics, Vol 31, No. 1 (January 9, 2012): pg. 495-504. DOI.

methods for tetrasubstituted olefins has gained a particular prominence in recent years, in part to meet the growing needs for the synthesis of pharmaceutical agents such as tamoxifen (anti-breast cancer drug) and rofecoxib (anti-inflammatory drug) as well as for photo-responsive organic materials.[3] Heck and Suzuki-type of Pd-catalyzed cross coupling methods have been shown to be highly effective in forming tetrasubstituted olefins in regio- and stereoselective fashion.[4] A number of Ni- and Rh-catalyzed exocyclization and nucleophilic coupling methods have been developed for the synthesis of highly substituted olefins.[5] The ring-closing olefin metathesis strategy has also been successfully employed for forming tetrasubstituted cyclic olefins.[6]

Even though conjugate addition of simple alkenes to α,β-unsaturated carbonyl compounds has long been recognized as a potentially powerful olefination method, its synthetic potential has not been fully exploited, in part due to the lack of reactivity on the olefin substrates coupled with the formation of homocoupling byproducts. Recently, Jamison and co-workers successfully developed catalytic conjugate addition and allylic substitution methods in forming substituted olefins.[7] Ogoshi and co-workers reported a similar direct conjugate addition of simple alkenes to enones by using a Ni(0)/PR_3 catalyst.[8] Chelate-assisted C–H insertion methods have been successfully extended to the catalytic couplings of enones with simple alkenes.[9] Bergman and Toste's group recently reported cobalt-catalyzed intramolecular conjugate addition of vinylic C–H bonds to enones in forming tetrasubstituted cyclic compounds.[10]

Transition metal catalyzed oxidative C–H coupling methods have also emerged as an expedient olefination protocol for arene compounds.[11] Compared to the traditional catalytic olefination methods such as Heck and Suzuki coupling reactions, these oxidative C–H coupling methods directly introduce olefinic group without employing any reactive reagents. Since Fagnou's seminal report on the C–H oxidative coupling of two different arene substrates,[12] considerable progress has been made in the area of catalytic C–H alkenylation of arene compounds. For example, Kakiuchi successfully developed chelate-assisted direct *ortho*-C–H alkenylation of arene compounds by using a Ru catalyst.[13] Glorius and Yu's research groups reported a series of regioselective C–H olefination of arene compounds

using carbonyl directing groups.[14,15] Following Milstein and Ishii's work on the catalytic oxidative coupling reactions of arenes to acrylic substrates,[16] a number of research groups reported chelate assisted C–H alkenylation of arene compounds.[17] Ackermann also reported a number of chelate-assisted alkenylation and arylation of arenes by using Ru catalysts.[18] These catalytic C–H alkenylation methods typically require a stoichiometric amount of oxidants or additives, and the substrate scope is generally limited to arene sp^2 C–H bonds,[19] although an olefination to sp^3 C–H bond has recently been achieved.[20] Detailed mechanistic insights as well as on the factors influencing these catalytic C–H oxidative coupling reactions are still remained to be established.

We recently disclosed that the cationic ruthenium-hydride complex $[(C_6H_6)(CO)(PCy_3)RuH]^+BF_4^-$ (**1**) is a highly effective catalyst precursor for a number of coupling reactions involving vinyl C–H activation.[21] We observed an unusual selectivity pattern of the catalyst **1** in mediating these coupling reactions in that C–H and C=O olefination products are directly resulted from the coupling of arylketones with alkenes,[21c] instead of the *ortho*-arene C–H insertion products typically observed in Ru-catalyzed C–H activation reactions.[22] We have been able to extend the synthetic utility of the C–H olefination method to the conjugate addition reaction of α,β-unsaturated carbonyl compounds in affording tetrasubstituted olefins.[23] This report delineates full details on the scope as well mechanistic insights for the coupling reaction of α,β-unsaturated carbonyl compounds with alkenes.

Results and Discussion

Reaction Scope

We recently reported a novel catalytic synthesis of (*Z*)-selective tetrasubstituted olefins from the intermolecular conjugate addition of simple alkenes to α,β-unsaturated carbonyl compounds.[22] Among initially screened metal catalysts, the cationic ruthenium hydride complex **1** was found to exhibit distinctively high activity in yielding the coupling products. In a typical setting, the treatment of ethyl cinnamate (0.6 mmol) with propene (2.9 mmol) in the presence of the

Organometallics, Vol 31, No. 1 (January 9, 2012): pg. 495-504. DOI.

ruthenium catalyst **1** (3 mol %) at 70 °C in CH_2Cl_2 led to the exclusive formation of the tetrasubstituted olefin product **2** (eq 1). Both 1- and 2-alkenes gave the same coupling product, indicating that a rapid rate of olefin isomerization prior to the coupling reaction. The cationic nature of the ruthenium-hydride complex **1** was found to be critical for the catalytic activity, since the neutral ruthenium catalysts showed no activity for the coupling reaction under similar conditions.

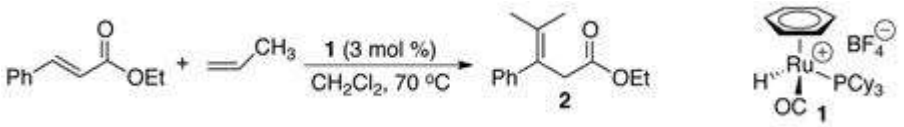

(1)

In an effort to extend the scope of the coupling reaction, we examined the substituent effect of the α,β-unsaturated carbonyl compounds on the coupling reaction (Table 1). In general, a-substituted cinnamic esters and amides were found to undergo the coupling reaction with 1-alkenes to give the corresponding olefin products **3a-3o**. Both α-methyl- and α-phenylcinnamides with propene gave the coupling products **3d-3g** in excellent yields (entries 4–7), but a sterically demanding *N,N*-disubstituted cinnamide failed to give the coupling product under the similar conditions (entry 8). A *E/Z* mixture of the coupling products was formed from a a-substituted cinnamide with ethylene, while the coupling reaction with both 1-butene and 2-butenes gave the same product **3j** in a highly (*Z*)-selective fashion (entries 9–11). The alkene stereochemistry of **3j** was assigned from the observation of NOE signals between phenyl and the methyl triplet peaks (δ 7.24 (Ph) ↔ 0.84 (CH_3)) and between the CH proton and the methyl singlet peaks (δ 3.59 (CH) ↔ 1.82 (CH_3)), as analyzed by the NOESY NMR. Sterically less demanding α-olefins such as 1-hexene and 4-phenyl-1-butene also yielded (*Z*)-selective tetrasubstituted olefin products **3k** and **3l** (entries 12, 13). The coupling reaction of α-methyl cinnamide with cyclopentene gave a diastereoselective coupling products **3m** and **3n** (7:2), in which three different chiral centers are created in one step (entry 14). The relative stereochemistry of **3m** and **3n** was definitively assigned from the ^{1}H NMR spectroscopic data by examining vicinal coupling of the diastereotopic protons. A furan-substituted acrylic substrate with propene rapidly yielded the corresponding tetrasubstituted olefin product **3o** (entry 15).

Organometallics, Vol 31, No. 1 (January 9, 2012): pg. 495-504. DOI.

Table 1. Conjugate Addition Reaction of Simple Alkenes to α-Substituted α,β-Unsaturated Carbonyl Compounds[a]

entry	carbonyl compd	alkene	product (s)	t (h)	temp (°C)	yd (%)
1	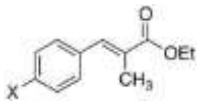	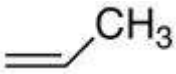	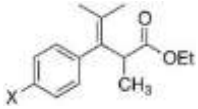	14	70	91
2				14	70	94
3				14	70	95
	X = H X = Me X = Cl		**3a** **3b** **3c**			
4	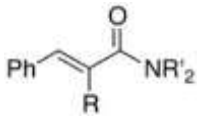	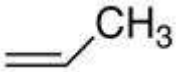	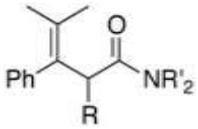	14	70	92
5				14	70	82
6				14	70	95
7				14	70	91
8	R = Me R′ = H, Me R = Ph R′ = H, Bz R = Me R′ = H, Ph R = Me R′ = H, Bz R = Me R′ = Me, Me		**3d** **3e** **3f** **3g**	14	70	<5[b]
9	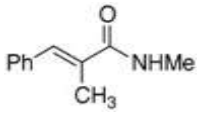	$H_2C{=}CH_2$	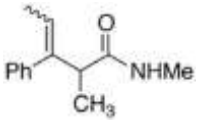	14	50	80
			(*Z*)/(*E*)-**3i** = 2:1			
10		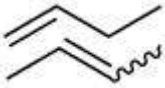	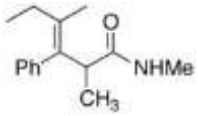	14	50	38
11				14	50	37
			3j			
12		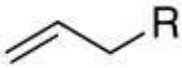	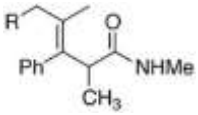	14	50	80
13				14	50	80
			3k (R = n-Pr) **3l** (R = Bz))			
14	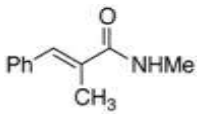		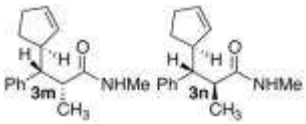	14	20	89
15	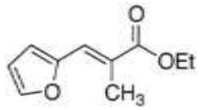	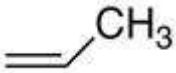	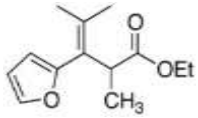	2	70	95
			3o			

[a]Reaction conditions: carbonyl compound (0.6 mmol), alkene (3.0 mmol), **1** (3 mol %), CH_2Cl_2 (3 mL).
[b]Due to low conversion, the product yield was determined by GC.

Organometallics, Vol 31, No. 1 (January 9, 2012): pg. 495-504. DOI.

The analogous coupling reaction with aryl-substituted alkenes led to the selective formation of the oxidative C–H coupling products **4a-4k** (Table 2). Among initially screened cinnamic acid derivatives, only a-methylcinnamide with styrene led to the significant amount of the coupling product **4e** (entry 5). Both steric and electronic environments on the carbonyl substrate seem to be important in effecting the oxidative coupling reaction, since neither cinnamic esters nor sterically demanding *N,N*-disubstituted cinnamides yielded any significant amount of the coupling products (entries 1–4). Also, an electron-deficient *p*-chlorostyrene gave only 10% of the oxidative coupling product **4f**, resulting in a mixture of linear and branched insertion products **3p** and **3q** predominantly (entry 6). Styrenes with electron donating group were found to promote the oxidative C–H coupling reaction in yielding (*E*)-diene products **4g** and **4h** (entries 7, 8). 2-Vinylnaphthalenes were also found to be suitable substrates for giving the oxidative coupling products **4j** and **4k** (entries 10, 11). Unlike other catalytic C–H oxidative coupling methods which typically require stoichiometric oxidants,[14–17] our catalytic method does not require any external oxidants, as the alkene substrate is effectively serving as the hydrogen acceptor.

Table 2. Oxidative C–H Coupling Reaction of α,β-Unsaturated Carbonyl Compounds with Arylalkenes[a]

entry	carbonyl compd	alkene	product	yield (%)
1	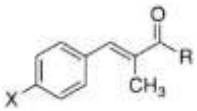	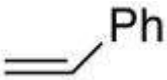	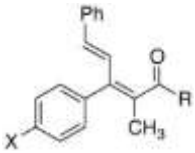	<5[b]
2				<5[b]
3				<5[b]
4				<5[b]
5	X = H R = OEt X = Me R = Ph X = Cl R = Ph X = H X = H R = NHMe		**4a** **4b** **4c** **4d** **4e**	51
6	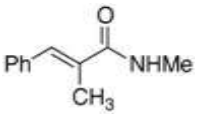	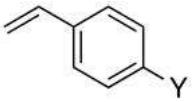		10[c]
7				62
8				56
9		Y = Cl Y = OMe Y = Me Y = Ph	**4f** **4g** **4h** **4i**	29
10				70

Organometallics, Vol 31, No. 1 (January 9, 2012): pg. 495-504. DOI.

entry	carbonyl compd	alkene	product	yield (%)
11	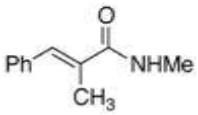	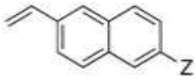 Z = H Z = OMe	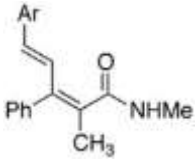 **4j**(Ar = $C_{10}H_7$) **4k**(Ar = $C_{10}H_6$-6-OMe)	71

[a]Reaction conditions: carbonyl compound (0.6 mmol), alkene (3.0 mmol), **1** (5 mol %), CH_2Cl_2 (3 mL), 50 °C, 12–14 h.
[b]Due to low conversion, the product yield was determined from GC analysis.
[c]A complex mixture of the insertion products **3p** and **3q** was formed (55% combined yield).

We next pursued an intramolecular version of the coupling reaction to further demonstrate its synthetic utility. Both 1,2-disubstituted arene and cycloalkene substrates were employed to examine the conformational effects on the insertion vs the oxidative coupling products. These substrates were readily synthesized in two or three steps by using Wittig and Suzuki coupling protocols (Scheme S1, Supporting Information).[24] The coupling reaction of *ortho*-alkenylated cinnamate substrates proceeded smoothly to give the 1,2-disubstituted indene products **5a** and **5b** (Table 3, entries 1–3). Both allyl and homoallyl-substituted substrates gave the same indene product **5b**, and this is in line with the previously observed rapid olefin isomerization rate prior to the coupling reaction.[25] The analogous coupling reaction with 1,2-disubstituted cycloalkenes led to the oxidative C–H coupling reaction to form bicyclic fulvene products **6a-6f** (entries 4–9). The (*Z*)-stereochemistry of the *exo*-acrylate moiety on the fulvene product was established from the NOESY NMR analysis, where a strong correlation has been observed between α-vinyl hydrogen and CH_2 group of the product **6**. In these cases, ca. 5–10% of side products including the hydrogenated substrate were also detected in the crude mixture. These results suggest that the conformational orientation between two acrylic and alkene units is important in modulating the formation of the indene products **5** (insertion pathway) vs the fulvene products **6** (oxidative coupling pathway).

Table 3. Intramolecular Coupling Reaction of α,β-Unsaturated Carbonyl Compounds[a]

entry	substrate	product	yield (%)
1	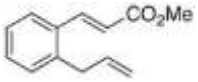	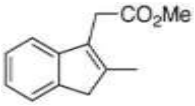 **5a**	78
2	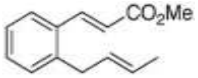	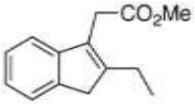 **5b**	76
3	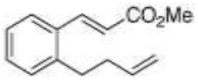	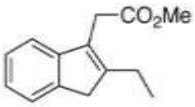 **5b**	76
4	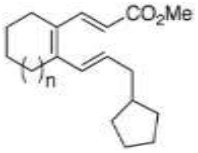 n = 1	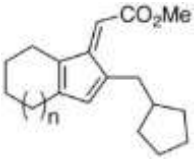 **6a**	51
5	n = 2	**6b**	71
6	n = 3	**6c**	83
7	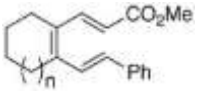 n = 1	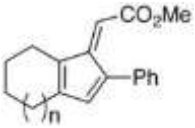 **6d**	84
8	n = 2	**6e**	82
9	n = 3	**6f**	88

[a]Reaction conditions: carbonyl substrate (0.6 mmol), 1 (5 mol %), CH_2Cl_2 (3 mL), 50 °C, 12–14 h.

Because of their unique physicochemical properties, fulvene derivatives have long been utilized in a broad range of material science and medicinal applications, but the traditional synthetic methods to such compounds often require multiple steps and reactive stoichiometric reagents.[26] Catalytic methods to fulvenes and related benzocyclic compounds have not been extensively developed, although this group and others have recently reported catalytic C–H coupling methods to synthesize fulvene and structurally related indene derivatives.[21a,27] From a synthetic point of view, one of the most salient features of our intramolecular coupling method is that

synthetically valuable indene and fulvene derivatives are efficiently constructed without employing any reactive reagents or additives.

Kinetics and Mechanistic Study: Determination of the Empirical Rate Law

In an effort to establish the reaction mechanism, we sought to deduce an empirical rate law from the coupling reaction of ethyl cinnamate with propene. The reaction rate of ethyl cinnamate (70 μmol) and propene (5 equiv) in CD_2Cl_2 (0.5 mL) at 20 °C was monitored as a function of the catalyst concentration of **1** (2.1–34 mM). Initial rate was determined from a first-order plot of the product **2** vs time at each concentration of **1**. The linear plot of the reaction rate as a function of the catalyst concentration established the first order dependence on [**1**] (Figure 1).

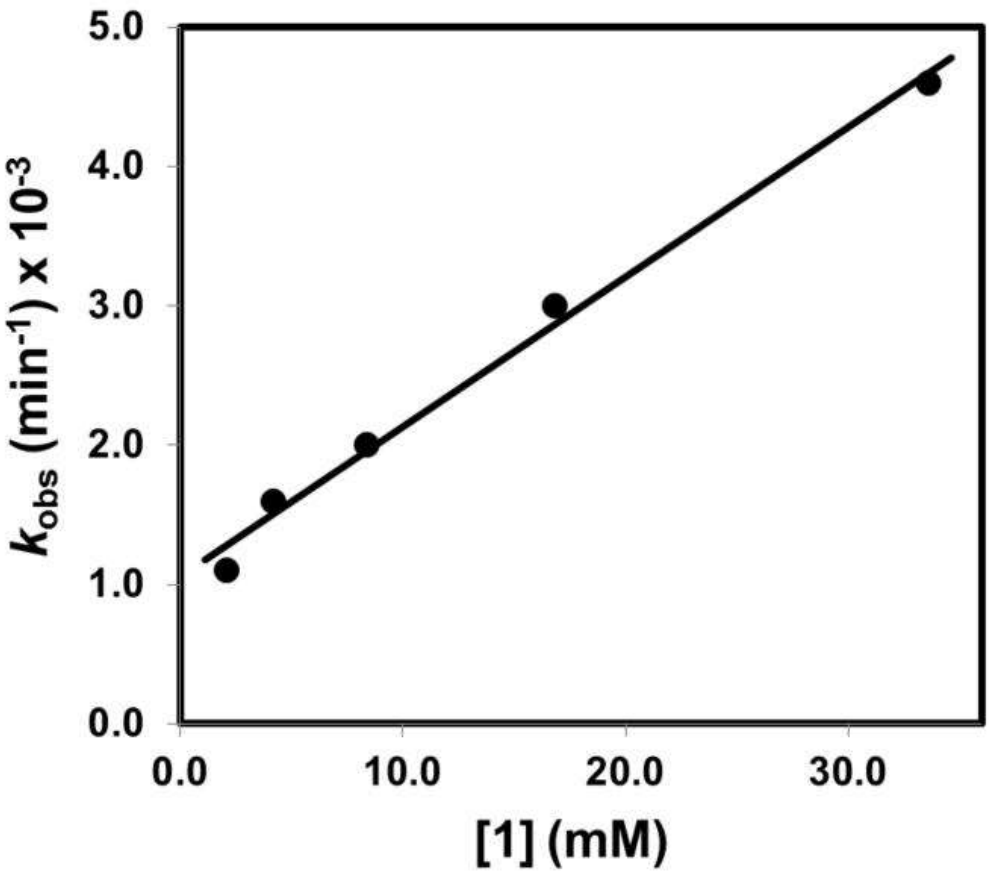

Figure 1. Plot of the Rate vs Catalyst Concentration (2.1–34 mM) for the Coupling Reaction of (*E*)-$C_6H_5CH{=}CHCO_2Et$ and Propene

Organometallics, Vol 31, No. 1 (January 9, 2012): pg. 495-504. DOI.

The analogous procedure was used to obtain the rate dependence on both cinnamate and propene substrates. Two separate linear plots of the rate vs [cinnamate] and with [propene] revealed that the rate is independent on [propene] in the range of 0.6–1.8 M (Figure 2), but exhibited an inverse dependence on [cinnamate] (Figure 3). The inverse rate dependence on [cinnamate] suggests that the second cinnamate substrate is serving as an effective inhibitior. To further demonstrate zero-order dependence of [alkene] under preparatory-scale reaction conditions, we separately measured the product conversion from the coupling reaction of *N*-methyl cinnamide with different amounts of styrene (3–10 equiv) under otherwise similar conditions. In all cases, exactly same product conversion (10%) was resulted after 30 min at 50 °C. By combining these experimental results, the empirical rate law of the reaction has been deduced as shown in eq 2.

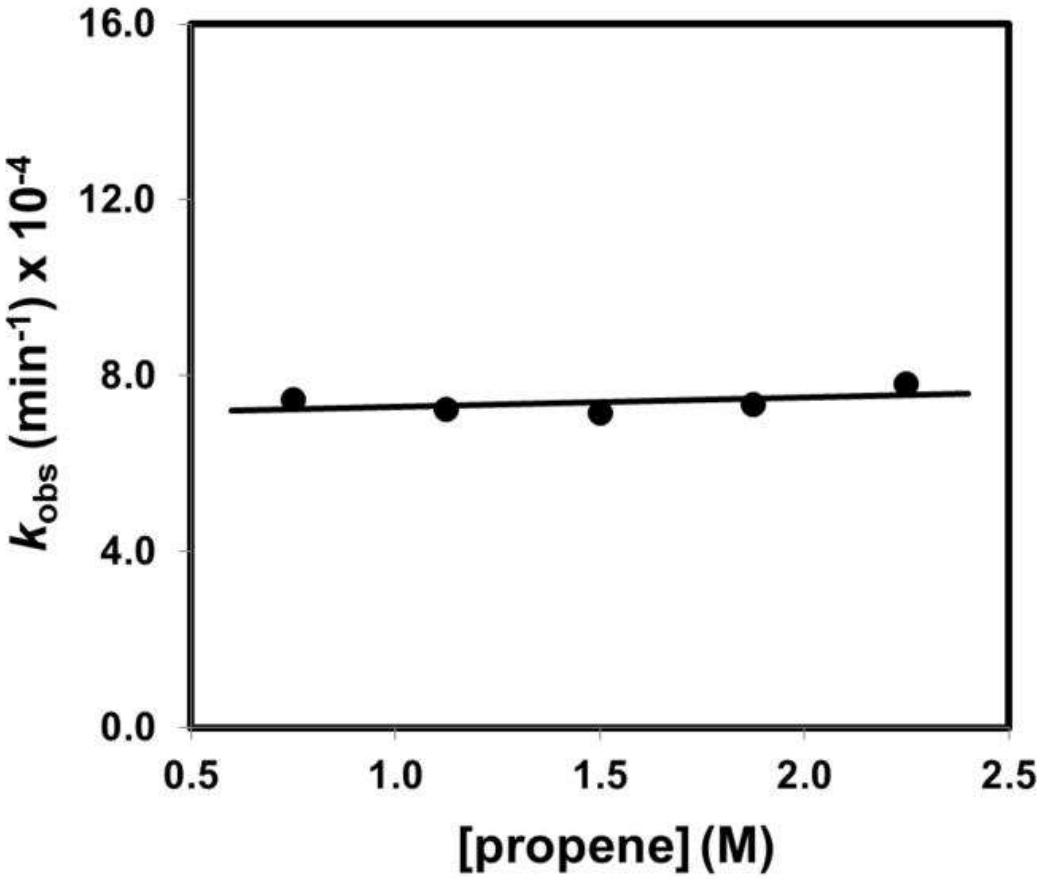

Figure 2. Plot of the Rate vs Propene Concentration (0.6–1.8 M) for the Coupling Reaction of (*E*)-$C_6H_5CH{=}CHCO_2Et$ and Propene

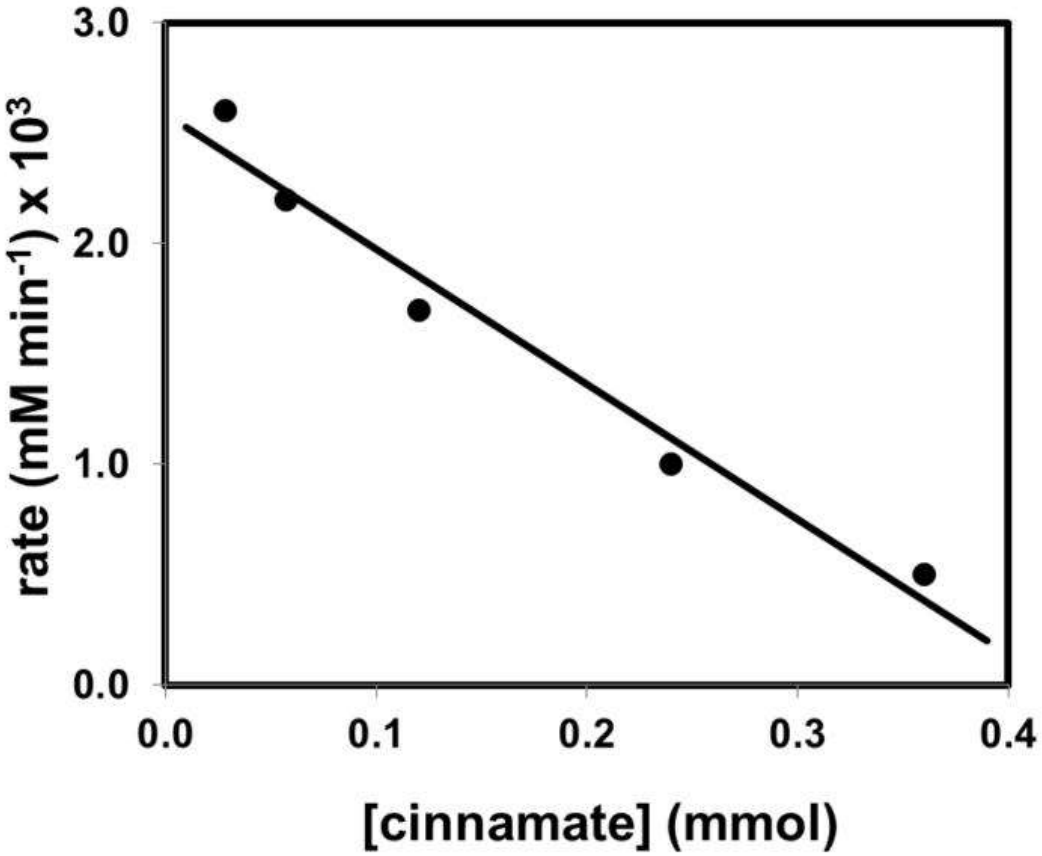

Figure 3. Plot of the Rate vs (*E*)-$C_6H_5CH{=}CHCO_2Et$ (0.12–0.36 M) for the Coupling Reaction of (*E*)-$C_6H_5CH{=}CHCO_2Et$ and Propene

$$\text{rate}=k[\mathbf{1}]^1[\text{propene}]^0[\text{cinnamate}]^{-1} \tag{2}$$

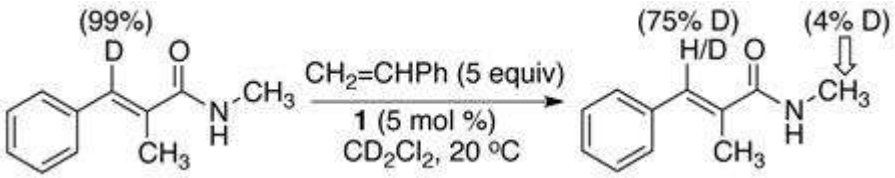

(3)

Deuterium Labeling Study

We previously observed that the coupling reaction of (*E*)-$C_6D_5CD{=}CDCONMe_2$ with an excess amount of propene led to the selective H/D exchange on the α-methylene position of the product (55% D), but only 5% D on the δ-methyl positions.[23] To examine the

H/D exchange pattern of the oxidative coupling reaction, the treatment of (*E*)-$C_6H_5CD{=}C(CH_3)CONHCH_3$ (70 μmol, 99% D) with an excess amount of styrene (5 equiv) in the presence of **1** (2 mg, 5 mol %) in CD_2Cl_2 was monitored by NMR (eq 3). After 15 h at 20 °C, a significant H/D exchange between the vinyl hydrogen of the cinnamide (75% D) and styrene (4% D) substrates was observed without forming the coupling product **3q**, as analyzed by ^{1}H and ^{2}H NMR (Figure S1, Supporting Information). A relatively facile H/D exchange pattern is consistent with a reversible vinyl C–H bond activation of the cinnamide substrate, and further suggests that the vinyl C–H bond activation step is not rate-limiting for the oxidative coupling reaction.

Kinetic Isotope Effects

We next measured the deuterium kinetic isotope effect from the coupling reaction of cinnamic acid derivatives with alkenes. As for the formation of insertion products, we separately measured the rate from the treatment of (*E*)-$C_6H_5CH{=}CHCO_2Et$ with ethylene and with ethylene-d_4 at 60 °C in CD_2Cl_2, which led to a negligible kinetic isotope effect of k_H/k_D = 1.1±0.1 (Figure S2, Supporting Information). We also measured the deuterium isotope effect from both (*E*)-$C_6H_5CH{=}C(CH_3)CONHCH_3$ and (*E*)-$C_6H_5CD{=}C(CH_3)CONHCH_3$ with styrene under the same reaction conditions in forming the oxidative coupling product **4e**. The pseudo first-order plots from both (*E*)-$C_6H_5CH{=}C(CH_3)CONHCH_3$ and (*E*)-$C_6H_5CD{=}C(CH_3)CONHCH_3$ with styrene led to $k_{obs} = 9.2 \times 10^{-2}$ h^{-1} and $k_{obs} = 8.8 \times 10^{-2}$ h^{-1}, respectively, which translated to a negligible isotope effect of k_H/k_D = 1.1 ± 0.1 (Figure S3, Supporting Information). These results further support that the vinyl C–H bond activation of the cinnamic acid derivative is not the rate-limiting step in forming the oxidative coupling product **4**.

In sharp contrast, a normal deuterium isotope effect was measured from the coupling reaction of (*E*)-$C_6H_5CH{=}C(CH_3)CONHCH_3$ with styrene and styrene-d_8 at 40 °C in CH_2Cl_2 (Figure 4). The pseudo first-order plots from the reaction of (*E*)-$C_6H_5CH{=}C(CH_3)CONHCH_3$ with both styrene and styrene-d_8 led to $k_{obs} = 9.2 \times 10^{-2}$ h^{-1} and 5.3×10^{-2} h^{-1}, respectively, which translated to a normal deuterium isotope effect of k_H/k_D = 1.7±0.1 (Figure 4). The results clearly indicate that

the styrenyl C–H bond cleavage is the most likely turnover-limiting step in forming the oxidative coupling product **4**.

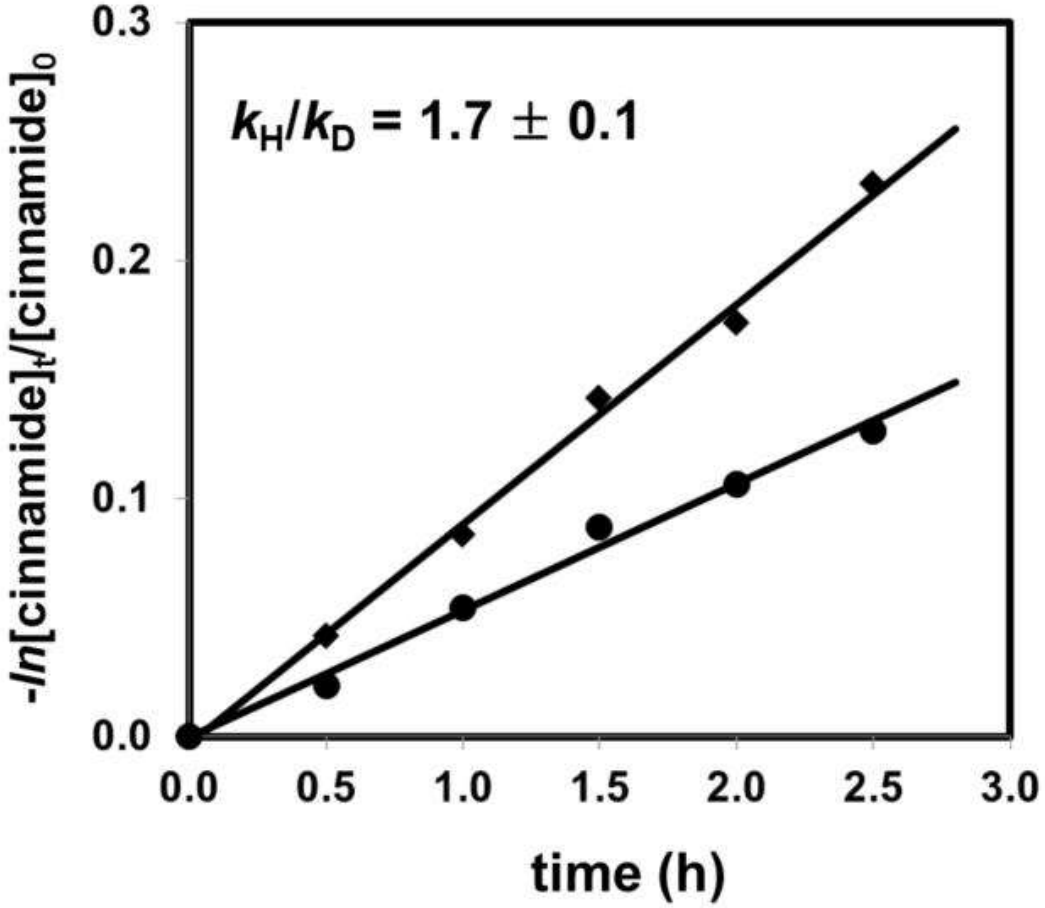

Figure 4. First-Order Plots of $-ln([\text{cinnamide}]_t/[\text{cinnamide}]_0)$ vs Time for the Coupling Reaction of (*E*)-$C_6H_5CH{=}C(CH_3)CONHCH_3$ with Styrene (◆) and Styrene-d_8 (●)

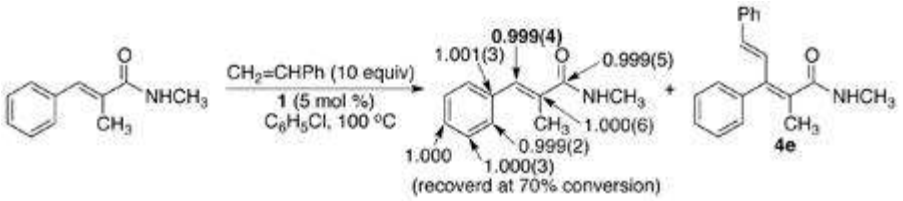

(4)

To further discern rate-limiting step of the oxidative coupling reaction, $^{12}C/^{13}C$ carbon isotope effect was measured from the coupling reaction of a α-substituted cinnamide with styrene by employing Singleton's high-precision NMR technique (eq 4).[28] No significant carbon isotope

effect on the β-carbon of the cinnamide substrate was observed from the coupling reaction of (*E*)-$C_6H_5CH{=}C(CH_3)CONHCH_3$ with styrene (^{13}C(recovered)/^{13}C(virgin) of C_β = 0.999(4); average of two runs at 70% conversion) (Table S1 and Figure S4, Supporting Information). The results reinforced the notion that the styrenyl C–H activation is the rate-limiting step in forming the oxidative coupling product **4**.

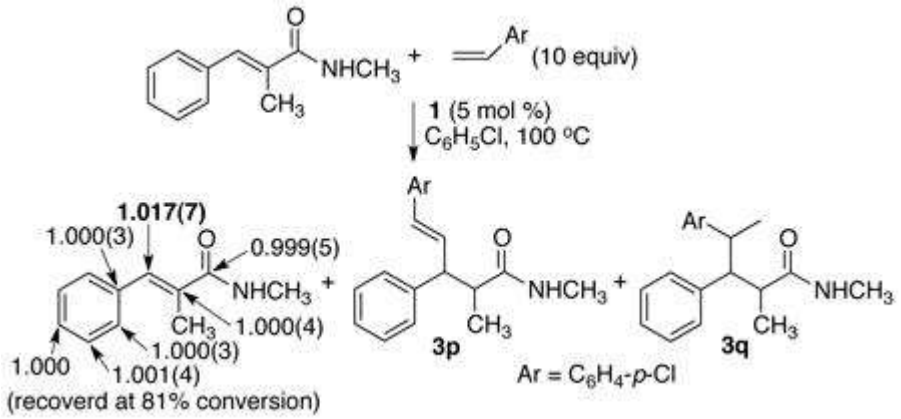

(5)

To demonstrate the propensity of carbon isotope effect in determining the rate-determining step, we measured the analogous carbon isotope effect from the coupling reaction of a α-substituted cinnamide with 4-chlorostyrene, which was found to yield the insertion product **3p** predominantly as described in Table 2 (eq 5). In this case, a definitive carbon isotope effect was observed on the β-carbon of the cinnamide substrate, when the ^{13}C ratio of recovered (*E*)-$C_6H_5CH{=}C(CH_3)CONHCH_3$ at 80% and 82% conversion was compared to that of the virgin sample (^{13}C(recovered)/^{13}C(virgin) at C_β = 1.017(7); average of two runs) (Table S2 and Figure S5, Supporting Information). Previously, we also observed similar results from the coupling reaction of (*E*)-$C_6H_5CH{=}CHCO_2Et$ with propene in forming the insertion product **2**.[23] It should be mentioned that the coupling reaction of (*E*)-$C_6H_5CH{=}C(CH_3)CONHCH_3$ with an electron-deficient alkene such as 4-chlorostyrene led to a mixture of linear and branched insertion products **3p** and **3q** and the oxidative coupling product **4f** **((3p + 3q):4f** = 85 : 15), and we observed the noticeable carbon isotope effect only from the insertion products **3p** and **3q**.

Hammett Study

To probe electronic effects on the product formation, we determined the Hammett ρ values from the coupling reaction of α,β-unsaturated carbonyl compounds with alkenes.[29] The correlation of the relative rate with σ_p for a series of *para*-substituted *p*-X-$C_6H_4CH{=}CHCO_2Et$ (X = OCH_3, CH_3, H, F, Cl, CO_2Me, CF_3) with propene in the presence of **1** (3 mol %) at 20 °C led to a positive ρ value (ρ = +1.1±0.1) in forming the insertion products **2** (Figure 5A). The promotional effect by an electron-withdrawing group as indicated by a positive slope is consistent with a decreasing positive charge on the β-carbon of cinnamate substrate during the alkene insertion step. The observed Hammett ρ value is well within the range of other Michael-type of conjugate addition of nucleophiles to acrylic substrates.[30]

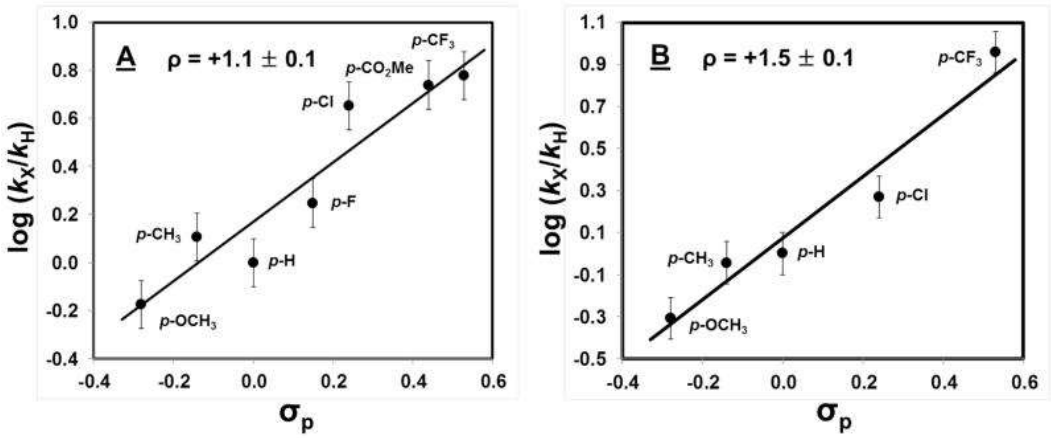

Figure 5. Hammett Plots of the Coupling Reaction of *para*-Substituted *p*-X-$C_6H_4CH{=}CHCO_2Et$ (X = OCH_3, CH_3, H, F, Cl, CO_2Me, CF_3) with Propene (A), and (*E*)-$C_6H_4CH{=}CHCO_2Et$ with *para*-Substituted *p*-Y-$C_6H_4CH{=}CH_2$ (Y = OCH_3, CH_3, H, Cl, CF_3) (B)

An analogous correlation from the reaction of (*E*)-$C_6H_5CH{=}CHCO_2Et$ with a series of *para*-substituted styrene derivatives *p*-Y-$C_6H_4CH{=}CH_2$ (Y = OCH_3, CH_3, H, Cl, CF_3) at 50 °C in CH_2Cl_2 resulted in a substantially higher Hammett ρ value (ρ = +1.5±0.1) for the formation of the insertion products **2** (Figure 5B). In this case, a strong promotional effect by an electron-withdrawing group of styrene can be readily rationalized by invoking the formation of a cationic Ru-vinyl species Ru–CH=CHAr. A higher +ρ value compared to the insertion reaction suggests of a considerable build-up of ionic character on the cationic Ru-vinyl species, and a linear Hammett correlation also

indicates the same operating mechanism for these cinnamate and styrene derivatives. While overall conversion is relatively high, the coupling reaction with styrene derivatives generally led to a lower selectivity toward the insertion product **2;** the formation of a nearly 1:1 mixture of the linear and branched insertion products along with other minor double bond isomers as well as the oxidative coupling product **4** was observed in the crude reaction mixture (combined insertion products **2 : 4** = 4 : 1 to 5 : 1). The product ratio for these reactions were determined by NMR.

For the coupling reaction of the α-substituted cinnamide (*E*)-$C_6H_5CH{=}C(CH_3)CONHCH_3$ with *para*-substituted styrenes *p*-Y-$C_6H_4CH{=}CH_2$ (Y = OCH_3, CH_3, H, F, Cl, CF_3), electronic nature of the *para*-substituent group was found to be the dominant factor in modulating the product selectivity (Scheme 1). Thus, the coupling reaction of (*E*)-$C_6H_5CH{=}C(CH_3)CONHCH_3$ with styrenes with a *para*-electron donating group (Y = OCH_3, CH_3, H) yielded the oxidative coupling products **4** over the insertion products **3 (3 : 4** = 1 : 2.5 to 1 : 8). In contrast, the analogous coupling reaction with styrenes having a *para*-electron deficient group (Y = F, Cl, CF_3) resulted in a mixture of the branched and linear insertion products **3** predominantly (**3 : 4** = 3 : 1 to 5.5 : 1). Hammett ρ values were measured for the coupling reaction with these *para*-substituted styrene derivatives to further probe electronic effects of the alkene substrate on the product selectivity.

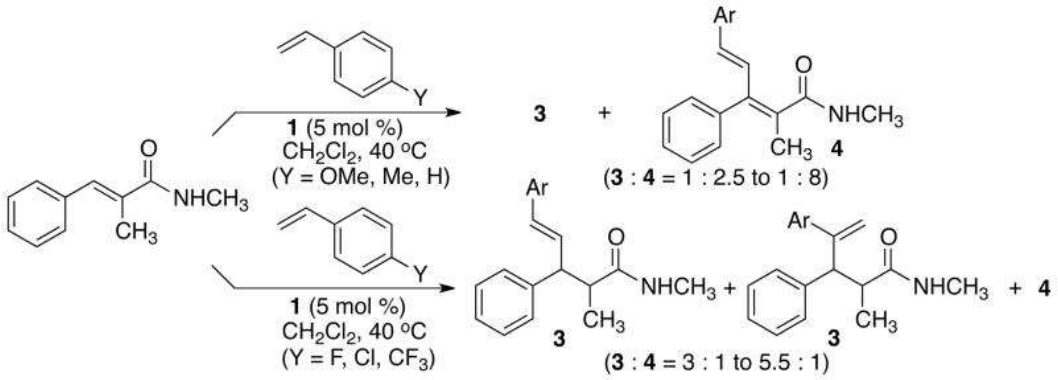

Scheme 1

Interestingly, the Hammett correlation from the reaction of (*E*)-$C_6H_5CH{=}C(CH_3)CONHCH_3$ with a series of *para*-substituted styrene *p*-

Y-$C_6H_4CH{=}CH_2$ (Y = OCH_3, CH_3, H, F, Cl, CF_3) in the presence **1** (5 mol %) at 40 °C in CH_2Cl_2 led to the positive ρ values for both electron-donating and electron-withdrawing groups (ρ = +1.1±0.1 with electron-donating group; ρ = +0.9±0.1 with electron-withdrawing group) (Figure 6). The results suggest that two opposing electronic factors promote the product selectivity. Thus, for the styrene derivatives having an electron-withdrawing group, the formation of the conjugate addition product **3** is promoted by a facile olefin insertion resulted from increasing olefinic bond polarity. On the other hand, for styrenes with an electron-donating group, the predominant formation of the oxidative coupling product **4** can be rationalized by invoking promotional effect from the styrenyl C–H activation.

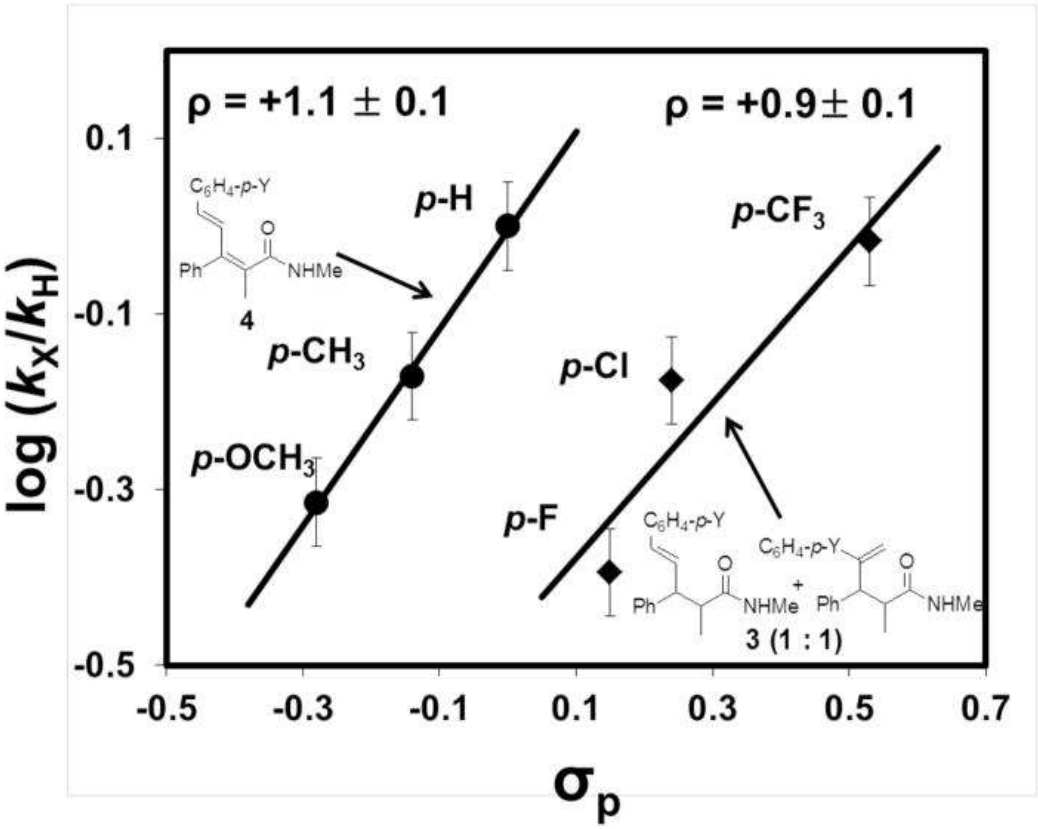

Figure 6. Hammett Plots for the Coupling Reaction of (*E*)-$C_6H_4CH{=}C(CH_3)CONHCH_3$ with *para*-Substituted Styrenes *p*-Y-$C_6H_4CH{=}CH_2$ (Y = OCH_3, CH_3, H (●) and Y = F, Cl, CF_3 (◆))

Thermodynamic Parameters

The thermodynamic parameters were successfully obtained from measuring the rates of the coupling reaction as a function of the temperature. The reaction rate was measured from the treatment of (*E*)-$C_6H_4CH{=}CHCO_2Et$ (0.12 mmol) with an excess amount of propene (0.60 mmol) and the catalyst **1** (3 mol %) in the temperature range of 20–40 °C at 5 °C intervals by using the standard VT NMR technique. Excess propene concentration was employed to maintain a pseudo zero-order [propene], which minimized the cinnamate inhibition during the reaction. The thermodynamic parameters, $\Delta H^{\ddagger}$ = 20.3±2.2 kcal/mol and $\Delta S^{\ddagger}$ = −42.1±4.5 e.u., were obtained from the standard Eyring analysis (Figure 7).[29] A relatively large negative $\Delta S^{\ddagger}$ value is consistent with an organized transition state formed from combining two substrate molecules.

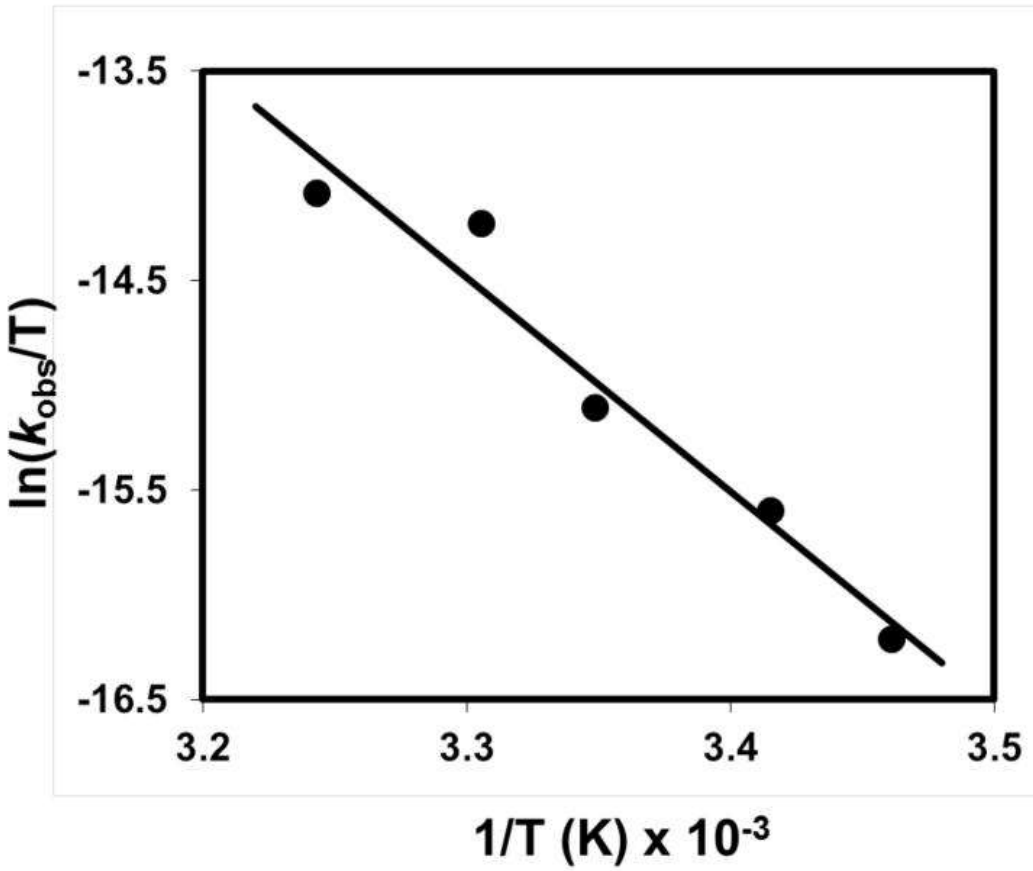

Figure 7. Eyring Plot for the Coupling Reaction of (*E*)-$C_6H_5CH{=}CHCO_2Et$ with Propene

Organometallics, Vol 31, No. 1 (January 9, 2012): pg. 495-504. DOI.

Proposed Mechanism

We present two separate mechanistic pathways to explain the formation of the coupling products **3** and **4**. We propose a cationic Ru–H species **7**, which is initially formed from the ligand exchange reaction of **1** with the carbonyl substrate, as the common intermediate species for both mechanistic pathways (Scheme 2). To explain the formation of the insertion product **3**, we propose a mechanistic pathway via the cationic Ru-alkene-alkyl species **8**, which is formed from the chelate-directed regioselective alkene insertion. The zero-order dependence on [alkene] indicates that the alkene coordination step is quite facile in the presence of excess [alkene]. On the other hand, the inverse dependence on [cinnamate] suggests that the cinnamate substrate inhibits competitively by binding to the metal center, where an excess [alkene] would be needed to overcome the competitive inhibition from the cinnamate substrate.

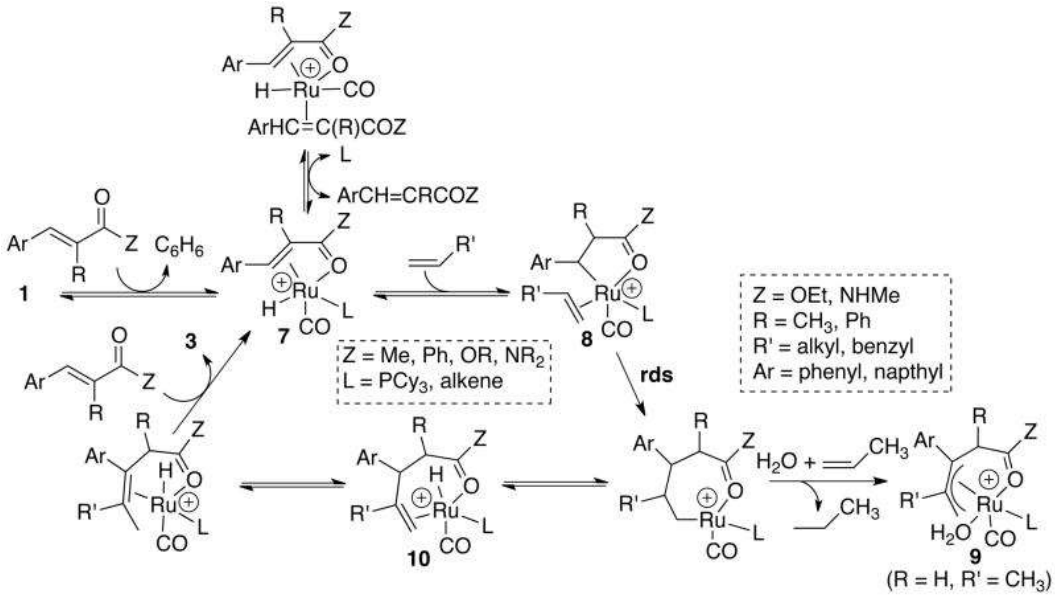

Scheme 2. Proposed Mechanism for the Conjugate Addition Reaction of α,β-Unsaturated Carbonyl Compounds with Simple Alkenes

Both the observation of the carbon isotope effect on the β-carbon of α,β-unsaturated carbonyl substrate and a negligible deuterium isotope effect of k_H/k_D = 1.1±0.1 from the reaction with ethylene/ethylene-d_4 support the olefin insertion as the rate-limiting step. The positive Hammett ρ value obtained from the correlation of

para-substituted cinnamate substrates is also consistent with the formation of the carbonyl-chelated species **8**, where an electron-releasing group would promote the regioselective olefin insertion and β-hydride elimination steps. It has been well established that both olefin bond polarity and the chelation of the carbonyl group are important in directing regioselective insertion of enamides and α,β-unsaturated carbonyl compounds.[31] In light of the recent deuterium labeling study on the alkene dimerization and isomerization reactions,[25] a facile olefin isomerization step is expected in forming the tetrasubstituted olefin products **3** and the regeneration of **7**. Previously, we have successfully trapped and isolated the catalytically relevant ruthenium-allyl species **9**, which provides another supporting evidence for the Ru-alkene-hydride complex **10**.[23]

We propose an alternative mechanistic pathway involving vinyl C–H bond activation to explain the formation of the oxidative coupling product **4** (Scheme 3). The olefin insertion to the electrophilic Ru-H complex **7** followed by the vinyl C–H bond activation of the carbonyl substrate and olefin insertion steps would form a cationic Ru(IV) species **11**. The reductive elimination (dehydrogenation) and the coordination of another olefin substrate would lead to the formation of a cationic ruthenium-alkenyl species **12**. Alternatively, one can envision a σ-bond metathesis mechanism in forming the alkenyl complex **12**, the possibility which cannot be rigorously excluded at this time.[32] All of the kinetic data, including the observation of a normal isotope effect of k_H/k_D = 1.7±0.1 from the coupling reaction of styrene and styrene-d_8 as well as a negligible deuterium isotope effect from (*E*)-$C_6H_5CH{=}C(CH_3)CONHCH_3$ and (*E*)-$C_6H_5CD{=}C(CH_3)CONHCH_3$, are consistent with the styrenyl C–H bond activation rate-limiting step. Both carbon isotope effect and the deuterium labeling studies also provide supporting evidences for the rate-limiting styrenyl C–H bond activation step. It is imperative to mention that the C–C bond formation step has been generally found to be the turnover-limiting step in Murai-type of chelate-assisted C–H insertion reactions catalyzed by neutral Ru catalysts.[22,33] In our case, the electrophilic nature of the Ru catalyst appears to promote the vinyl C–H bond activation of electron-deficient alkenes in forming the oxidative coupling product **4**, where the formation of ethylbenzene from dehydrogenation should also serve as the driving force for the vinyl C–H activation. Hammett study of *para*-substituted styrene derivatives

revealed a fine electronic balance on dictating the olefin insertion vs oxidative coupling pathways, and the vinyl C–H activation is favored over the alkene insertion for electron-deficient alkenes.

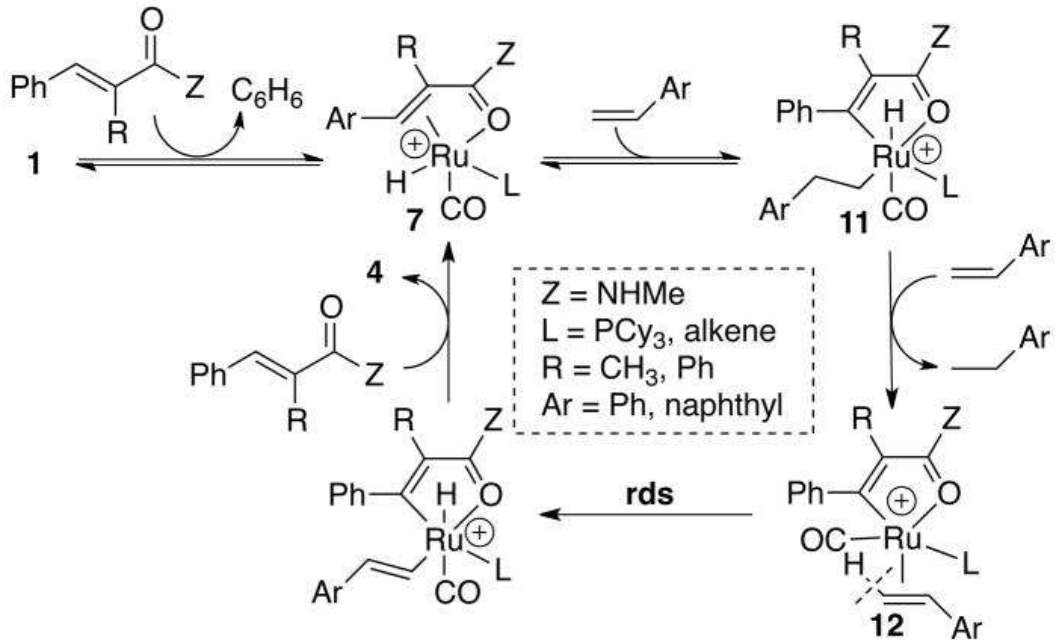

Scheme 3. Proposed Mechanism for the Coupling Reaction of α,β-Unsaturated Carbonyl Compounds with Aryl-Substituted Alkenes

Table 4 compares the major kinetic data between the insertion and oxidative coupling pathways. The coupling reaction of cinnamic acid derivatives with simple alkenes normally favors the insertion pathway in forming the coupling product **3**. As inferred from the kinetic isotope effect data, we found that the alkene insertion step (C–C bond formation) is the most likely turnover-limiting step for this pathway. By employing α-substituted cinnamides and electron-poor alkene substrates, we have been able to alter the reaction path toward the oxidative coupling product **4**, for which case, the kinetic data are consistent with the vinyl C–H activation rate-limiting step.

Table 4. Summary of the Kinetic Data for the Coupling Reaction of α,β-Unsaturated Carbonyl Compounds with Alkenes

	Alkene Insertion Path	**Oxidative Coupling Path**
Hammett ρ Value[a]	+1.1 to +1.4	+0.9 to +1.1
Carbon Isotope Effect[b]	Yes (C_β = 1.018)	No (C_β = 0.999)
Deuterium Isotope Effect[c]	No (k_H/k_D = 1.1)	Yes (k_H/k_D = 1.7)
Rate Limiting Step	Alkene Insertion	Vinyl C–H Activation

Organometallics, Vol 31, No. 1 (January 9, 2012): pg. 495-504. DOI.

[a]Hammett ρ values obtained from the reaction of (*E*)-*p*-X-$C_6H_4CH{=}CHCO_2Et$ with propene and with styrene.
[b]^{13}C ratio (recovered/virgin) obtained from the reaction of (*E*)-$C_6H_4CH{=}CHCON(CH_3)_2$ with propene with styrene and from the (*E*)-$C_6H_4CH{=}CH(CH_3)CONHMe$ with styrene.
[c]Deuterium isotope effect obtained from the reaction of (*E*)-$C_6H_4CH{=}CHCO_2Et$ with ethylene/ethylene-d_4 and from the reaction of (*E*)-$C_6H_4CH{=}CH(CH_3)CONHCH_3$ with styrene/styrene-d_8.

Both the conformation of the cinnamide substrate and the electronic nature of the olefin substrate have been found to be important in promoting the C–H oxidative coupling product **4**. A simple conformational analysis indicates that a normally facile hydride migration to the α,β-unsaturated carbonyl substrate would be less favored for α-substituted cinnamide substrate, due to the steric interaction between phenyl and the α-substitutent in forming the alkyl species **8**. As illustrated in Table 3, such conformational flexibility has been successfully exploited for an intramolecular version of the coupling reaction to form the fulvene products **6**.

Hammett study from the coupling reaction of (*E*)-$C_6H_5CH{=}C(CH_3)CONHCH_3$ with *para*-substituted styrenes (Figure 6) also revealed that the electronic environment on the alkene substrate significantly influences the oxidative C–H coupling pathway. That styrenes with electron-releasing group yielding the oxidative coupling products **4**, suggests that the olefin insertion is the key step in modulating the product selectivity by promoting the styrenyl C–H bond activation while discouraging the olefin insertion pathway.

Conclusions

Scope and mechanistic aspects of the ruthenium-catalyzed coupling reaction of a,β-unsaturated carbonyl compounds and alkenes have been delineated. The coupling reaction of a,β-unsaturated carbonyl compounds with simple electron-rich alkenes exclusively gave (*Z*)-selective conjugate addition products **3**, while the analogous reaction of cinnamides with electron-poor alkenes predominantly yielded the C–H oxidative coupling products **4**. Intramolecular version of the coupling reaction has led to an efficient synthesis for indene and fulvene derivatives **5** and **6**. Detailed kinetic studies revealed that the olefin insertion into an α,β-unsaturated carbonyl substrate is the most likely rate-limiting step in forming the insertion products **3**. In contrast, the kinetic data are consistent with the vinyl C–H activation

rate-limiting step for the oxidative coupling products **4**. Further, both kinetic and mechanistic studies illuminated that the conformation of α,β-unsaturated carbonyl substrate as well as the alkene electronic environments are important factors in modulating between the insertion vs oxidative coupling pathways. We anticipate that the catalytic coupling method would provide an efficient synthetic methodology to highly substituted olefins as well as indene and fulvene derivatives from readily available cinnamic acid derivatives and simple alkenes.

Experimental Section

Representative Procedure of the Catalytic Reaction

In a glove box, complex **1** (10 mg, 17 μmol), a carbonyl compound (0.60 mmol) and an alkene (3.0 mmol) were dissolved in CH_2Cl_2 (2 mL) in a 25 mL Schlenk tube equipped with a Teflon stopcock and a magnetic stirring bar. The tube was brought out of the box, and was stirred for 12–14 h in an oil bath which was preset at 70 °C, after which it was chilled in a dry ice/acetone bath. After the tube was open to air, the solution was filtered through a small pad of silica gel (hexanes/EtOAc = 2:1), and the resulting solution was analyzed by GC. Analytically pure product was isolated after a simple column chromatography on silica gel (hexanes/EtOAc = 20:1 to 4:1). All substrates for the intramolecular coupling reaction listed in Table 3 were prepared by following the literature methods.[24] See the Supporting Information for a detailed experimental procedure for the preparation of these substrates.

General Procedure for the Rate Measurements

In a glove box, complex **1** (1.5–12 mol %) and (*E*)-$C_6H_5CH{=}CHCO_2Et$ (0.03–0.38 mmol) were dissolved in CD_2Cl_2 (0.4 mL) in a thick-walled J-Young NMR tube with a Teflon screw cap. The tube was cooled in a liquid nitrogen bath, and excess propene (0.3–0.9 mmol) was condensed via a vacuum line transfer. The tube was gradually warmed to room temperature. The sample was inserted into the NMR probe which was preset at 20 °C. The initial rate at each concentration of **1** was determined by measuring the appearance of

the product signals in 5 min intervals, and these were normalized against an internal standard (solvent resonance). The k_{obs} was estimated from a first-order plot of $-ln\{[(E)\text{-}C_6H_5CH{=}CHCO_2Et]_t/[(E)\text{-}C_6H_5CH{=}CHCO_2Et]_o\}$ vs time.

Deuterium Kinetic Isotope Effect Study: Reaction in CD_2Cl_2

In a glove box, complex **1** (2 mg, 3.5 μmol) and (*E*)-$C_6H_5CH{=}CHCO_2Et$ (20 mg, 0.12 mmol) were dissolved in CD_2Cl_2 (0.4 mL) in a thick-walled J-Young NMR tube with a Teflon screw cap. The tube was cooled in a liquid nitrogen bath, and excess ethylene or ethylene-d_4 (0.6 mmol) was condensed via a vacuum line transfer. The tube was gradually warmed to room temperature, and the sample tube was inserted into the NMR probe which was preset at 20 °C. The rate was measured by monitoring the ^1H integration of the product signals in 5 min intervals, and these were normalized against an internal standard (solvent resonance). The k_{obs} was estimated from a first-order plot of $-ln([C_6H_5CH{=}CHCO_2Et]_t/[C_6H_5CH{=}CHCO_2Et]_o)$ vs time.

Reaction in CH_2Cl_2

In a glove box, complex **1** (20 mg, 35 μmol), (*E*)-$C_6H_5CH{=}C(CH_3)CONHCH_3$ (122 mg, 0.7 mmol) or $C_6H_5CD{=}C(CH_3)CONHCH_3$ (122 mg, 0.7 mmol) and styrene or styrene-d_8 (0.36 g, 35 mmol) were dissolved in CH_2Cl_2 (6.0 mL) in a 25 mL Schlenk tube equipped with a Teflon screw cap stopcock and a magnetic stirring bar. After the solution was stirred at room temperature for 10 min, an equal amount of the solution (1.0 mL) was placed in 5 different Schlenk tubes. The tubes were brought out of the box, and they were stirred in an oil bath set at 50 °C. Each reaction tube was taken out from the oil bath in 30 min intervals, and was immediately cooled in a dry ice/acetone bath. After filtering through a small silica gel column (hexanes/EtOAc = 2:1), the solution was analyzed by GC. The k_{obs} was determined from a first-order plot of $-ln([\text{cinnamide}]_t/[\text{cinnamide}]_o)$ vs time.

Carbon Isotope Effect Study

In a glove box, complex **1** (164 mg, 0.28 mmol), (*E*)-$C_6H_5CH{=}CH(CH_3)CONEt_2$ (1.0 g, 5.7 mmol) and styrene (57 mmol) in CH_2Cl_2 (10 mL) were placed in three separate 100 mL Schlenk tubes, each equipped with a Teflon screw cap stopcock and a magnetic stirring bar. The tubes were brought out of the box, and stirred for 14 h in an oil bath which was preset at 100 °C. Unreacted (*E*)-$C_6H_5CH{=}CH(CH_3)CONEt_2$ was collected separately after filtering through a short silica gel column (hexanes/EtOAc = 2:1), and the solution was analyzed by GC (68–82% conversion). The NMR sample of the virgin and recovered (*E*)-$C_6H_5CH{=}CH(CH_3)CONEt_2$ was prepared identically by dissolving an equal amount of (*E*)-$C_6H_5CH{=}CH(CH_3)CONEt_2$ (100 mg) in $CDCl_3$ (0.5 mL) in a 5 mm high precision NMR tube. The $^{13}C\{^1H\}$ NMR spectra of both samples were recorded by following Singleton's NMR method.[28] The $^{13}C\{^1H\}$ NMR spectra were recorded with H-decoupling and 45 degree pulses, and a 60 s delay was imposed to minimize T_1 variations (d1 = 60 s, at = 5.0 s, np = 245098, nt = 704) between each aquisition.

Hammett Study: Reaction in CD_2Cl_2

In a glove box, *para*-substituted *p*-X-$C_6H_4CH{=}CHCO_2Et$ (X = OCH_3, CH_3, H, F, Cl, CO_2Me, CF_3) (0.12 mmol) and complex **1** (2 mg, 3.5 μmol) were dissolved in CD_2Cl_2 (0.4 mL) in a thick-walled J-Young NMR tube with a Teflon screw cap. The tube was cooled in a liquid nitrogen bath, and excess propene (0.60 mmol) was condensed via a vacuum line transfer. The tube was gradually warmed to room temperature, and the sample was inserted into the NMR probe which was preset at 20 °C. The reaction rate was measured by monitoring the ^1H integration of the product signals, which were normalized against an internal standard (solvent resonance) in 5 min intervals. The k_{obs} was estimated from a first-order plot of $-ln([\text{cinnamate}]_t/[\text{cinnamate}]_o)$ vs time.

Reaction in CH_2Cl_2

In a glove box, complex **1** (20 mg, 35 μmol), (*E*)-$C_6H_5CH{=}C(CH_3)CONHCH_3$ (122 mg, 0.7 mmol) and *para*-substituted *p*-

Y-$C_6H_4CH{=}CH_2$ (X = OCH_3, CH_3, H, F, Cl, CF_3) (3.5 mmol) were dissolved in CH_2Cl_2 (6.0 mL) in a 25 mL Schlenk tube equipped with a Teflon stopcock and a magnetic stirring bar. After the solution was stirred at room temperature for 10 min, an equal amount of the solution (1.0 mL) was divided and placed in 5 different Schlenk tubes. The tubes were brought out of the box, and were stirred in an oil bath set at 50 °C. Each reaction tube was taken out from the oil bath in 30 min intervals, and was immediately cooled in a dry ice/acetone bath. After filtering through a small silica gel column (hexanes/EtOAc = 2:1), an internal standard (C_6Me_6) was added, and the resulting solution was analyzed by GC. The k_{obs} was determined from a first-order plot of – $ln([C_6H_5CH{=}C(CH_3)CONHCH_3]_t/[C_6H_5CH{=}C(CH_3)CONHCH_3]_o)$ vs time.

General Procedure for the Erying Analysis

In a glove box, complex **1** (2 mg, 3.5 μmol) and (*E*)-$C_6H_5CH{=}CHCO_2Et$ (20 mg, 0.12 mmol) were dissolved in CD_2Cl_2 (0.5 mL) in a thick-walled J-Young NMR tube with a Teflon screw cap. The tube was brought out of the box, and cooled in a liquid nitrogen bath. Excess propene (0.60 mmol) was condensed via a vacuum line transfer. After the tube was gradually warmed to room temperature, the sample tube was inserted into the NMR probe which was preset at 20–40 °C. The rate was measured by monitoring the ^1H integration of the product signals in 5 min intervals, and these were normalized against an internal standard (solvent resonance). The k_{obs} was estimated from a first-order plot of – $ln([C_6H_5CH{=}CHCO_2Et]_t/[C_6H_5CH{=}CHCO_2Et]_o)$ vs time.

Acknowledgments

Financial support from the National Science Foundation (CHE-1011891) and the National Institute of Health General Medical Sciences (R15 GM55987) is gratefully acknowledged.

Footnotes

Supporting Information Available: Experimental procedures and spectroscopic data of organic products (39 pages, print/PDF). This material is available free of charge via the Internet at http//:pubs.acs.org.

References

[1] Anastas PT, Kirchhoff MM. Acc Chem Res. 2002;35:686–694. **(b)** Sheldon RA, Arends IWCE, Hanefeld U. Green Chemistry and Catalysis. Wiley-VCH; Weinheim: 2007. **(c)** Anastas PT, editor. Green Catalysis; Homogeneous Catalysis. Vol. 1 Wiley-VCH; Weinheim: 2009.

[2] Recent reviews on Wittig-type olefination methods: **(a)** Maryanoff BE, Reitz AB. Chem Rev. 1989;89:863–927.**(b)** Cristau HJ. Chem Rev. 1994;94:1299–1313.**(c)** Shen Y. Acc Chem Res. 1998;31:584–592.

[3] Recent reviews: **(a)** Flynn AB, Ogilvie WW. Chem Rev. 2007;107:4698–4745.**(b)** Arai T, Suemitsu Y. Pure Appl Chem. 2010;82:1458–1490.

[4] **(a)** Negishi E, Huang Z, Wang G, Mohan S, Wang C, Hattori H. Acc Chem Res. 2008;41:1474–1485. and the references cited therein.**(b)** Itami K, Kamei T, Yoshida J. J Am Chem Soc. 2003;125:14670–14671.**(c)** Zhou C, Larock RC. J Org Chem. 2005;70:3765–3777.**(d)** Zhou C, Larock RC. J Org Chem. 2006;71:3184–3191. **(e)** McKinley NF, O'Shea DF. J Org Chem. 2006;71:9552–9555.

[5] **(a)** Itami K, Kamei T, Yoshida JI. J Am Chem Soc. 2003;125:14670–14671. **(b)** Lemay AB, Vulic KS, Ogilvie WW. J Org Chem. 2006;71:3615–3618. **(c)** Hojo D, Noguchi K, Tanaka K. Angew Chem, Int Ed. 2009;48:8129–8132. **(d)** Ni Y, Kassab RM, Chevliakov MV, Montgomery J. J Am Chem Soc. 2009;131:17714–17718.

[6] **(a)** Gansäuer A, Pierobon M, Bluhm H. Angew Chem, Int Ed. 2002;114:3341–3343.**(b)** Berlin JM, Campbell K, Ritter T, Funk TW, Chlenov A, Grubbs RH. Org Lett. 2007;9:1339–1342. **(c)** Vorfalt T, Leuthäußer S, Plenio H. Angew Chem, Int Ed. 2009;48:5191–5194. **(d)** Stenne B, Timperio J, Savoie J, Dudding T, Collins SK. Org Lett. 2010;12:2032–2035. **(e)** Donohoe TJ, Race NJ, Bower JF, Callens CK. Org Lett. 2010;12:4094–4097.

[7] **(a)** Ho CY, Ohmiya H, Jamison TF. Angew Chem, Int Ed. 2008;47:1893–1895. **(b)** Matsubara R, Jamison TF. J Am Chem Soc. 2010;132:6880–6881.

[8] Ogoshi S, Hada T, Ohashi M. J Am Chem Soc. 2009;131:10350–10351.

[9] **(a)** Kakiuchi F, Tanaka Y, Sato T, Chatani N, Murai S. Chem Lett. 1995:679–680.**(b)** Trost BM, Imi K, Davies IW. J Am Chem Soc. 1995;117:5371–5372.**(c)** Sato T, Kakiuchi F, Chatani N, Murai S. Chem Lett. 1998:893–894.**(d)** Jun C-H, Moon CW, Lim Y-M, Lee H, Lee JH. Tetrahedron Lett. 2002:4233–4236.**(e)** Colby DA, Bergman RG, Ellman JA. J Am Chem Soc. 2006;128:5604–5605. **(f)** Ogoshi S, Hada T, Ohashi M. J Am Chem Soc. 2009;131:10350–10351.

[10] Zhao C, Toste FD, Bergman RG. J Am Chem Soc. 2011;133:10787–10789.

[11] **(a)** Wasa M, Engle KM, Yu JQ. J Am Chem Soc. 2010;132:3680–3681. **(b)** Rakshit S, Patureau FW, Glorius F. J Am Chem Soc. 2010;132:9585–9587.

[12] **(a)** Stuart DR, Fagnou K. Science. 2007;317:1172–1175. **(b)** Stuart DR, Villemure E, Fagnou K. J Am Chem Soc. 2007;129:12072–12073. **(c)** Stuart DR, Bertrand-Laperle M, Burgess KMN, Fagnou K. J Am Chem Soc. 2008;130:16474–16475.

[13] Matsuura Y, Tamura M, Kochi T, Sato M, Chatani N, Kakiuchi F. J Am Chem Soc. 2007;129:9858–9859.

[14] **(a)** Patureau FW, Glorius F. J Am Chem Soc. 2010;132:9982–9983. **(b)** Rakshit S, Grohmann C, Besset T, Glorius F. J Am Chem Soc. 2011;133:2350–2353. **(c)** Patureau FW, Besset T, Glorius F. Angew Chem, Int Ed. 2011;50:1064–1067.

[15] **(a)** Giri R, Maugel N, Li JJ, Wang DH, Breazzano SP, Saunders LB, Yu JQ. J Am Chem Soc. 2007;129:3510–3511. **(b)** Giri R, Yu JQ. J Am Chem Soc. 2008;130:14082–14083. **(c)** Zhang YH, Shi BF, Yu JQ. J Am Chem Soc. 2009;131:5072–5074. **(d)** Shi BF, Zhang YH, Lam JK, Wang DH, Yu JQ. J Am Chem Soc. 2010;132:460–461. **(e)** Lu Y, Wang DH, Engle KM, Yu JQ. J Am Chem Soc. 2010;132:5916–5921. **(f)** Engle KM, Wang DH, Yu JQ. J Am Chem Soc. 2010;132:14137–14151. **(g)** Ye M, Gao GL, Yu JQ. J Am Chem Soc. 2011;133:6964–6967.

[16] **(a)** Weissman H, Song X, Milstein D. J Am Chem Soc. 2001;123:337–338. **(b)** Yokota T, Tani M, Sakaguchi S, Ishii Y. J Am Chem Soc. 2003;125:1476–1477.

[17] **(a)** Umeda N, Tsurugi H, Satoh T, Miura M. Angew Chem, Int Ed. 2008;47:4019–4021.**(b)** Wang F, Song G, Li X. Org Lett. 2010;12:5430–5433. **(c)** Su Y, Zhao M, Han K, Guoyong Song G, Xingwei Li X. Org Lett. 2010;12:5462–5465. **(d)** Ueyama T, Mochida S, Fukutani T, Hirano K, Satoh T, Miura M. Org Lett. 2011;13:706–708. **(e)** Tsai AS, Brasse M, Bergman RG, Ellman JA. Org Lett. 2011;13:540–542. **(f)** Zhu C, Falck JR. Org Lett. 2011;13:1214–1217. **(g)** Park SH, Kim JY, Chang S. Org Lett. 2011;13:2372–2375. **(h)** Yu M, Liang Z, Wang Y, Zhang Y. J Org Chem. 2011;76:4987–4994. **(i)** Pintori DG, Greaney MF. J Am Chem Soc. 2011;133:1209–1211. **(j)** Huang C, Chattopadhyay B, Gevorgyan V. J Am Chem Soc. 2011;133:12406–12409.

[18] **(a)** Ackermann L, Althammer A, Born R. Synlett. 2007:2833–2836.**(b)** Ackermann L, Vicente R, Potukuchi HK, Pirovano V. Org Lett. 2010;12:5032–5035. **(c)** Ackermann L, Lygin AV, Hofmann N. Org Lett. 2011;13:3278–3281. **(d)** Ackermann L, Pospech J. Org Lett. 2011;13:4153–4155.

[19] Recent reviews: **(e)** Beccalli EM, Broggini G, Martinelli M, Sottocornola S. Chem Rev. 2007;107:5318–5365. **(b)** Colby DA, Bergman RG, Ellman JA. Chem Rev. 2010;110:624–655.

[20] **(a)** Wasa M, Engle KM, Yu JQ. J Am Chem Soc. 2010;132:3680–3681. **(b)** Yoo EJ, Wasa M, Yu JQ. J Am Chem Soc. 2010;132:17378–17380.

[21] **(a)** Yi CS, Lee DW. Organometallics. 2009;28:4266–4268. **(b)** Yi CS, Lee DW. Organometallics. 2010;29:1883–1885. **(c)** Kwon KH, Lee DW, Yi CS. Organometallics. 2010;29:5748–5750.

[22] **(a)** Kakiuchi F, Murai S. In: Activation of Unreactive Bonds and Organic Synthesis. Murai S, editor. Springer; New York: 1999. **(b)** Kakiuchi F. In: Topics in Organometallic Chemistry. Chatani N, editor. Vol. 24. Springer; Berlin: 2007. pp. 1–33.

[23] Kwon KH, Lee DW, Yi CS. Angew Chem, Int Ed. 2011;50:1692–1695.

[24] We followed the procedures described in: **(a)** Liu L, Zhang Y, Xin B. J Org Chem. 2006;71:3994–3997. **(b)** Lee DH, Jung JY, Lee IM, Jin MJ. Eur J Org Chem. 2008;73:356–360.

[25] Lee DW, Yi CS. Organometallics. 2010;29:3413–3417.

[26] Selected recent reviews on the synthesis and usage of indene and fulvene derivatives: **(a)** Gao H, Katzenellenbogen JA, Garg R, Hansch C. Chem Rev. 1999;99:723–744. **(b)** Strohfeldt K, Tacke M. Chem Soc Rev. 2008;37:1174–1187. **(c)** Guo LN, Duan XH, Liang YM. Acc Chem Res. 2011;44:111–122.

[27] **(a)** Tang J-M, Bhunia S, Sohel SMA, Lin M-Y, Liao H-Y, Datta S, Das A, Liu R-S. J Am Chem Soc. 2007;129:15677–15683. **(b)** Patureau FW, Besset T, Kuhl N, Glorius F. J Am Chem Soc. 2011;133:2154–2156.

[28] **(a)** Singleton DA, Thomas AA. J Am Chem Soc. 1995;117:9357–9358.**(b)** Frantz DE, Singleton DA, Snyder JP. J Am Chem Soc. 1997;119:3383–3384.

[29] **(a)** Anslyn EV, Dougherty DA. Modern Physical Organic Chemistry. University Science Books; Sausalito, CA: 2006. **(b)** Isaacs NS. Physical Organic Chemistry. Longman Scientific; Harlow: 1995.

[30] **(a)** Bernasconi CF, Renfrow RA, Tia PR. J Am Chem Soc. 1986;108:4541–4549.**(b)** Oh HK, Kim IK, Lee HW, Lee I. J Org Chem. 2004;69:3806–3810. **(c)** Weston MH, Nakajima K, Back TG. J Org Chem. 2008;73:4630–4637.

[31] Hartwig JF. Organotransition Metal Chemistry: From Bonding to Catalysis. Chapter 15 University Science Books; Sausalito, CA: 2010.

[32] For a recent example of σ-bond metathesis mechanism in C–H activation reactions, see: Foley NA, Lee JP, Ke Z, Gunnoe TB, Cundari TR. Acc Chem Res. 2009;42:585–597.

[33] **(a)** Kakiuchi F, Murai S. Acc Chem Res. 2002;35:826–834. **(b)** Kakiuchi F, Kochi T, Mizushima E, Murai S. J Am Chem Soc. 2010;132:17741–17750.

Supplementary Material

Supporting Information

Scope and Mechanistic Study of the Coupling Reaction of α,β-Unsaturated Carbonyl Compounds with Alkenes: Uncovering Electronic Effects on Alkene Insertion vs Oxidative Coupling Pathways

Ki-Hyeok Kwon, Do W. Lee and Chae S. Yi*

Department of Chemistry, Marquette University, Milwaukee, Wisconsin 53201-1881

Table of Contents

General Information. All operations were carried out in an inert-atmosphere glove box or by using standard high vacuum and Schlenk techniques unless otherwise noted. Tetrahydrofuran, benzene, hexanes and Et_2O were distilled from purple solutions of sodium and benzophenone immediately prior to use. The NMR solvents were dried from activated molecular sieves (4 Å). All organic substrates were received from commercial sources and used without further purification. The ^{1}H, ^{2}H, ^{13}C and ^{31}P NMR spectra were recorded on a Varian 300 or 400 MHz FT-NMR spectrometer. Mass spectra were recorded from a Agilent 6850 GC/MS spectrometer. The conversion of organic products was measured from a Hewlett-Packard HP 6890 GC spectrometer. FT-IR spectra were recorded on Perkin Elmer Spectrum 100. High-resolution mass spectra (EI) were obtained at the Center of Mass Spectrometry, Washington University, St. Louis, MO. Elemental analyses were performed at the Midwest Microlab, Indianapolis, IN.

Scheme S1. Representative Experimental Procedure for the Synthesis of Intramolecular Carbonyl Substrates.

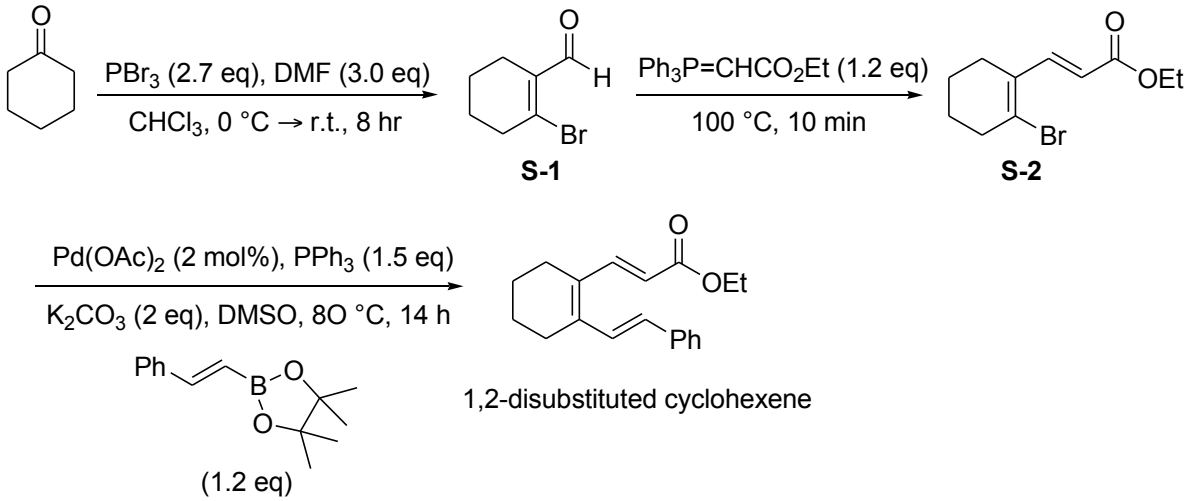

Synthesis of 2-bromo-cyclohex-1-enecarbaldehyde (S-1).[S1] In a 100 mL round bottom flask, PBr_3 (6.9 mL, 69 mmol) was added dropwise at 0 °C to a solution of DMF (5.9 mL, 76 mmol) and chloroform (25 mL), and the mixture was stirred for 2 h. Cyclohexanone (2.5 g, 26 mmol) was added to the reaction mixture, and the resulting solution was stirred for 8 h at room temperature. The solution was poured into a 150 mL water, neutralized with solid $NaHCO_3$, and the resulting mixture was extracted with CH_2Cl_2 (3 × 100 mL). The extract was washed with a

saturated brine solution, dried over anhydrous $MgSO_4$, and the solvent was removed under a reduced pressure. The residue was purified by column chromatography (*n*-hexanes:Et_2OAc = 20:1) on silica gel to afford the product **S-1** (3.8 g, 81% yield).

Synthesis of ethyl 3-(2'-bromocyclohex-1'-enyl)acrylate (S-2).[S2] In a 25 mL round bottom flask, **S1** (1.3 g, 6.9 mmol) and $Ph_3P{=}CHCO_2Et$ (3.0 g, 8.6 mmol) were heated at 100 °C for 10 min under neat condition. The resulting mixture was purified by column chromatography on silica gel (*n*-hexanes:Et_2OAc = 4:1) to yield compound **S-2** (1.6 g, 90% yield).

Synthesis of ethyl 3-(*trans*-2-styrylcyclohexen-l-yl)-*trans*-propene (S-3).[S3] In a 25 mL round bottom flask, a mixture of K_2CO_3 (0.28 g, 2.0 mmol), $Pd(OAc)_2$ (4 mg, 2 mol %), compound **S-2** (0.26 g, 1 mmol), *trans*-β-styrylboronic acid pinacol ester (0.28 g, 1.2 mmol) in DMSO (5 mL) was stirred for 14 h at 80 °C. The resulting solution was extracted with Et_2O (3 × 10 mL). The combined organic layer was washed with a saturated brine solution and removed the solvent under a reduced pressure. The residue was purified by column chromatography on silica gel (*n*-hexanes:Et_2OAc = 40:1 to 10:1) to give the product **S-3** (0.17 g, 60% yield).

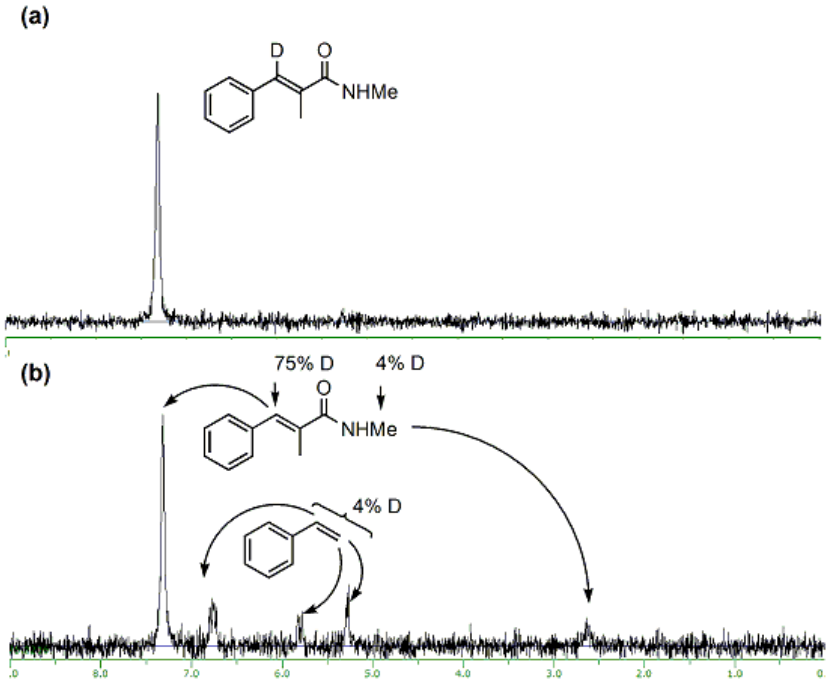

Figure S1: (a) ^2H NMR Spectrum of (*E*)-$C_6H_5CD{=}C(CH_3)CONHCH_3$, (b) ^2H NMR Spectrum of the Reaction Mixture of (*E*)-$C_6H_5CD{=}C(CH_3)CONHCH_3$ with Styrene.

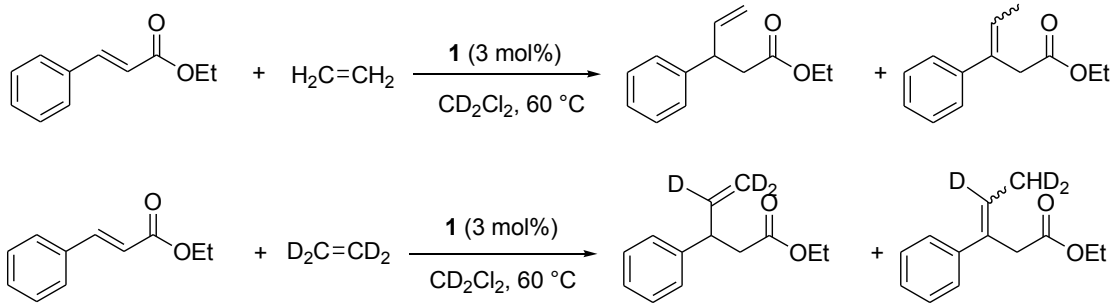

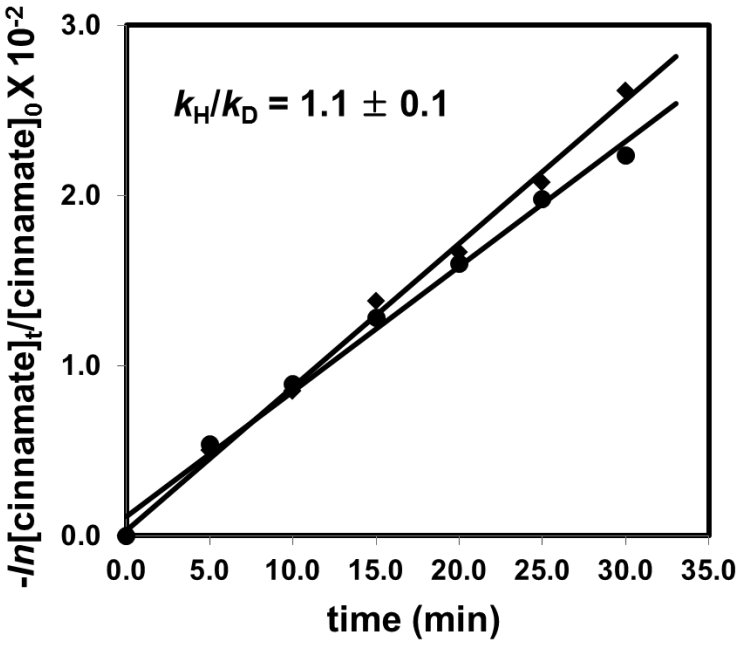

Figure S2. First-Order Plots of $-ln[\text{cinnamate}]_t/[\text{cinnamate}]_0$ vs Time for the Coupling Reaction of (*E*)-$C_6H_5CH{=}CHCO_2Et$ with Ethylene (◆) and Ethylene-d_4 (●).

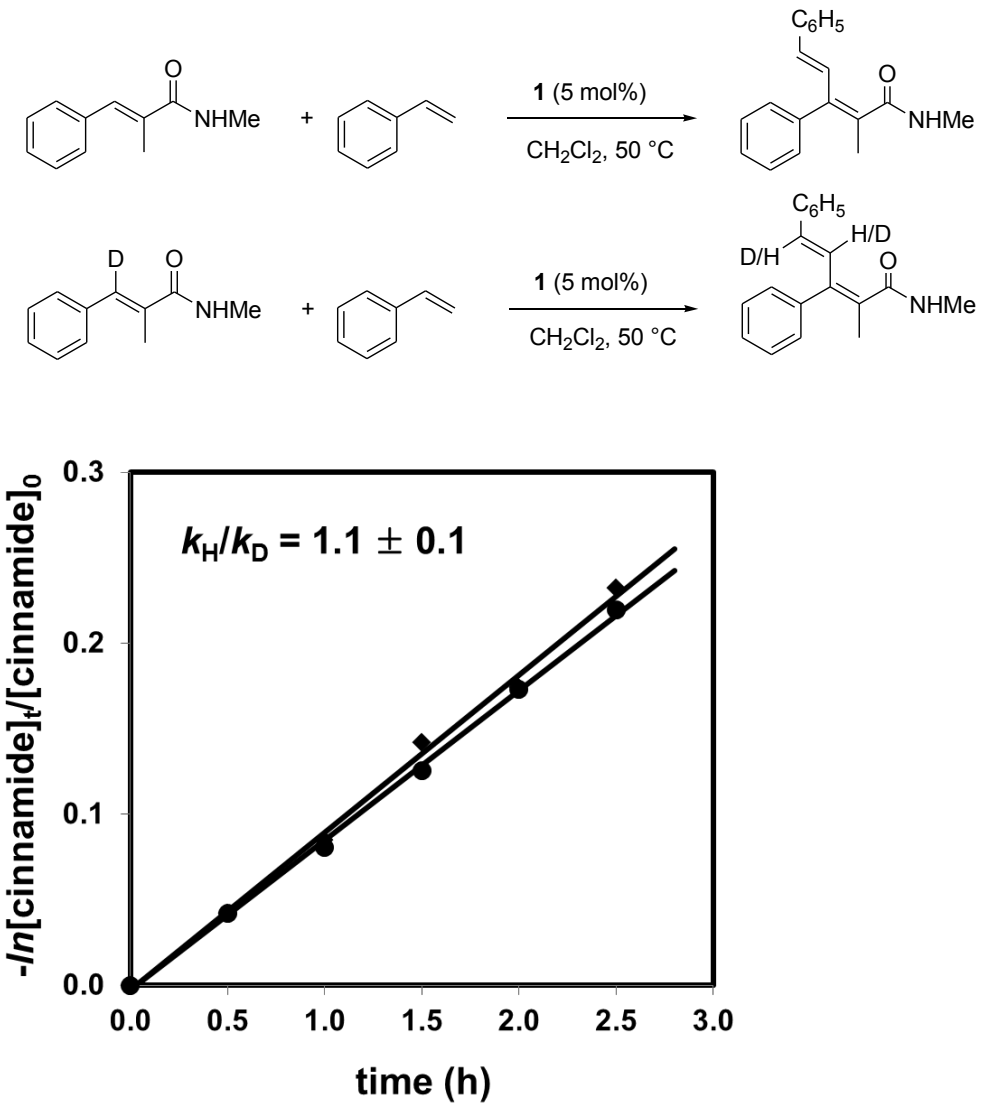

Figure S3. First-Order Plots of $-ln([\text{cinnamide}]_t/[\text{cinnamide}]_0)$ vs Time for the Coupling Reaction of (*E*)-$C_6H_5CH{=}C(CH_3)CONHMe$ (◆) and (*E*)-$C_6H_5CD{=}C(CH_3)CONHMe$ (●) with Styrene.

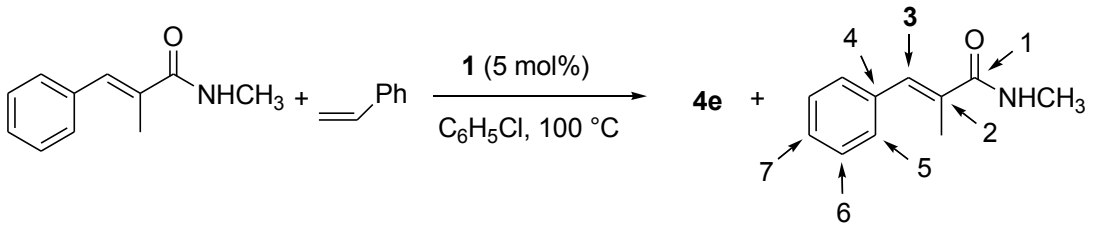

Table S1. Average ^{13}C KIEs of the Recovered and Virgin Sample of (*E*)-$C_6H_5CH{=}C(CH_3)CONHCH_3$ using Singleton's Method.

C #	virgin (4[a])	average ^{13}C integation (6[a])	R/R_o	KIE
1	1.0440(35)	1.0430(48)	0.999(6)	0.999(5)
2	1.0312(37)	1.0312(51)	1.000(6)	1.000(6)
3	**1.0073(24)**	**1.0067(32)**	**0.999(4)**	**0.999(4)**
4	0.9348(19)	0.9342(34)	1.002(4)	1.001(3)
5	2.0168(28)	2.0158(39)	0.999(4)	0.999(2)
6	2.1168(36)	2.1167(52)	1.000(3)	1.000(3)
7(ref)	1.0000	1.0000	1.000	1.000

[a] The total number of spectra obtained from 2 samples.

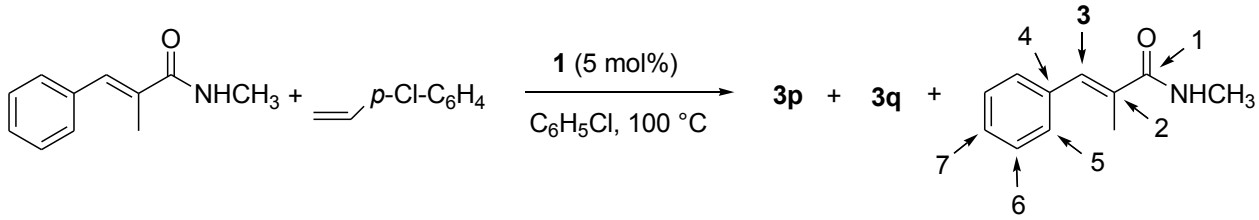

Table S2. Average ^{13}C KIEs of the Recovered and Virgin Sample of (*E*)-$C_6H_5CH{=}C(CH_3)CONHCH_3$ using Singleton's Method.

C #	virgin (4[a])	average ^{13}C integation (6[a])	R/R_o	KIE
1	1.0440(35)	1.0438(46)	0.999(6)	0.999(5)
2	1.0312(37)	1.0317(36)	1.000(5)	1.000(4)
3	**1.0073(24)**	**1.0352(76)**	**1.028(8)**	**1.017(7)**
4	0.9348(19)	0.9347(31)	1.000(4)	1.001(3)
5	2.0168(28)	2.0169(36)	0.999(2)	1.000(3)
6	2.1168(36)	2.1157(52)	1.002(3)	1.001(4)
7(ref)	1.0000	1.0000	1.000	1.000

[a] The total number of spectra obtained from 2 samples.

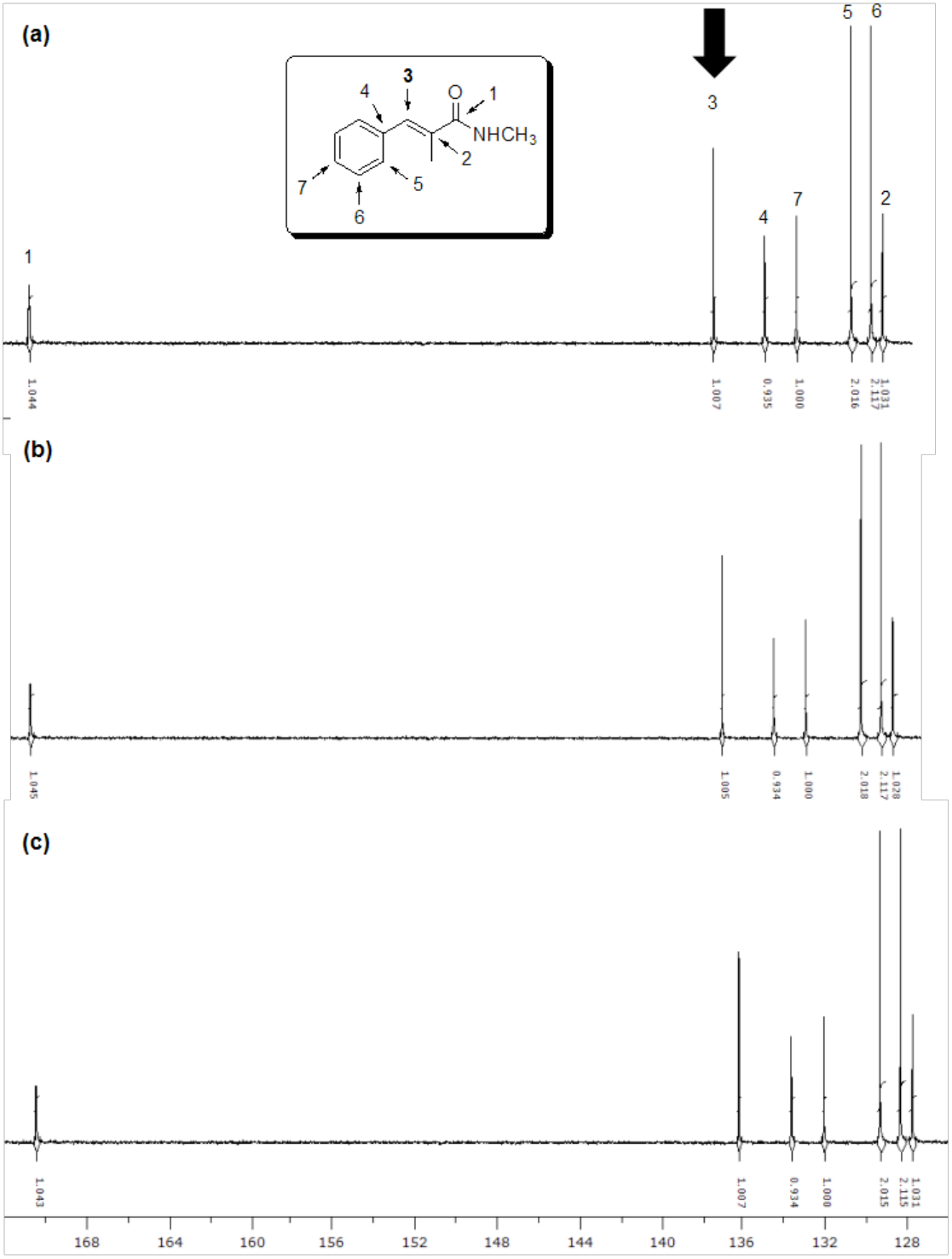

Figure S4. (a) ^{13}C NMR Spectrum of Virgin Sample of (*E*)-$C_6H_5CH{=}C(CH_3)CONHCH_3$. (b) ^{13}C NMR Spectrum of Recovered (*E*)-$C_6H_5CH{=}C(CH_3)CONHCH_3$ from the Coupling Reaction with Styrene at 68% conversion. (c) ^{13}C NMR Spectrum of Recovered (*E*)-$C_6H_5CH{=}C(CH_3)CONHCH_3$ from the Coupling Reaction with Styrene at 72% conversion.

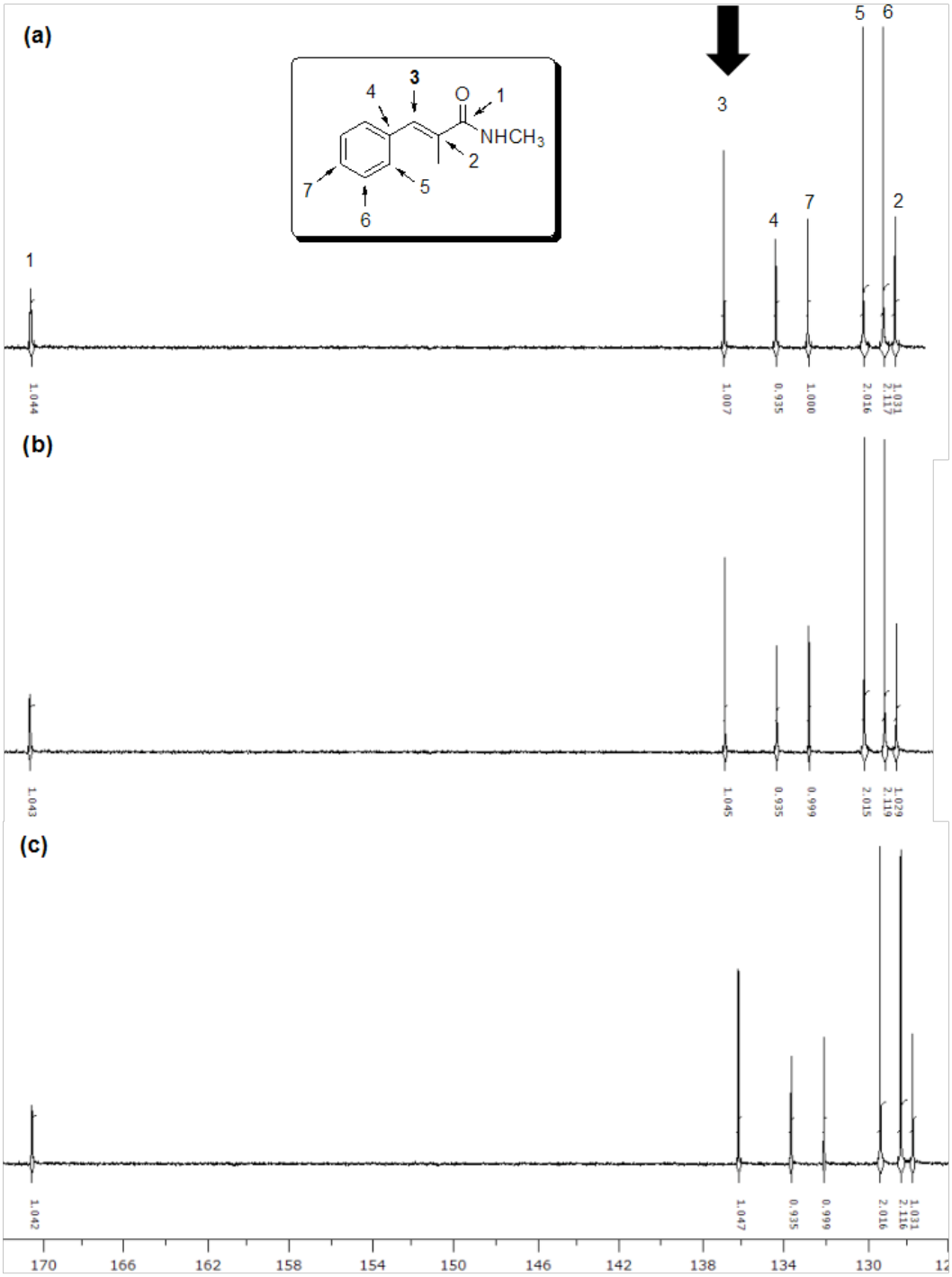

Figure S5. (a) ^{13}C NMR Spectrum of Virgin Sample of (*E*)-$C_6H_5CH{=}C(CH_3)CONHCH_3$ (b) ^{13}C NMR Spectrum of Recovered (*E*)-$C_6H_5CH{=}C(CH_3)CONHCH_3$ from the Coupling Reaction with 4-Chlorostyrene at 80% Conversion. (c) ^{13}C NMR Spectrum of Recovered (*E*)-$C_6H_5CH{=}C(CH_3)CONHCH_3$ from the Coupling Reaction with 4-Chlorostyrene at 82% Conversion.

Characterization Data of Organic Products.

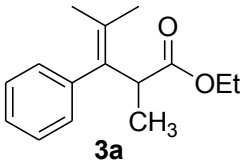

3a

For **3a**: ^{1}H NMR (400 MHz, $CDCl_3$) δ 7.3-7.0 (m, 4H), 4.07 (m, 2H), 3.80 (q, *J* = 7.1 Hz, 1H), 1.87 (s, 3H), 1.49 (s, 3H), 1.20 (t, *J* = 7.1 Hz, 3H), 1.15 (d, *J* = 7.1 Hz, 3H) ppm; ^{13}C{^{1}H} NMR (100 MHz, $CDCl_3$) δ 174.7, 141.0, 134.0, 131.0, 129.7, 127.9, 126.5, 60.5, 42.8, 22.7, 20.3, 15.9, 14.1 ppm; GC-MS *m/z* = 232 (M^+); Anal. Calcd for $C_{15}H_{20}O_2$: C, 77.55; H, 8.68. Found: C, 77.09; H, 8.62.

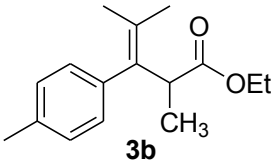

3b

For **3b**: ^{1}H NMR (400 MHz, $CDCl_3$) δ 7.1-6.9 (m, 4H), 4.08 (m, 2H), 3.80 (q, *J* = 7.1 Hz, 1H), 2.34 (s, 3H), 1.88 (s, 3H), 1.51 (s, 3H), 1.24 (t, *J* = 7.2 Hz, 3H) 1.16 (d, *J* = 7.1 Hz, 3H) ppm; ^{13}C{^{1}H} NMR (100 MHz, $CDCl_3$) δ 174.8, 137.9, 135.8, 133.9, 130.9, 129.5, 128.7, 60.5, 42.8, 22.8, 21.3, 20.3, 15.9, 14.2 ppm; GC-MS *m/z* = 246 (M^+); Anal. Calcd for $C_{16}H_{22}O_2$: C, 78.01; H, 9.00. Found: C, 77.75; H, 8.94.

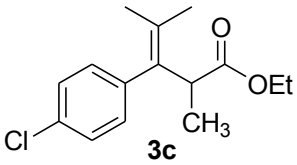

3c

For **3c**: ^{1}H NMR (400 MHz, $CDCl_3$) δ 7.2-6.9 (m, 4H), 4.05 (m, 2H), 3.77 (q, *J* = 7.1 Hz, 1H), 1.84 (s, 3H), 1.45 (s, 3H), 1.18 (t, *J* = 7.1 Hz, 3H) 1.09 (d, *J* = 7.1 Hz, 3H) ppm; ^{13}C{^{1}H} NMR (100 MHz, $CDCl_3$) δ 174.5, 139.3, 132.8, 132.4, 131.9, 131.1, 128.1, 60.5, 42.5, 22.7, 20.3, 15.9, 14.2 ppm; GC-MS *m/z* = 266 (M^+); Anal. Calcd for $C_{15}H_{19}ClO_2$: C, 67.54; H, 7.18. Found: C, 67.64; H, 7.20.

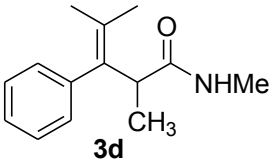

3d

For **3d**: ^{1}H NMR (400 MHz, $CDCl_3$) δ 7.2-6.9 (m, 5H), 5.88 (br, 1H), 3.62 (q, *J* = 7.2 Hz, 1H), 2.66 (d, *J* = 4.8 Hz, 3H), 1.79 (s, 3H), 1.43 (s, 3H), 1.01 (d, *J* = 7.2 Hz, 3H) ppm; ^{13}C{^{1}H} NMR (100 MHz, $CDCl_3$) δ 174.4, 140.5, 135.1, 131.2, 129.2, 127.7, 126.2, 43.2, 26,2, 22.6, 21.2, 15.4 ppm; GC-MS *m/z* = 217 (M^+); Anal. Calcd for $C_{14}H_{19}NO$: C, 76.38; H, 8.81. Found: C, 77.17; H, 8.73.

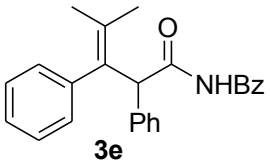

3e

For **3e**: ^{1}H NMR (400 MHz, $CDCl_3$) δ 7.2-6.8 (m, 15H), 6.01 (t, *J* = 5.8 Hz, 1H), 4.89 (s, 1H), 4.13 (dd, *J* = 6.0, 5.2 Hz, 2H), 1.71 (s, 3H), 1.43 (s, 3H) ppm; ^{13}C{^{1}H} NMR (100 MHz, $CDCl_3$) δ 172.1, 141.5, 138.3, 138.2, 133.5, 133.0, 130.1, 129.6, 128.6, 128.4, 127.8, 127.7, 127.0, 126.3, 57.5, 43.7, 23.2, 21.1 ppm; GC-MS *m/z* = 355 (M^+); HRMS (*m/z*): Calcd for $C_{25}H_{24}NO$ $(M-H)^+$, 354.1849. Found $(M-H)^+$, 354.1852.

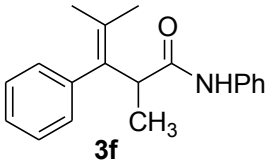

3f

For **3f**: ^{1}H NMR (400 MHz, $CDCl_3$) δ 7.47 (br, 1H), 7.4-6.9 (m, 10H), 3.79 (q, *J* = 7.0 Hz, 1H), 1.90 (s, 3H), 1.53 (s, 3H), 1.10 (d, *J* = 7.0 Hz, 3H) ppm; ^{13}C{^{1}H} NMR (100 MHz, $CDCl_3$) δ 172.1, 140.4, 138.1, 135.4, 132.8, 129.4, 129.2, 128.4, 126.9, 124.3, 119.9, 44.9, 23.1, 20.7, 15.5 ppm; GC-MS *m/z* = 279 (M^+); Anal. Calcd for $C_{19}H_{21}NO$: C, 81.68; H, 7.58. Found: C, 81.97; H, 7.71.

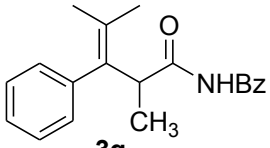

3g

For **3g**: ^{1}H NMR (400 MHz, $CDCl_3$) 7.2-6.8 (m, 10H), 6.15 (t, *J* = 5.5 Hz, 1H), 4.27 (dd, *J* = 5.9, 2.6 Hz, 2H), 3.62 (q, *J* = 7.2 Hz, 1H), 1.75 (s, 3H), 1.39 (s, 3H), 1.01 (d, *J* = 7.2 Hz, 3H) ppm; ^{13}C{^{1}H} NMR (100 MHz, $CDCl_3$) δ 173.7, 140.6, 138.6 135.1, 132.0, 129.4, 128.6, 127.9, 127.8, 127.3, 126.4, 43.6, 22.7, 20.4, 15.6 ppm; GC-MS *m/z* = 293 (M^+); Anal. Calcd for $C_{20}H_{23}NO$: C, 81.87; H, 7.90. Found: C, 81.66; H, 7.78.

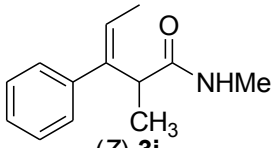

(*Z*)-**3i**

For (*Z*)**-3i**: ^{1}H NMR (400 MHz, $CDCl_3$) δ 7.4-7.1 (m, 5H), 5.99 (s, 1H), 5.81 (q, *J* = 6.8 Hz, 1H), 3.31 (q, *J* = 7.0 Hz, 1H), 2.71 (d, *J* = 4.9 Hz, 3H), 1.62 (d, *J* = 6.8 Hz, 3H), 1.32 (d, *J* = 7.0 Hz, 3H,) ppm: NOESY δ 3.31 ↔ 1.62 ppm (↔ denotes NOE correlation); ^{13}C{^{1}H} NMR (100 MHz, $CDCl_3$) δ 174.7, 141.7, 139.6, 128.7, 127.3, 126.9, 124.0, 49.3, 26.4, 16.4, 15.0 ppm; GC-MS *m/z* = 203 (M^+); Anal. Calcd for $C_{13}H_{17}NO$: C, 76.81; H, 8.43. Found: C, 76.76; H, 8.27.

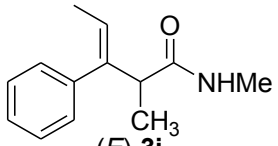

(*E*)-**3i**

For (*E*)-**3i**: ^{1}H NMR (400 MHz, $CDCl_3$) δ 7.4-7.1 (m, 5H), 5.86 (s, 1H), 5.83 (q, *J* = 6.8 Hz, 1H), 3.30 (q, *J* = 7.0 Hz, 1H), 2.78 (d, *J* = 4.9 Hz, 3H), 1.63 (d, *J* = 6.8 Hz, 3H), 1.29 (d, *J* = 7.0 Hz, 3H) ppm: NOESY δ 5.83 ↔1.63 ppm (↔ denotes NOE correlation); ^{13}C{^{1}H} NMR (100 MHz, $CDCl_3$) δ 174.7, 141.8, 139.6, 128.8, 127.3, 127.0, 124.1, 49.4, 26.5, 16.4, 15.0 ppm; GC-MS *m/z* = 203 (M^+); Anal. Calcd for $C_{13}H_{17}NO$: C, 76.81; H, 8.43. Found: C, 76.60; H, 8.27.

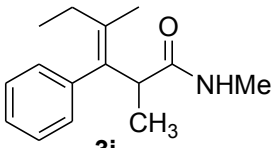

3j

For **3j**: ^{1}H NMR (400 MHz, $CDCl_3$) δ 7.2-6.9 (m, 5H), 5.72 (br, 1H), 3.59 (q, *J* = 7.1 Hz, 1H), 2.71 (d, *J* = 4.8 Hz, 3H), 1.82 (s, 3H), 1.75 (q, *J* = 7.5 Hz, 2H), 1.01 (d, *J* = 7.1 Hz, 3H), 0.84 (t, *J* = 7.5 Hz, 3H) ppm; NOESY δ 7.24 ↔ 0.84, 3.59 ↔ 1.82 ppm (↔ denotes NOE correlation); ^{13}C{^{1}H} NMR (100 MHz, $CDCl_3$) δ 174.4, 140.4, 137.3, 137.3, 135.3, 129.3, 128.2, 126.6, 43.0, 29.2, 26.6, 17.6, 15.5, 13.3 ppm; GC-MS *m/z* = 231 (M^+); HRMS Calcd for $C_{15}H_{22}NO$ $(M+H)^+$, 232.1700; Found: 232.1696.

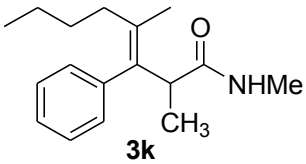

3k

For **3k**: ^{1}H NMR (400 MHz, $CDCl_3$) δ 7.3-7.0 (m, 5H), 5.78 (br, 1H), 3.66 (q, *J* = 7.2 Hz, 1H), 2.78 (d, *J* = 4.9 Hz, 3H), 1. 86 (s, 3H), 1.82 (m, 2H), 1.30 (m, 2H), 1.11 (m, 2H,), 1.06 (d, *J* = 7.2 Hz, 3H, CHCH_3), 0.75 (t, *J* = 7.5 Hz, 3H) ppm; NOESY δ 3.66 ↔1.86 ppm (↔ denotes NOE correlation); ^{13}C{^{1}H} NMR (100 MHz, $CDCl_3$) δ 174.4, 140.5, 136.1, 135.8, 129.5, 128.4, 128.0, 126.6, 43.8, 35.8, 30.7, 26.6, 22.7, 18.1, 15.6, 14.1 ppm; GC-MS *m/z* = 259; Anal. Calcd for $C_{17}H_{25}NO$: C, 78.72; H, 9.71. Found: C, 78.84; H, 9.55.

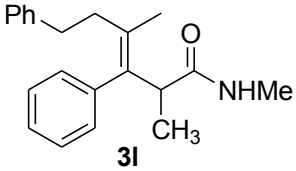

3l

For **3l**: ^{1}H NMR (400 MHz, $CDCl_3$) δ 7.2-6.8 (m, 10H), 5.48 (br, 1H), 3.59 (q, *J* = 7.0 Hz, 1H), 2.67 (t, *J* = 7.4 Hz, 2H), 2.64 (d, *J* = 4.8 Hz, 3H), 2.33 (m, 1H), 2.16 (m, 1H), 1.89 (s, 3H, CH_3), 1.01 (d, *J* = 7.0 Hz, 3H) ppm; NOESY δ 3.59 ↔1.87 ppm (↔ denotes NOE correlation); ^{13}C{^{1}H} NMR (100 MHz, $CDCl_3$) δ 174.1, 141.5, 140.1, 136.1, 131.0, 129.4, 128.6, 128.3, 128.0, 126.7, 126.1, 43.0, 37.0, 34.0, 26.6, 17.8, 15.3 ppm; GC-MS *m/z*: 307; Anal. Calcd for $C_{21}H_{25}NO$: C, 82.04; H, 8.20. Found: C, 81.65; H, 8.03.

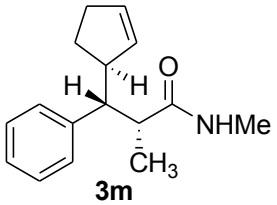

3m

For **3m**: ^{1}H NMR (400 MHz, $CDCl_3$) δ 7.3-7.1 (m, 5H), 6.61 (br, 1H), 5.71 (m, 1H), 5.69 (m, 1H), 3.14 (m, 1H), 2.97 (dd, *J* = 9.9, 9.8 Hz, 1H), 2.85 (d, *J* = 4.8 Hz, 3H), 2.72 (m, 1H), 2.10 (m, 1H), 2.01 (m, 1H), 1.83 (m, 1H), 1.51 (m, 1H), 0.94 (d, *J* = 6.8 Hz, 3H) ppm; NOESY δ 7.17 ↔ 1.83, 7.17 ↔ 1.51 ppm (↔ denotes NOE correlation); ^{13}C{^{1}H} NMR (100 MHz, $CDCl_3$) δ 177.1, 140.8, 132.5, 132.2, 129.6, 127.9, 126.3, 53.6, 48.8, 45.2, 32.0, 28.4, 26.4, 16.6 ppm; GC-MS *m/z* = 243 (M^+); HRMS (*m/z*): calcd for $C_{16}H_{22}NO$ $(M+H)^+$, 244.1705; Found: 244.1696.

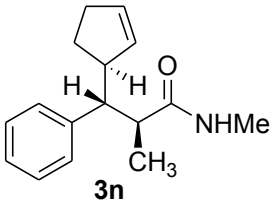

3n

For **3n**: ^{1}H NMR (400 MHz, $CDCl_3$) δ 7.3-7.1 (m, 5H), 6.16 (br, 1H), 5.66 (m, 1H), 5.58 (m, 1H), 3.13 (m, 1H), 3.05 (dd, *J* = 9.9, 4.8 Hz, 1H), 2.79 (d, *J* = 4.8 Hz), 2.76 (m, 1H), 2.10 (m, 1H), 2.01 (m, 1H), 1.81 (m, 1H), 1.53 (m, 1H), 0.96 (d, *J* = 7.2 Hz, 3H) ppm; NOESY δ 7.17 ↔1.81, 7.17↔1.53 ppm (↔ denotes NOE correlation); ^{13}C{^{1}H} NMR (100 MHz, $CDCl_3$) δ 176.8, 141.8, 130.1, 130.0, 129.1, 128.2, 126.4, 53.5, 45.7, 45.1, 37.9, 37.0, 31.7, 15.0 ppm; GC-MS *m/z* = 243 (M^+); HRMS (*m/z*): calcd for $C_{16}H_{22}NO$ $(M+H)^+$, 244.1705; Found: 244.1696.

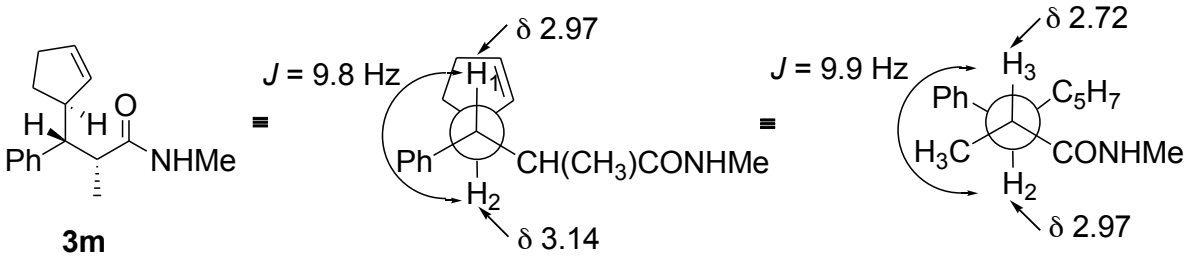

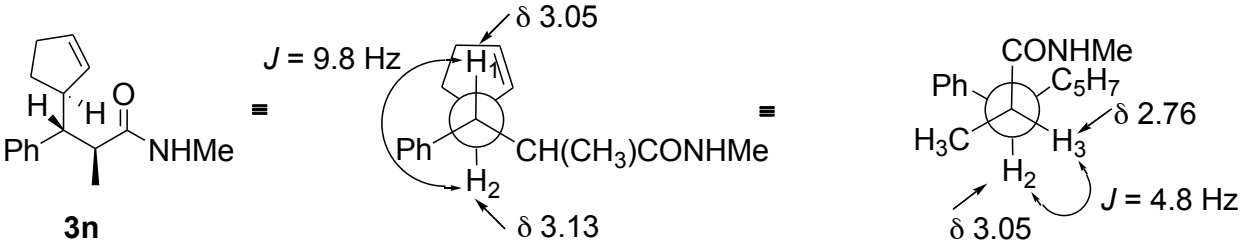

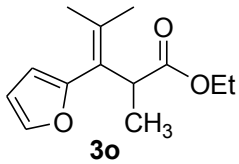

3o

For **3o**: ^{1}H NMR (400 MHz, $CDCl_3$) δ 7.30 (dd, *J* = 1.8, 1.1 Hz, 1H), 6.32 (dd, *J* = 3.2, 1.8 Hz, 1H), 6.10 (dd, *J* = 3.2, 0.8 Hz, 1H), 4.10 (m, 2H), 3.74 (q, J = 7.1 Hz, 1H), 1.87 (s, 3H), 1.80 (s, 3H), 1.22 (d, *J* = 7.1 Hz, 3H),

1.15 (t, J = 7.1 Hz, 3H) ppm; $^{13}C\{^1H\}$ NMR (100 MHz, $CDCl_3$) δ 174.6, 152.9, 140.7, 135.7, 125.2, 110.3, 108.5, 60.5, 41.8, 23.3, 22.1, 15.7, 14.73 ppm; GC-MS m/z = 222 (M^+); Anal. Calcd for $C_{13}H_{18}O_3$: C, 70.24; H, 8.16. Found: C, 70.45; H, 7.97.

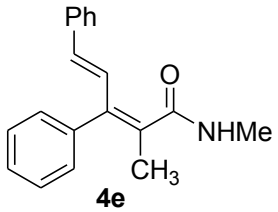

4e

For **4e**: ^1H NMR (400 MHz, $CDCl_3$) δ 7.4-7.1 (m, 10H), 7.32 (d, J = 15.9 Hz, 1H), 6.02 (d, J = 15.9 Hz, 1H), 5.97 (br, 1H), 3.00 (d, J = 4.9 Hz, 3H), 1.79 (s, 3H) ppm; $^{13}C\{^1H\}$ NMR (100 MHz, $CDCl_3$) δ 172.2, 140.4, 138.2, 137.2, 133.7, 133.3, 129.5, 128.7, 128.6, 128.3, 127.9, 127.5, 126.8, 26.6, 18.6 ppm; GC-MS m/z = 277 (M^+); Anal. Calcd for $C_{19}H_{19}NO$: C, 82.28; H, 6.90. Found: C, 81.98; H, 7.04.

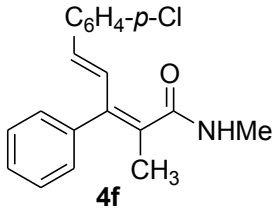

4f

For **4f**: ^1H NMR (400 MHz, $CDCl_3$) δ 7.4-7.1 (m, 9H), 7.31 (d, J = 15.8 Hz, 1H), 5.96 (d, J = 15.9 Hz, 1H), 5.94 (br, 1H), 2.99 (d, J = 4.9 Hz, 3H), 1.78 (s, 3H) ppm; $^{13}C\{^1H\}$ NMR (100 MHz, $CDCl_3$) δ 171.9, 140.2, 137.9, 135.6, 133.5, 133.3, 129.3, 128.8, 128.7, 128.6, 128.5, 127.8, 127.5, 26.6, 18.5 ppm; GC-MS m/z = 311 (M^+); Anal. Calcd for $C_{19}H_{18}ClNO$: C, 73.19; H, 5.82. Found: C, 73.27; H, 6.00.

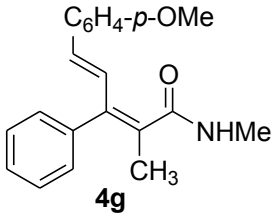

4g

For **4g**: ^1H NMR (400 MHz, $CDCl_3$) δ 7.4-6.8 (m, 9H), 7.18 (d, J = 15.9 Hz, 1H), 6.09 (br, 1H), 5.96 (d, J = 15.9 Hz, 1H), 3.75 (s, 3H), 2.98 (d, J = 4.9 Hz, 3H), 1.77 (s, 3H) ppm; $^{13}C\{^1H\}$ NMR (100 MHz, $CDCl_3$) δ 172.3, 159.5, 140.6, 138.4, 133.2, 132.1, 129.5, 128.5, 128.0, 127.4, 126.3, 114.1, 55.4, 26.5, 18.5 ppm; GC-MS m/z = 307 (M^+); Anal. Calcd for $C_{20}H_{21}NO_2$: C, 78.15; H, 6.89. Found: C, 77.91; H, 7.02.

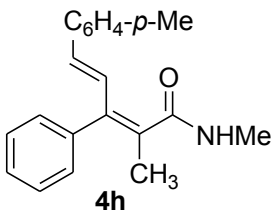

4h

For **4h**: ^1H NMR (400 MHz, $CDCl_3$) δ 7.4-7.0 (m, 9H), 7.29 (d, J = 15.9 Hz, 1H), 6.02 (d, J = 15.9 Hz, 1H), 5.92 (br, 1H, 3H), 3.00 (d, J = 4.9 Hz, 3H), 2.30 (s, 3H), 1.79 (s, 3H) ppm; $^{13}C\{^1H\}$ NMR (100 MHz, $CDCl_3$) δ 172.3, 140.6, 138.3, 137.9, 133.8, 132.7, 129.6, 129.5, 128.6,

127.5, 127.4, 126.7, 26.6, 21.4, 18.6 ppm; GC-MS *m/z* = 291 (M^+); Anal. Calcd for $C_{20}H_{21}NO$: C, 82.44; H, 7.26. Found: C, 82.04; H, 7.29.

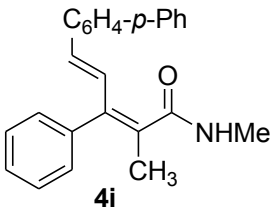

4i

For **4i**: ^{1}H NMR (400 MHz, $CDCl_3$) δ 7.4-7.1 (m, 14H), 7.31 (d, *J* = 15.9 Hz, 1H), 5.98 (d, *J* = 15.9 Hz, 1H), 5.80 (br, 1H), 2.93 (d, *J* = 4.9 Hz, 3H), 1.73 (s, 3H) ppm; $^{13}C\{^1H\}$ NMR (100 MHz, $CDCl_3$) δ 172.2, 140.7, 140.6, 140.5, 138.2, 136.3, 133.73, 129.6, 129.1, 129.0, 128.6, 128.4, 127.6, 127.5, 127.3, 127.2, 127.0, 26.7, 18.7 ppm; GC-MS *m/z* = 353 (M^+); Anal. Calcd for $C_{25}H_{23}NO$: C, 84.95; H, 6.56. Found: C, 83.94; H, 6.72.

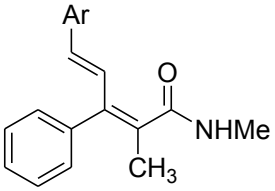

4j (Ar = naphthyl)

For **4j**: ^{1}H NMR (400 MHz, $CDCl_3$) δ 7.7-7.2 (m, 12H), 7.39 (d, *J* = 15.9 Hz, 1H), 6.20 (d, *J* = 15.9 Hz, 1H), 6.09 (br, 1H), 3.01 (d, *J* = 4.9 Hz, 3H), 1.82 (s, 3H) ppm; $^{13}C\{^1H\}$ NMR (100 MHz, $CDCl_3$) δ 172.2, 140.5, 138.2, 134.7, 133.8, 133.6, 133.3, 133.1, 129.5, 128.3, 128.1, 127.7, 127.5, 127.2, 126.4, 126.1, 123.5, 26.6, 18.7 ppm; GC-MS *m/z* = 327 (M^+); Anal. Calcd for $C_{23}H_{21}NO$: C, 84.37; H, 6.46. Found: C, 84.68; H, 6.50.

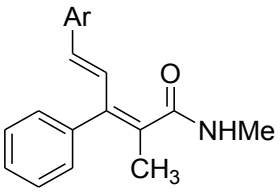

4k (Ar = 6-methoxynaphthyl)

For **4k**: ^{1}H NMR (400 MHz, $CDCl_3$) δ 7.6-7.0 (m, 11H), 7.41 (d, *J* = 15.9 Hz, 1H), 6.18 (d, *J* = 15.9 Hz, 1H), 5.92 (br, 1H), 3.98 (s, 3H), 3.05 (d, *J* = 4.9 Hz, 3H), 1.82 (s, 3H) ppm; $^{13}C\{^1H\}$ NMR (100 MHz, $CDCl_3$) δ 172.3, 158.0, 140.8, 138.4 and 134.4, 134.1, 132.7, 132.6, 129.7, 129.6, 129.1, 128.6, 127.7, 127.5, 127.3, 127.1, 55.5, 26.7, 18.7 ppm; GC-MS *m/z* = 357 (M^+); Anal. Calcd for $C_{24}H_{23}NO_2$: C, 80.64; H, 6.49. Found: C, 80.55; H, 6.59.

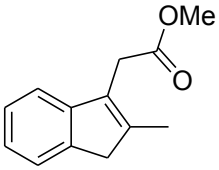

5a

For **5a**: ^{1}H NMR (400 MHz, $CDCl_3$) δ 7.4-7.2 (m, 4H), 3.72 (s, 3H), 3.60 (s, 2H), 3.39 (s, 2H), 2.18 (s, 3H) ppm; $^{13}C\{^1H\}$ NMR (100 MHz, $CDCl_3$) δ 171.7, 146.0, 142.3, 142.2, 129.8, 126.4, 124.1, 123.4, 118.5, 52.2, 42.9, 31.5, 14.3 ppm; GC-MS *m/z* = 202 (M^+); Anal. Calcd for $C_{13}H_{14}O_2$: C, 77.20; H, 6.98. Found: C, 77.61; H, 6.37.

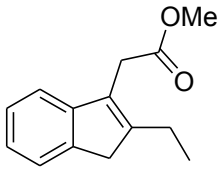

5b

For **5b**: ^{1}H NMR (400 MHz, $CDCl_3$) δ 7.5-7.2 (m, 4H), 3.73 (s, 3H), 3.60 (s, 2H), 3.42 (s, 2H), 2.60 (q, *J* = 7.6 Hz, 2H), 1.22 (t, *J* = 7.6 Hz, 3H) ppm; ^{13}C{^{1}H} NMR (100 MHz, $CDCl_3$) δ 171.7, 148.3, 146.0, 142.3, 129.0, 126.4, 124.2, 123.5, 118.7, 52.2, 40.1, 31.4, 22.0, 14.3 ppm; GC-MS *m/z* = 216 (M^+); Anal. Calcd for $C_{14}H_{16}O_2$: C, 77.75; H, 7.46. Found: C, 77.61; H, 7.37.

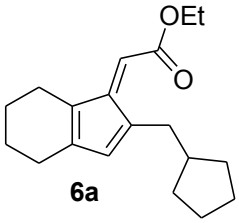

6a

For **6a**: ^{1}H NMR (400 MHz, $CDCl_3$) δ 7.59 (s, 1H, CH), 6.92 (s, 1H, CH), 4.34 (q, *J* = 7.1 Hz, 2H), 2.91 (d, *J* = 7.2 Hz, 2H), 2.76 (m, 4H), 2.07 (m, 1H), 1.80 (m, 4H), 1.65 (m, 4H), 1.53 (m, 4H), 1.38 (t, *J* = 7.1 Hz, 3H) ppm; NOESY δ 6.92 ↔2.76 ppm (↔ denotes NOE correlation); ^{13}C{^{1}H} NMR (100 MHz, $CDCl_3$) δ 168.4, 141.3, 140.8, 138.5, 132.2, 131.0, 127. 1, 60.7, 42.2, 39.7, 36.8, 36.3, 33.7, 28.5, 28.4, 25.0, 14.5 ppm; GC-MS *m/z* = 286 (M^+); HRMS (*m/z*): calcd for $C_{19}H_{27}O_2$ $(M+H)^+$, 287.2002; Found: 287.2004.

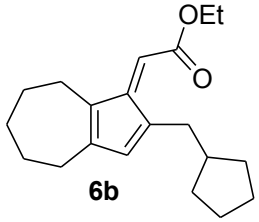

6b

For **6b**: ^{1}H NMR (400 MHz, $CDCl_3$) δ 7.53 (s, 1H), 6.82 (s, 1H), 4.26 (q, *J* = 7.1 Hz, 2H), 2.84 (d, *J* = 7.2 Hz, 2H), 2.70 (m, 4H), 1.96 (m, 1H), 1.66 (m, 2H), 1.57 (m, 4H), 1.43 (m, 4H), 1.35 (m, 4H), 1.31 (t, *J* = 7.1 Hz, 3H) ppm; NOESY δ 6.82 ↔ 2.70 ppm (↔ denotes NOE correlation); ^{13}C{^{1}H} NMR (100 MHz, $CDCl_3$) δ 168.2, 141.6, 140.7, 134, 132.2, 131.4, 127. 3, 60.7, 42.1, 39.8, 32.7, 29.6, 29.0, 25.0, 23.3, 23.2, 14.3 ppm; GC-MS *m/z* = 300 (M^+); HRMS (*m/z*): calcd for $C_{20}H_{29}O_2$ $(M+H)^+$, 301.2162; Found: 301.2076.

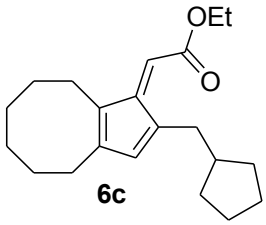

6c

For **6c**: ^{1}H NMR (400 MHz, $CDCl_3$) δ 7.62 (s, 1H), 6.96 (s, 1H), 4.34 (q, *J* = 7.2 Hz, 2H), 2.94 (d, *J* = 7.1 Hz, 2H), 2.75 (m, 4H), 2.06 (m, 1H), 1.68 (m, 4H), 1.64 (m, 4H), 1.35 (t, *J* = 7.1 Hz, 3H), 1.19 (m, 4H) ppm; NOESY δ 6.96 ↔2.75 ppm (↔ denotes NOE correlation); ^{13}C{^{1}H} NMR (100 MHz, $CDCl_3$) δ 168.5, 145.5, 141.9, 135.6, 132.4, 131.3, 127. 7, 60.7, 42.2, 39.9, 34.2, 32.7, 32.4, 32.3, 32.0, 26.1, 25.9, 25.0, 14.6 ppm; GC-MS *m/z* = 314 (M^+); HRMS (*m/z*): calcd for $C_{21}H_{31}O_2$ $(M+H)^+$, 315.2322; Found: 315.2319.

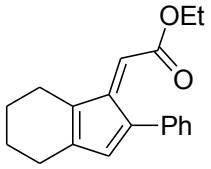

6d

For **6d**: ^{1}H NMR (400 MHz, $CDCl_3$) δ 7.60 (s, 1H), 7.4-7.3 (m, 5H), 7.08 (s, 1H), 4.09 (q, *J* = 7.1 Hz, 2H), 2.83 (m, 4H), 1.85 (m, 4H), 1.00 (t, *J* = 7.1 Hz, 3H) ppm; NOESY δ 7.08 ↔2.83 ppm (↔ denotes NOE correlation); ^{13}C{^{1}H} NMR (100 MHz, $CDCl_3$) δ 169.0, 141.9, 140.9, 140.9, 136.4, 131.5, 130.8, 128.6, 128.4, 128.0, 126.9, 60.8, 29.5, 29.1, 23.3, 23.2, 13.8 ppm; GC-MS *m/z* = 280 (M^+); HRMS (*m/z*): calcd for $C_{19}H_{21}O_2$ $(M+H)^+$, 281.1542; Found: 281.1534.

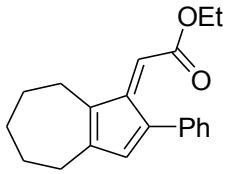

6e

For **6e**: ^{1}H NMR (400 MHz, $CDCl_3$) δ 7.50 (s, 1H), 7.3-7.2 (m, 5H), 7.01 (s, 1H), 3.98 (q, *J* = 7.1 Hz, 2H), 2.77 (m, 4H), 1.76 (m, 2H), 1.58 (m, 4H), 0.88 (t, *J* = 7.1 Hz, 3H) ppm; NOESY δ 7.01 ↔ 2.77 ppm (↔ denotes NOE correlation); ^{13}C{^{1}H} NMR (100 MHz, $CDCl_3$) δ 169.0, 147.2, 142.6, 141.8, 140.5, 131.6, 130.5, 128.6, 128.5, 128.4, 127.0, 60.8, 36.7, 36.3, 32.7, 28.3, 28.2, 13.8 ppm; ; GC-MS *m/z* = 294 (M^+); HRMS (*m/z*): calcd for $C_{20}H_{23}O_2$ $(M+H)^+$, 295.1698; Found: 295.1692.

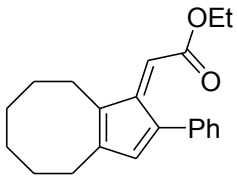

6f

For **6f**: ^{1}H NMR (400 MHz, $CDCl_3$) δ 7.51 (s, 1H), 7.3-7.2 (m, 5H), 6.92 (s, 1H), 3.98 (q, *J* = 7.2 Hz, 2H), 2.70 (m, 4H), 1.61 (m, 4H), 1.29 (m, 4H), 0.88 (t, *J* = 7.2 Hz, 3H) ppm; NOESY δ 6.92 ↔ 2.70 ppm (↔ denotes NOE correlation); ^{13}C{^{1}H} NMR (100 MHz, $CDCl_3$) δ 169.1, 145.1, 140.5, 139.6 138.5, 132.0, 131.5, 130.7, 128.6, 127.9, 126.9, 126.3, 60.7, 32.3, 32.2, 32.1, 31.9, 26.0, 25.9, 13.8 ppm; GC-MS *m/z* = 308 (M^+); HRMS (*m/z*): calcd for $C_{21}H_{25}O_2$ $(M+H)^+$, 309.1855; Found: 309.1847.

References

(S1) Tang, J.-M.; Bhunia, S.; Sohel, S. M. A.; Lin, M,-Y.; Liao, H,-Y.; Datta, S.; Das, A.; Liu, R.-S. *J. Am. Chem. Soc.* **2007**, *129*, 15677-15683.

(S2) Thiemann, T.; Watanabe, M.; Tanaka, Y.; Mataka, S. *New J. Chem.* **2004**, *28*, 758-584.

(S3) (a) Liu, L.; Zhang, Y.; Xin, B. *J. Org. Chem.* **2006**, *71*, 3994-3997. (b) Lee, D.-H.; Jung, J.-Y.; Lee, I.-M.; Jin, M.-J. *Eur. J. Org. Chem.* **2008**, 356-360.

^{1}H and ^{13}C NMR Spectra of Selected Organic Products.

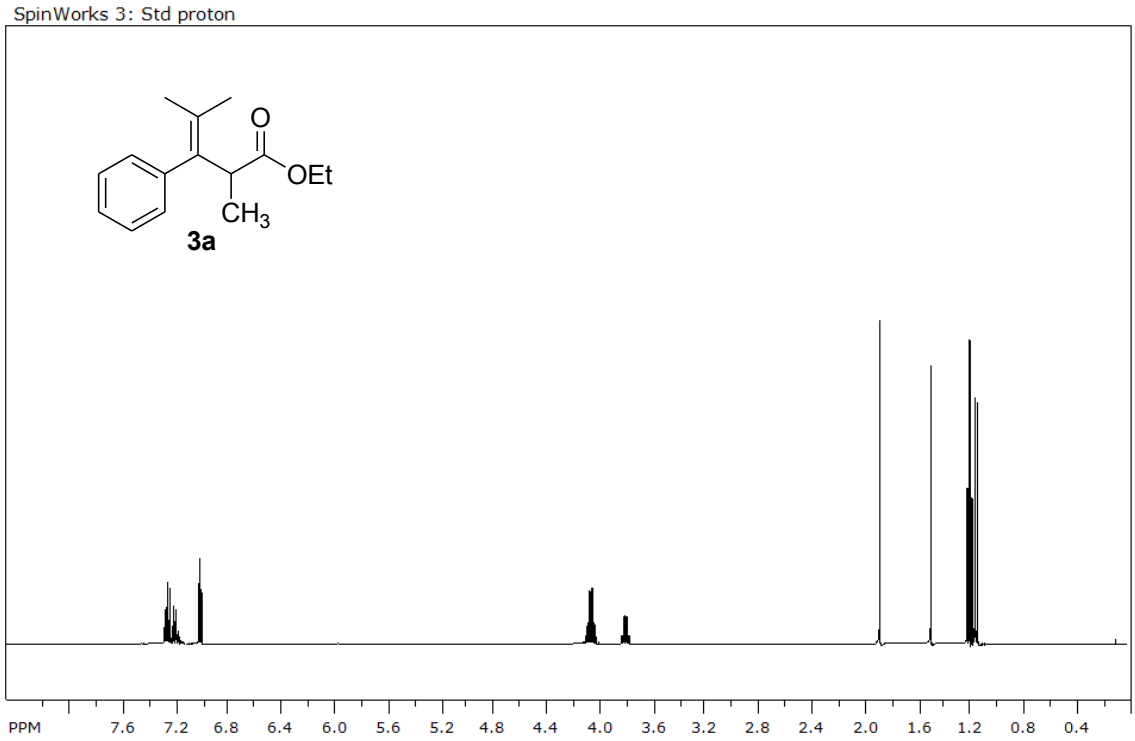

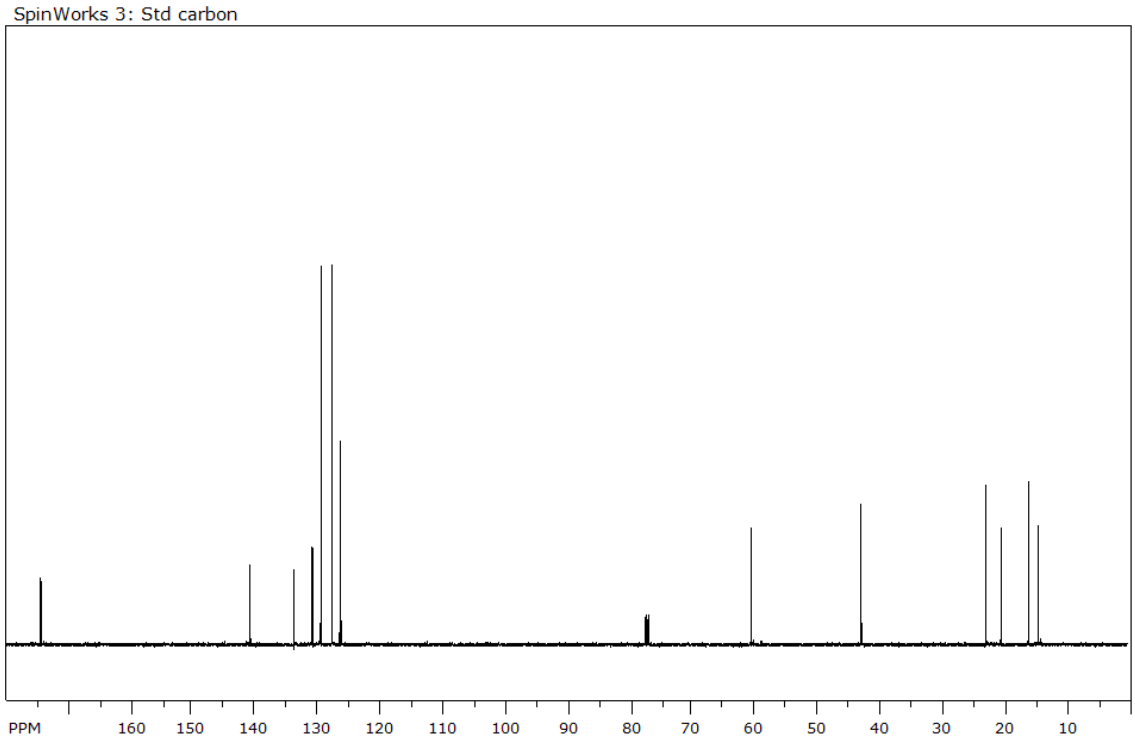

SpinWorks 3: Std proton

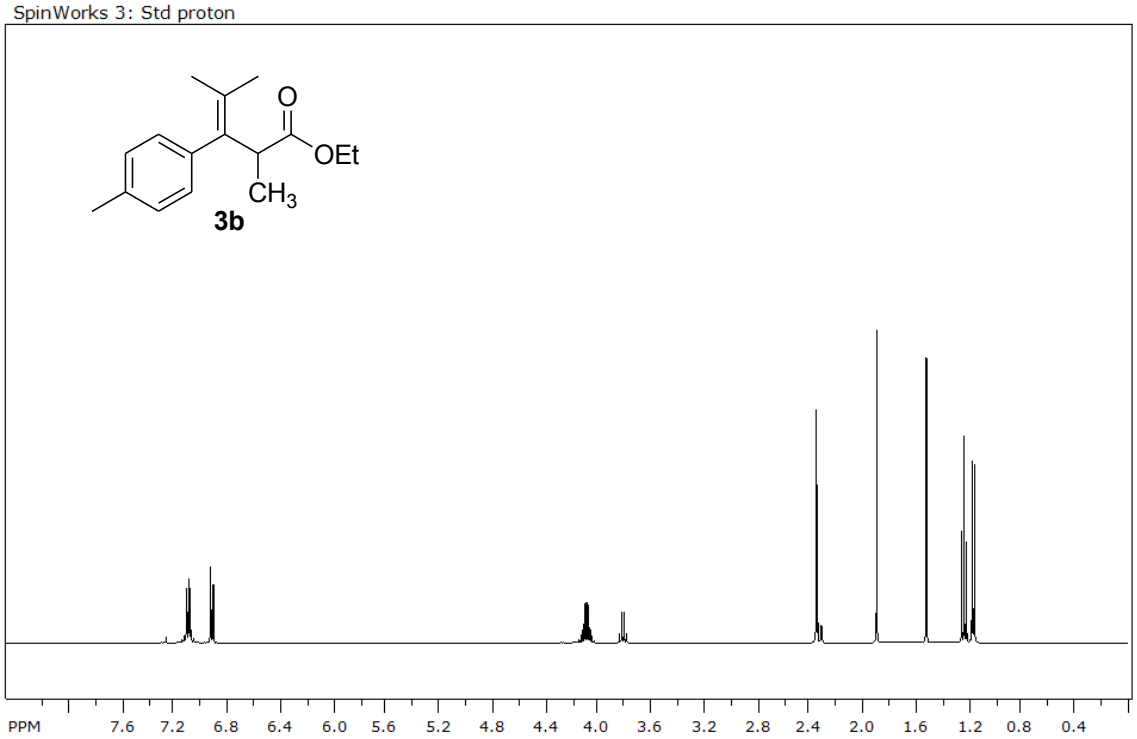

SpinWorks 3: Std carbon

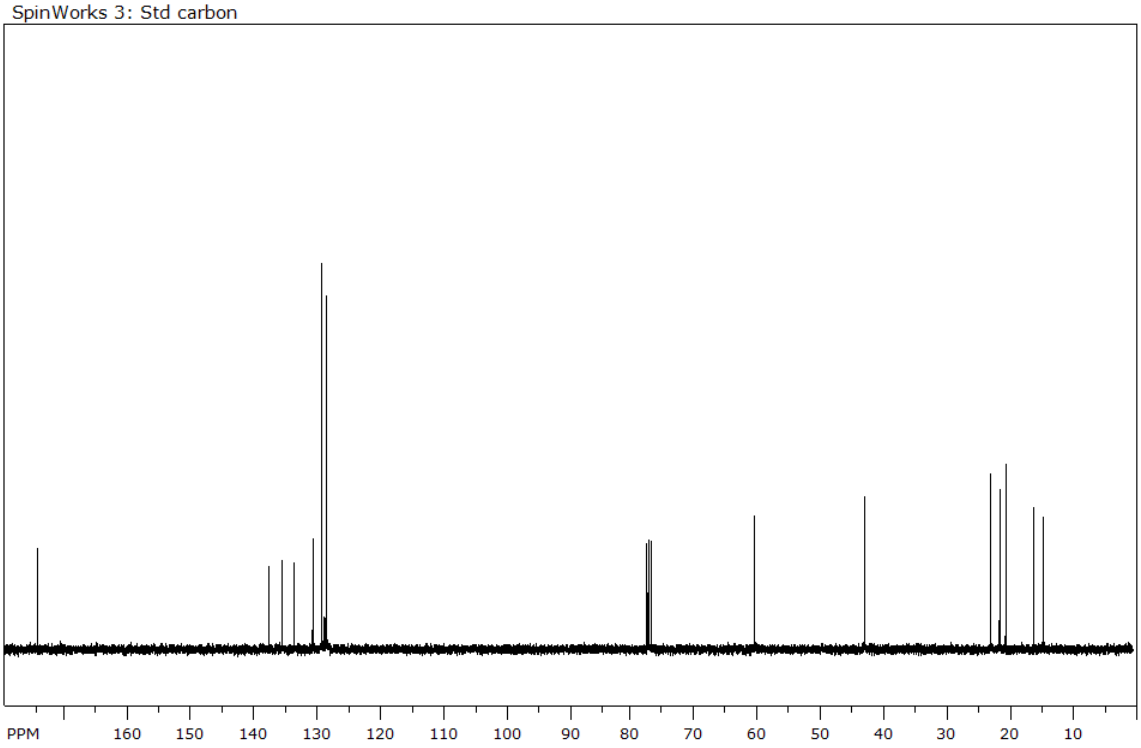

SpinWorks 3: Std proton

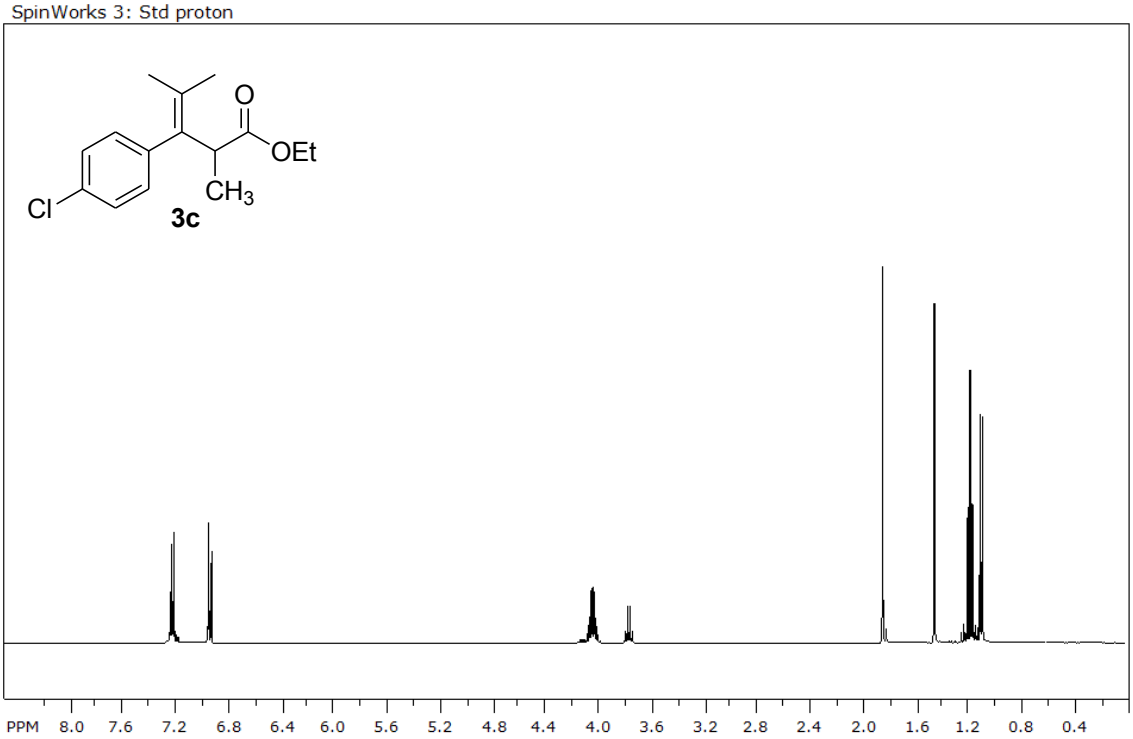

SpinWorks 3: Std carbon

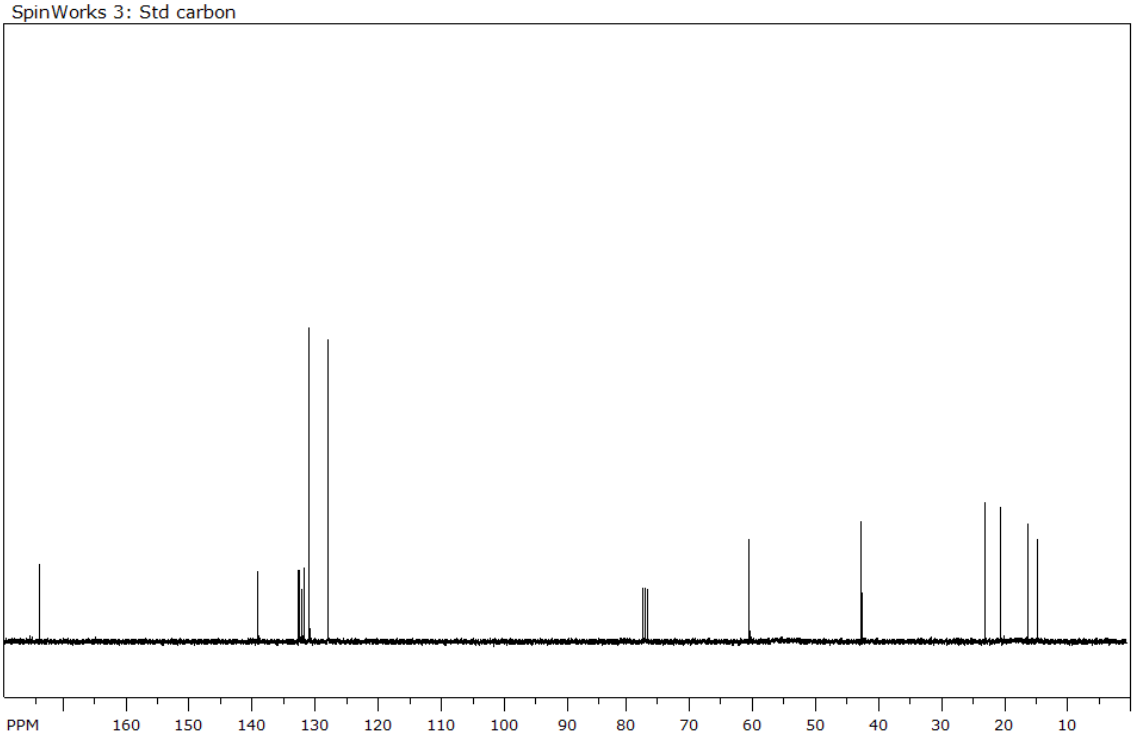

SpinWorks 3: Std proton

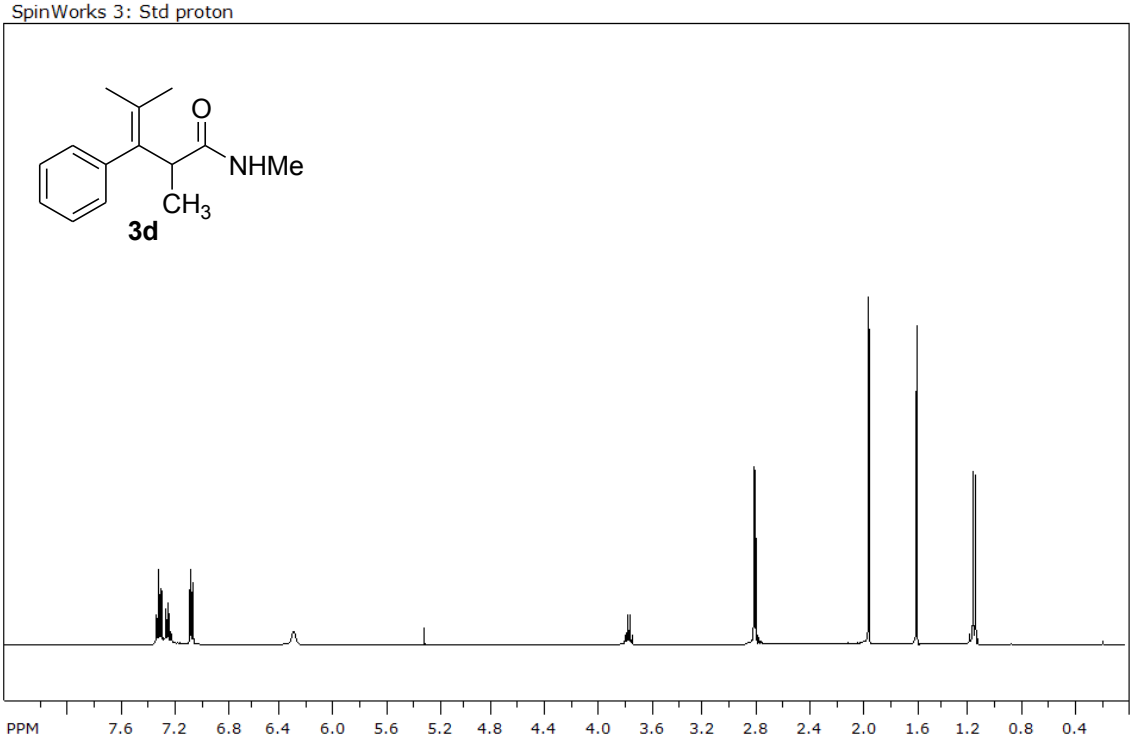

SpinWorks 3: Std carbon

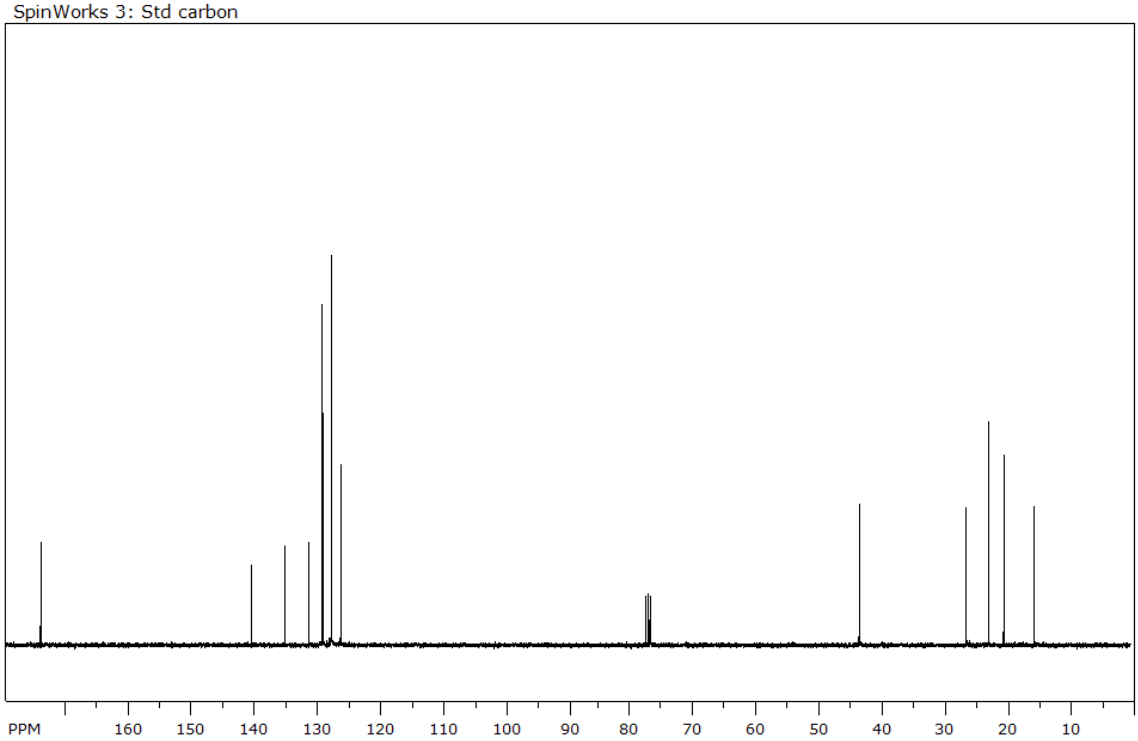

SpinWorks 3: Std proton

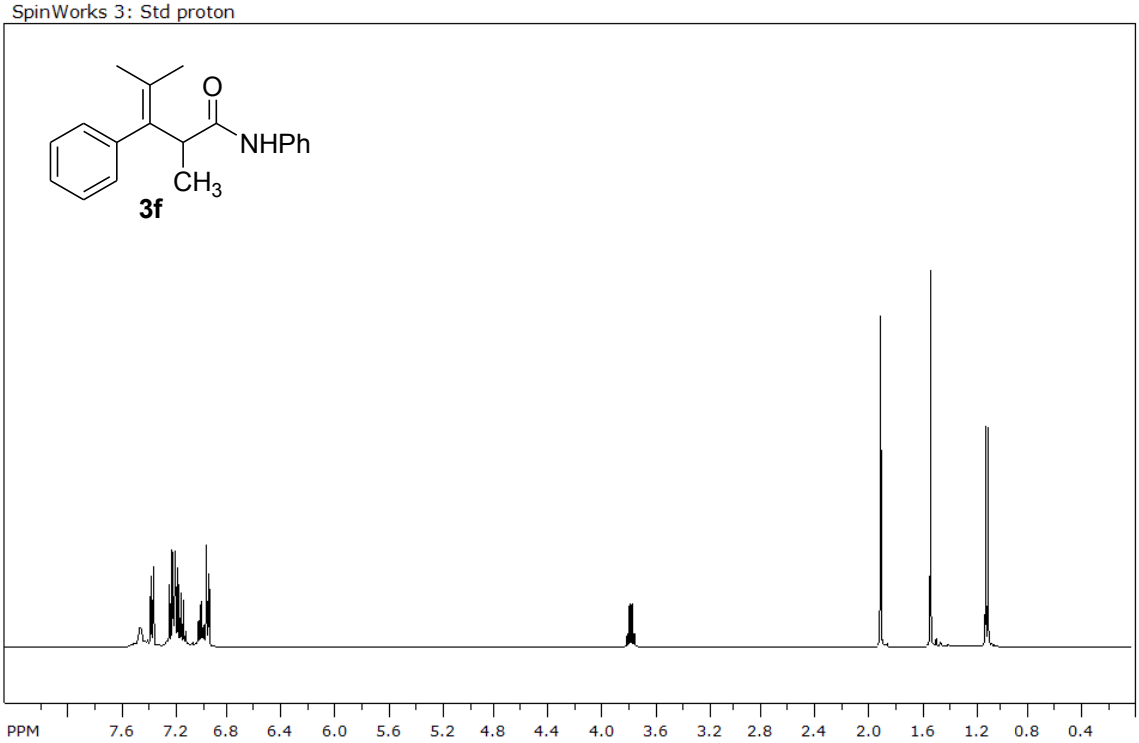

SpinWorks 3: Std carbon

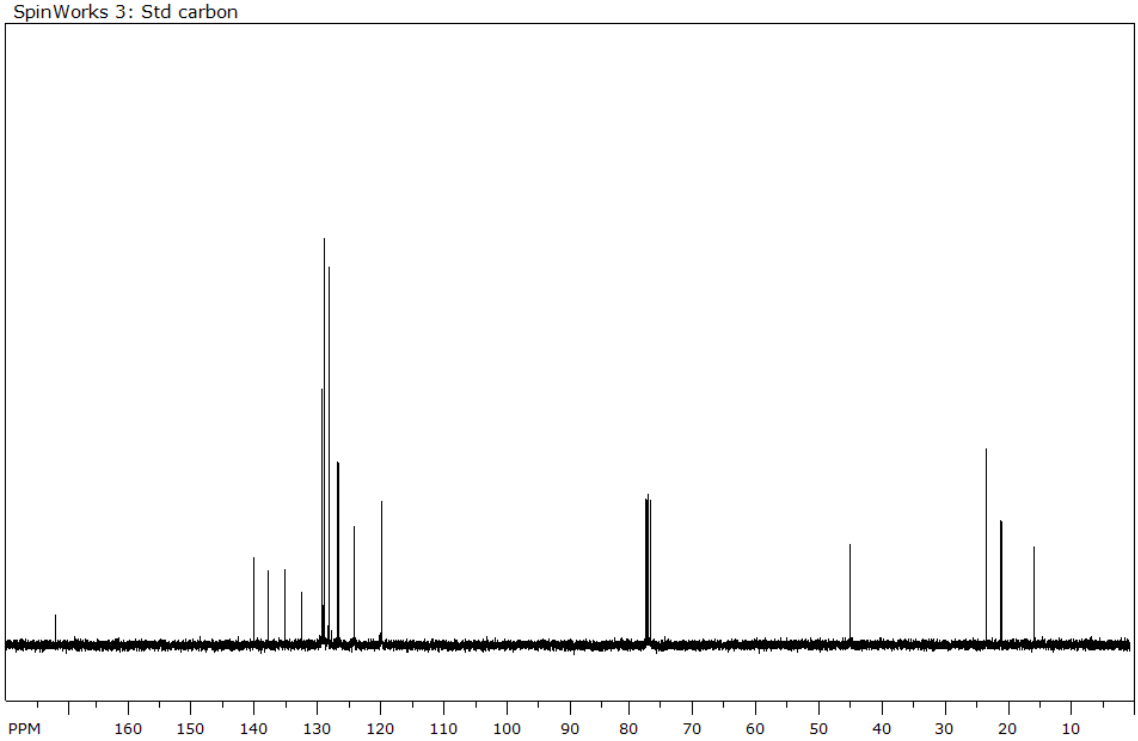

SpinWorks 3: Std proton

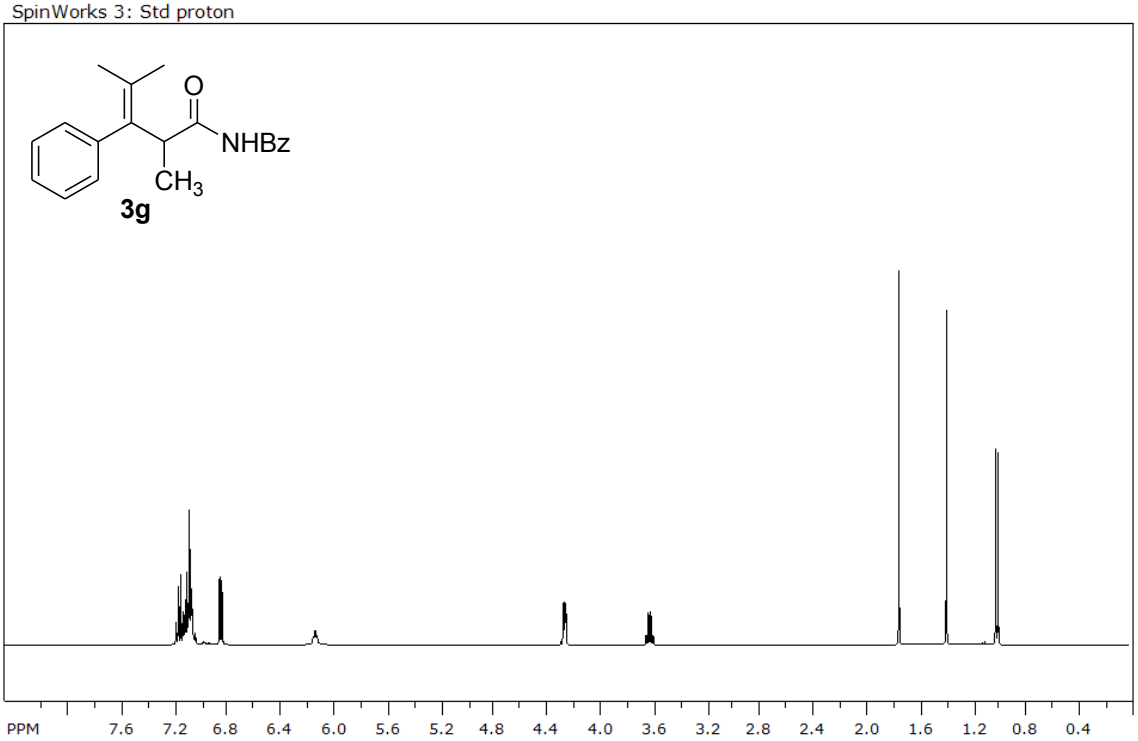

SpinWorks 3: Std carbon

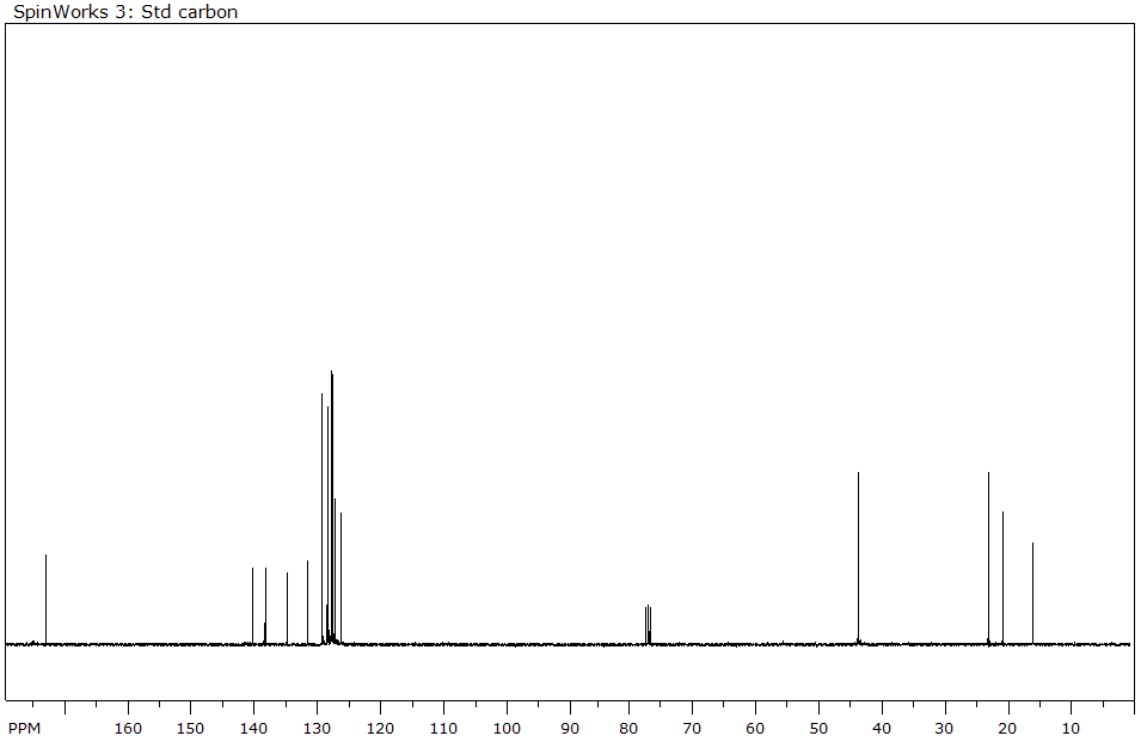

SpinWorks 3: Std proton

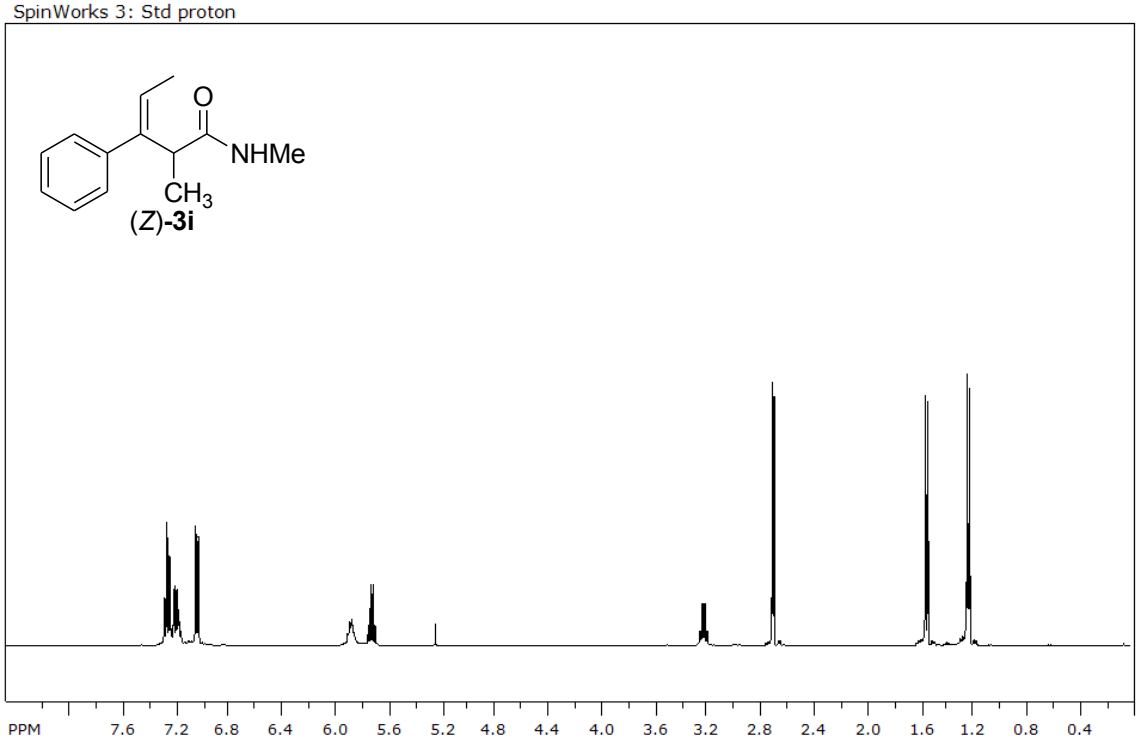

SpinWorks 3: Std carbon

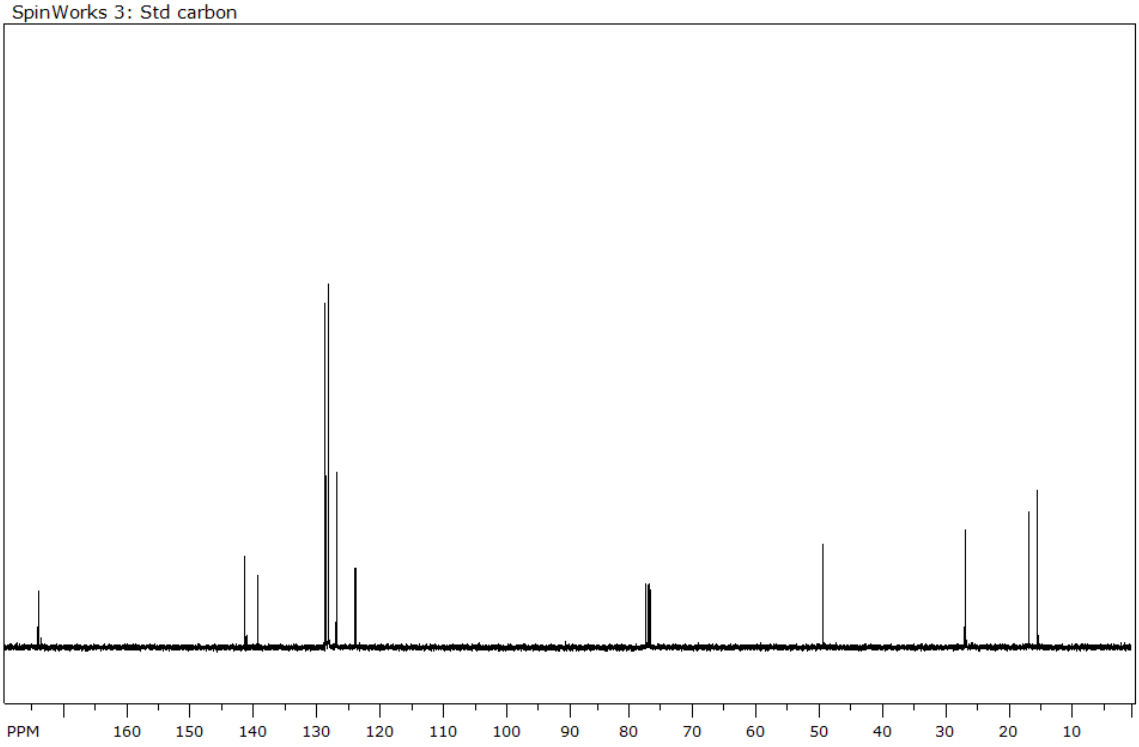

SpinWorks 3: Std proton

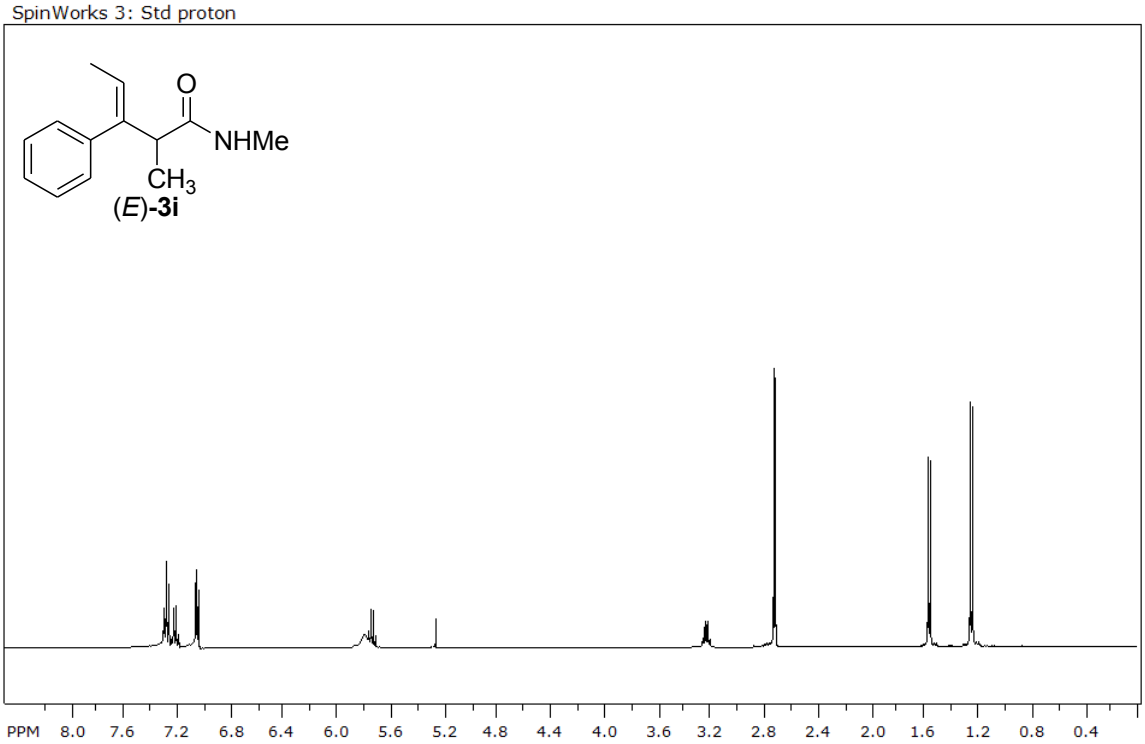

SpinWorks 3: Std carbon

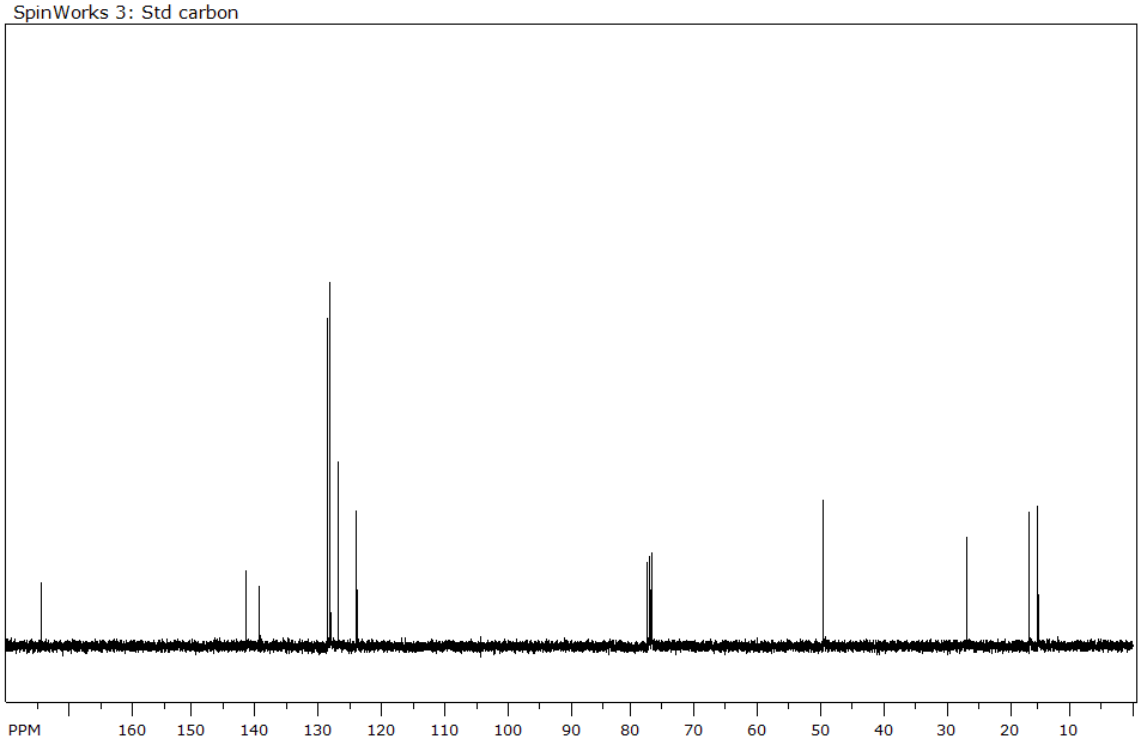

SpinWorks 3: Std proton

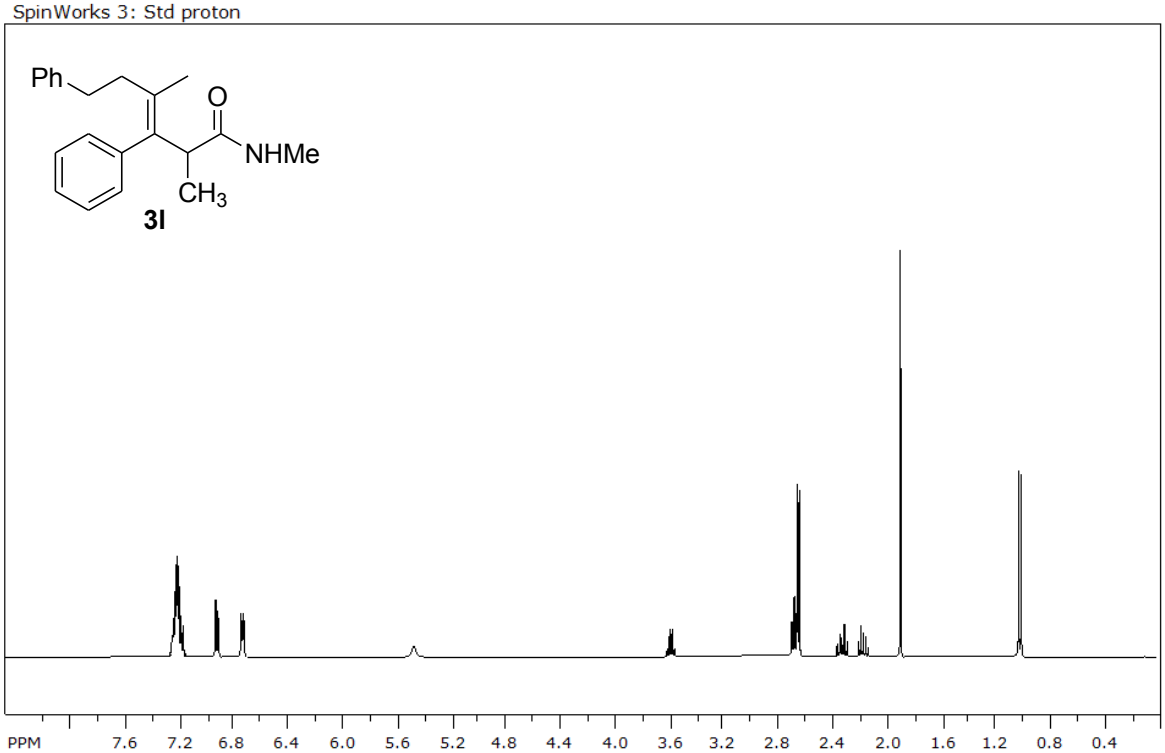

SpinWorks 3: Std carbon

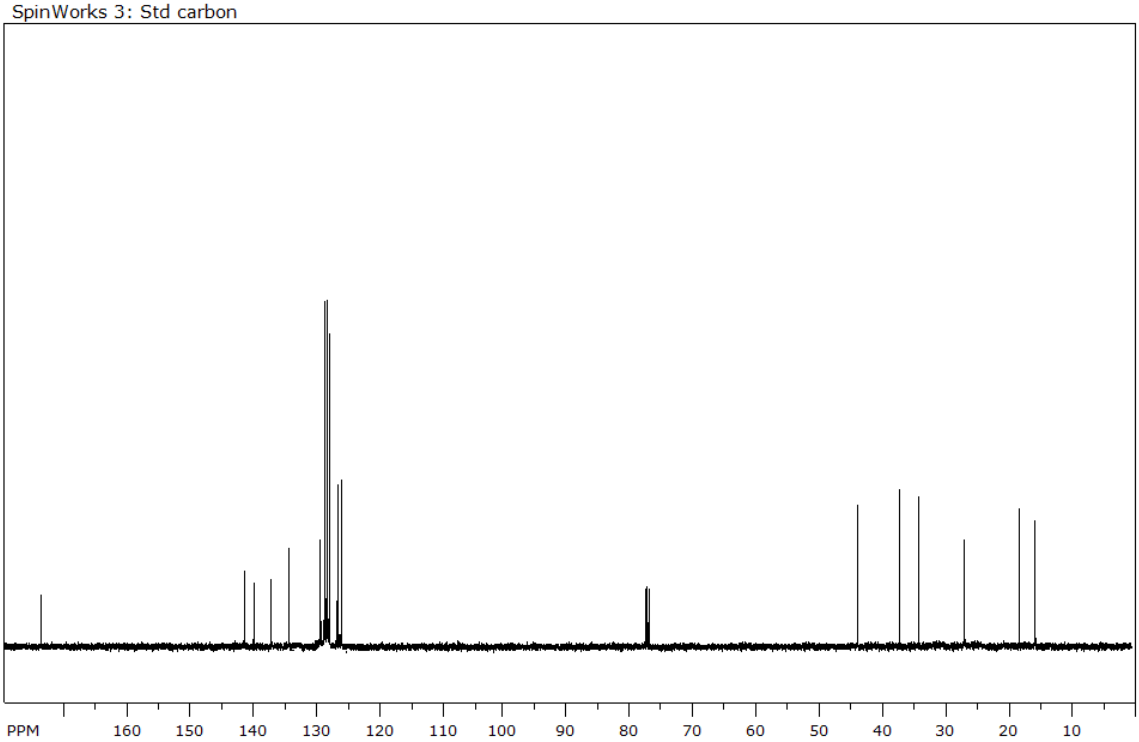

SpinWorks 3: Std proton

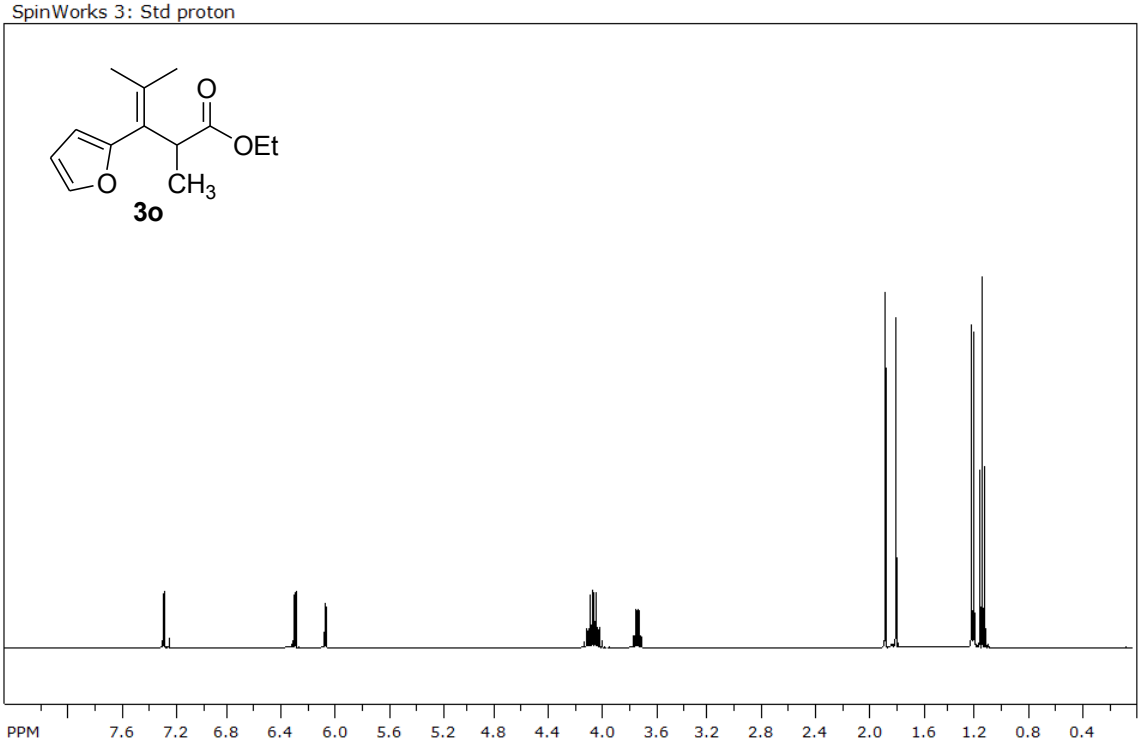

SpinWorks 3: Std carbon

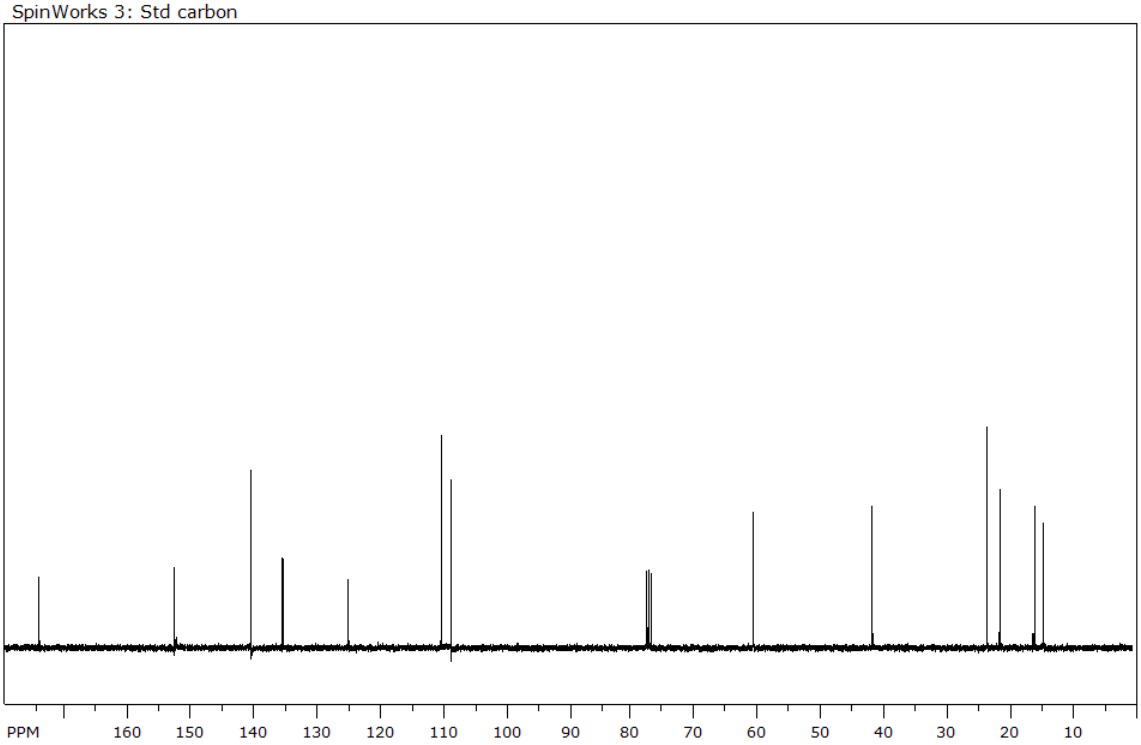

SpinWorks 3: Std proton

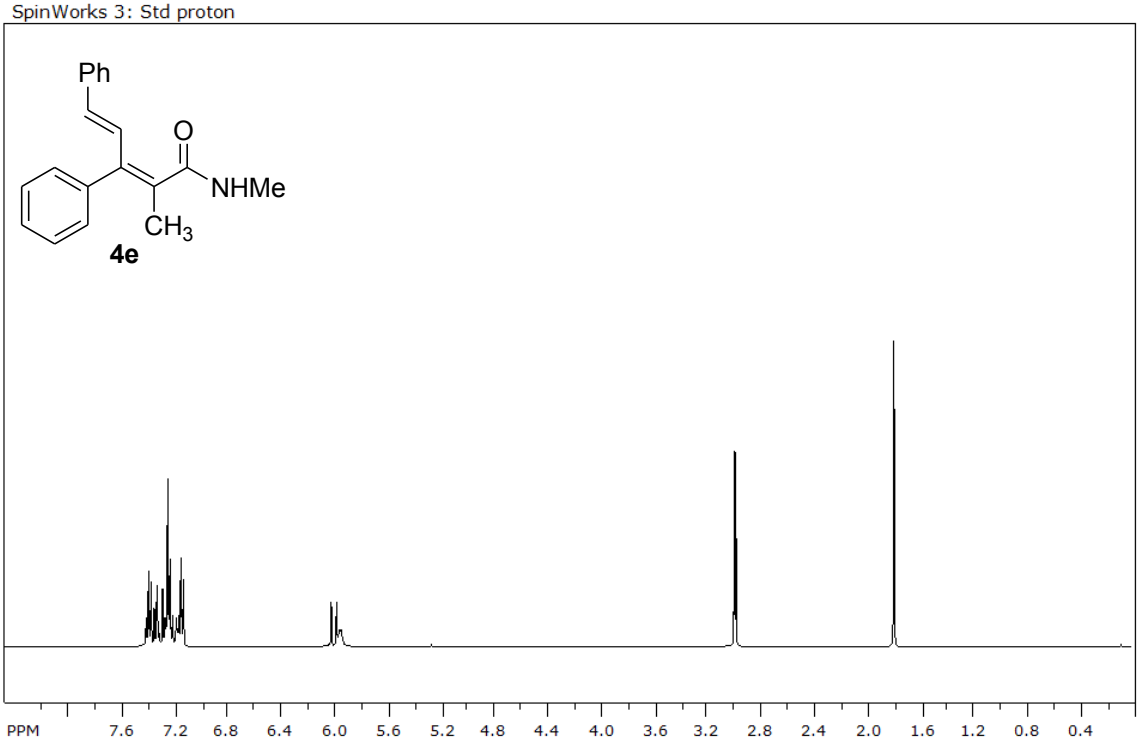

SpinWorks 3: Std carbon

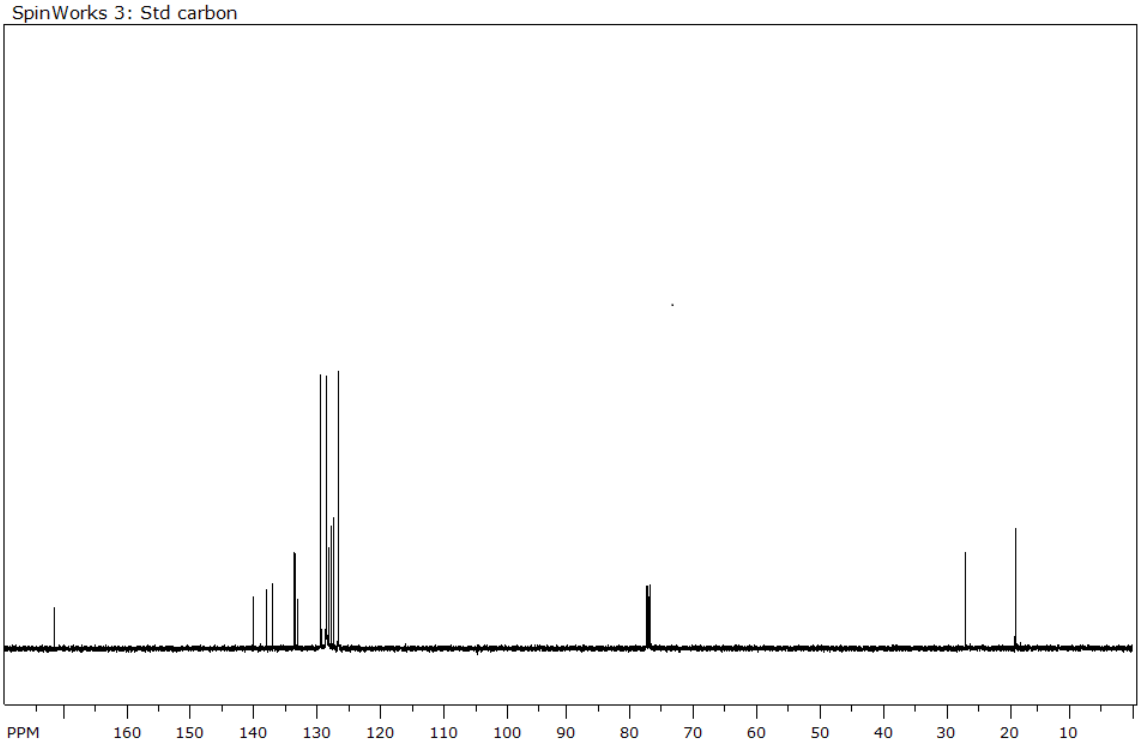

SpinWorks 3: Std proton

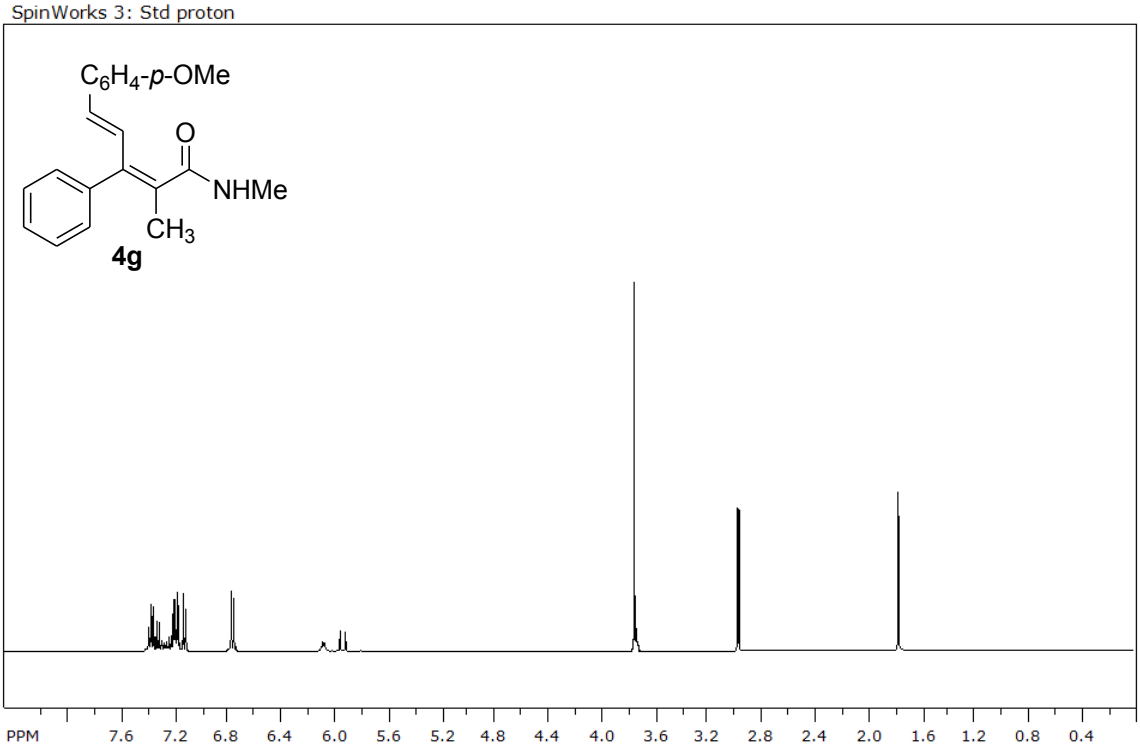

SpinWorks 3: Std carbon

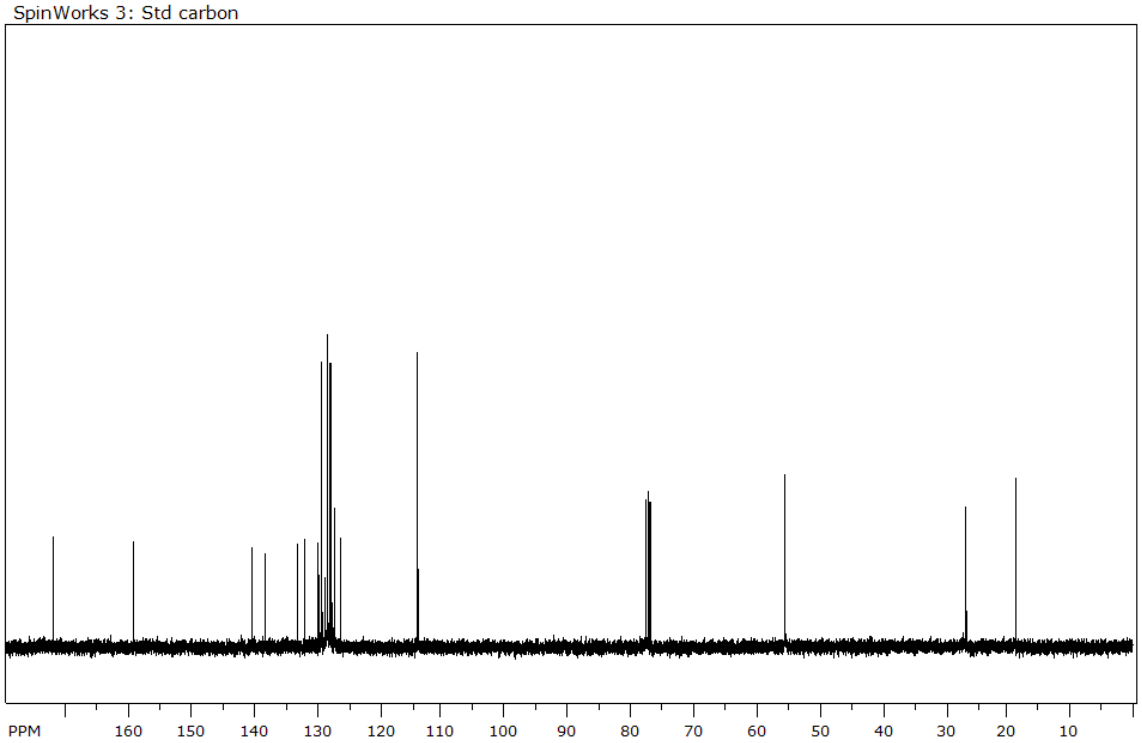

SpinWorks 3: STANDARD 1H OBSERVE

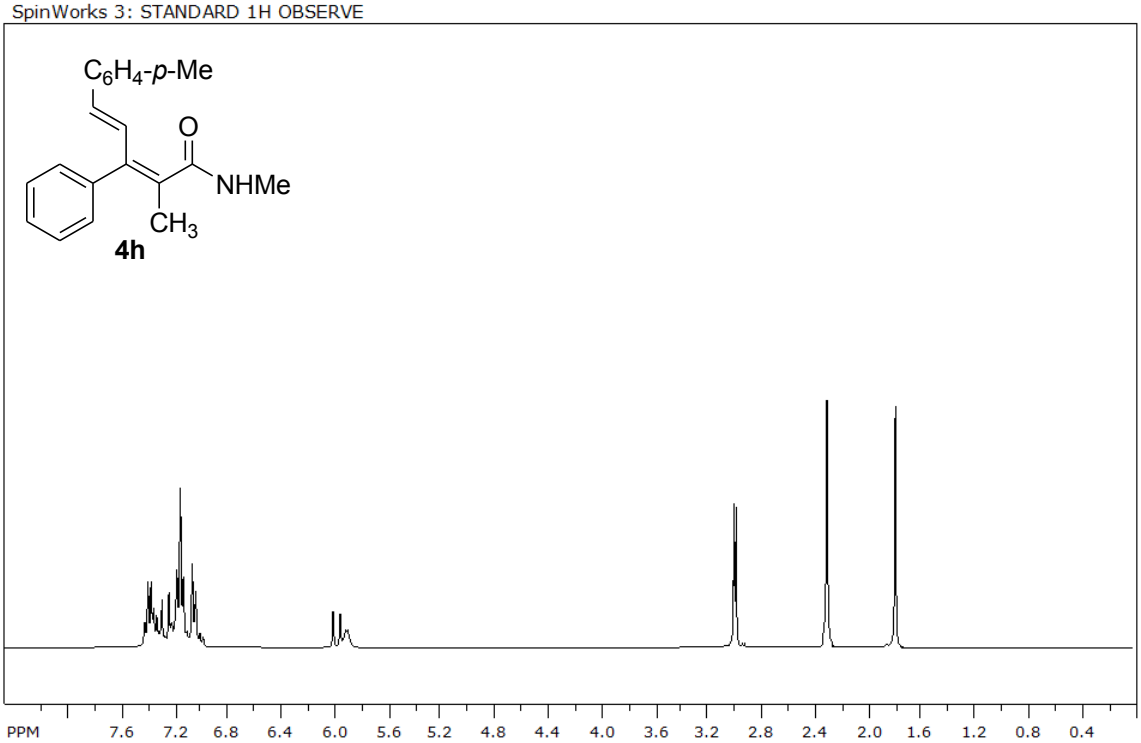

SpinWorks 3: 13C OBSERVE

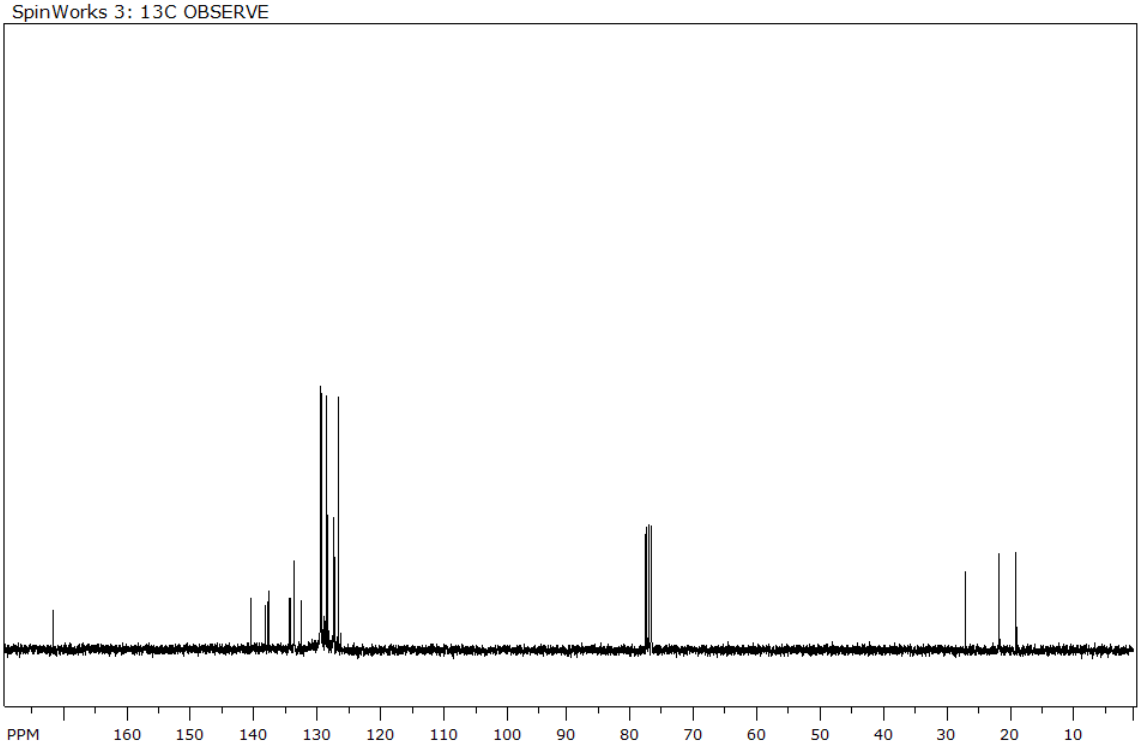

SpinWorks 3: Std proton

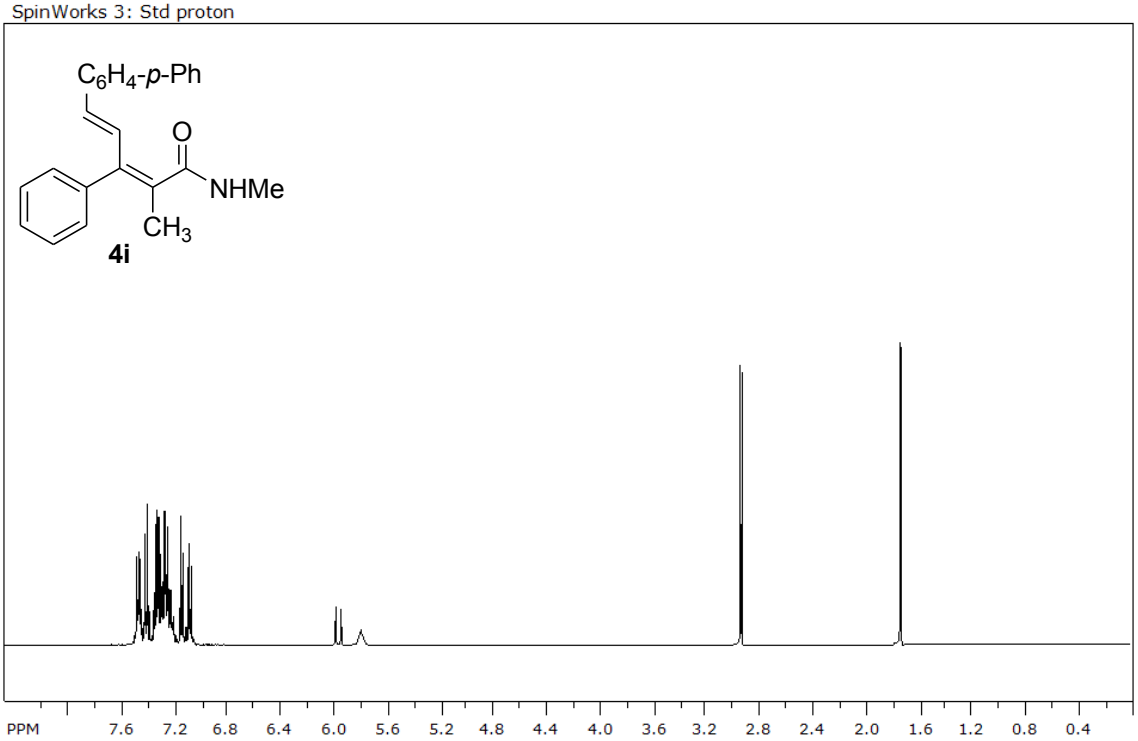

SpinWorks 3: Std carbon

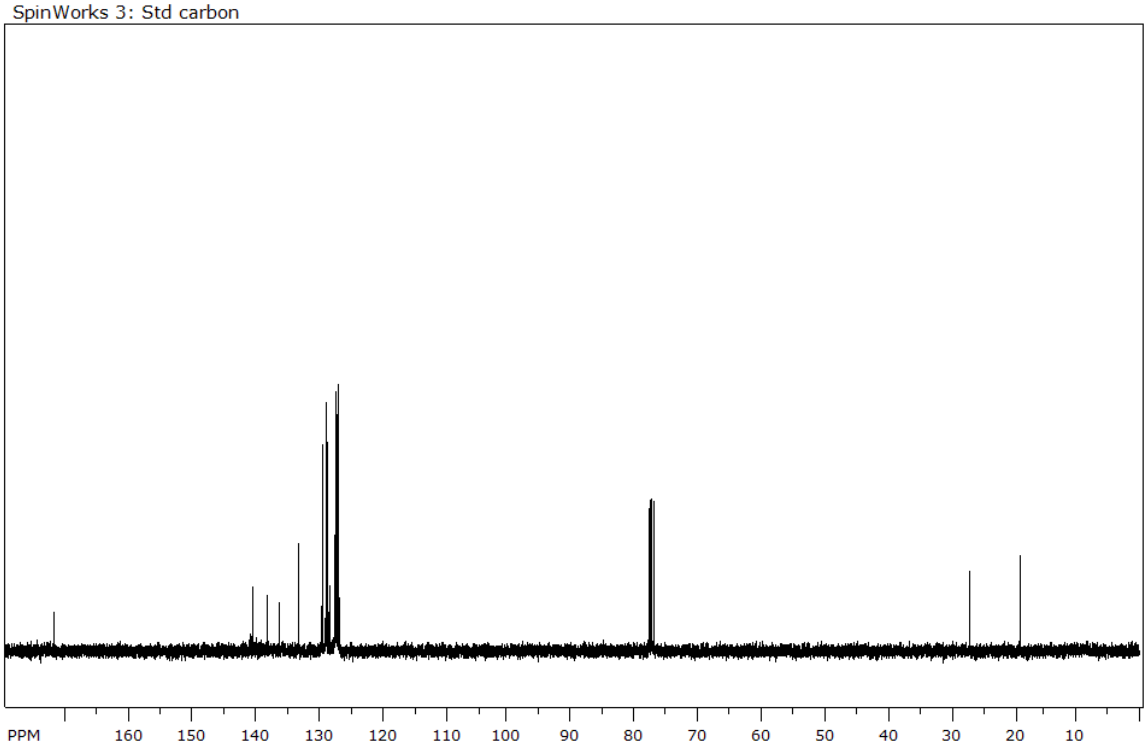

SpinWorks 3: Std proton

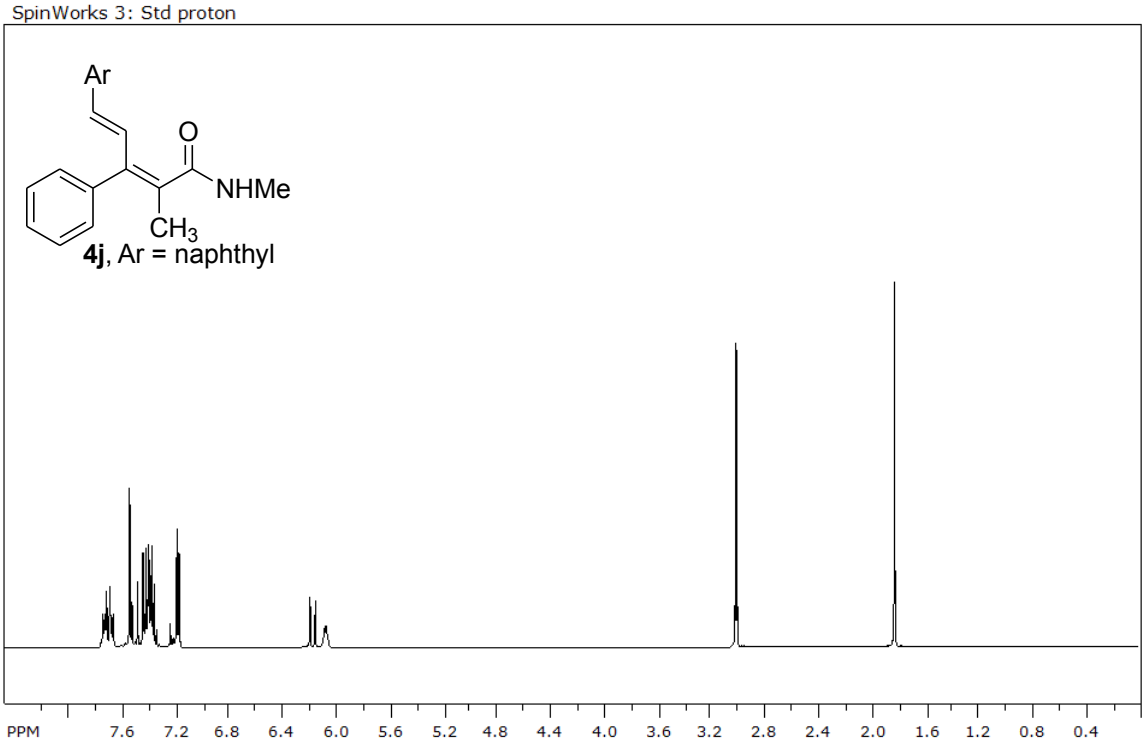

SpinWorks 3: Std carbon

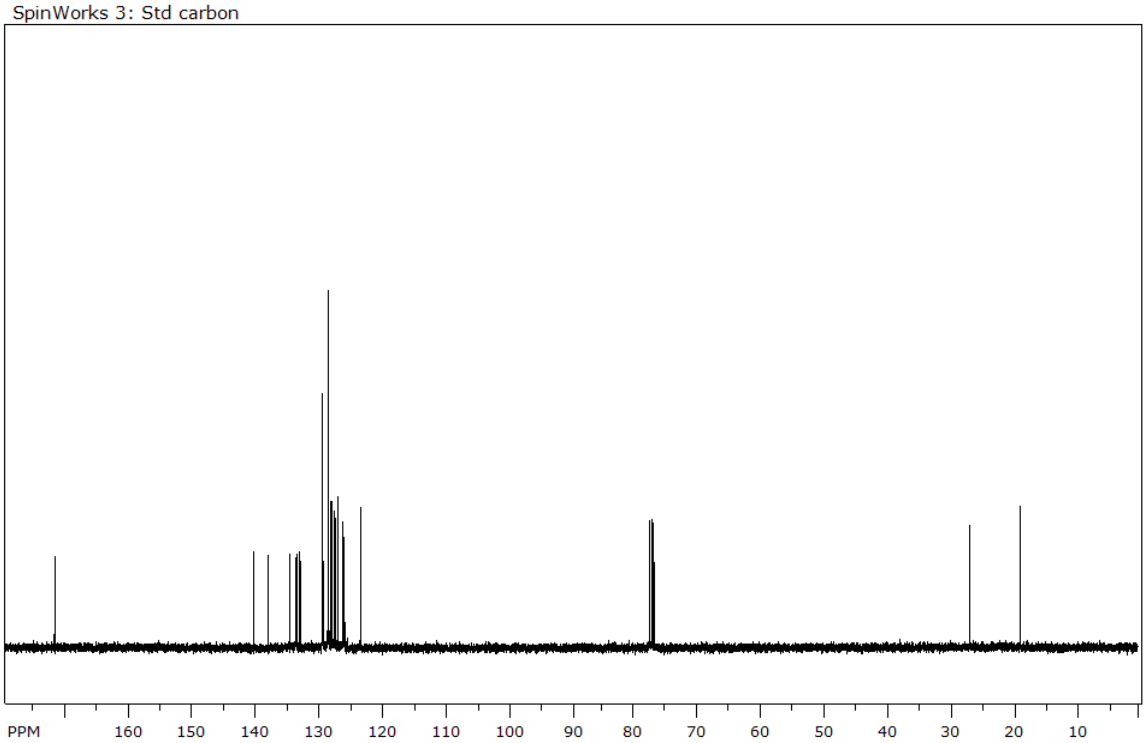

SpinWorks 3: Std proton

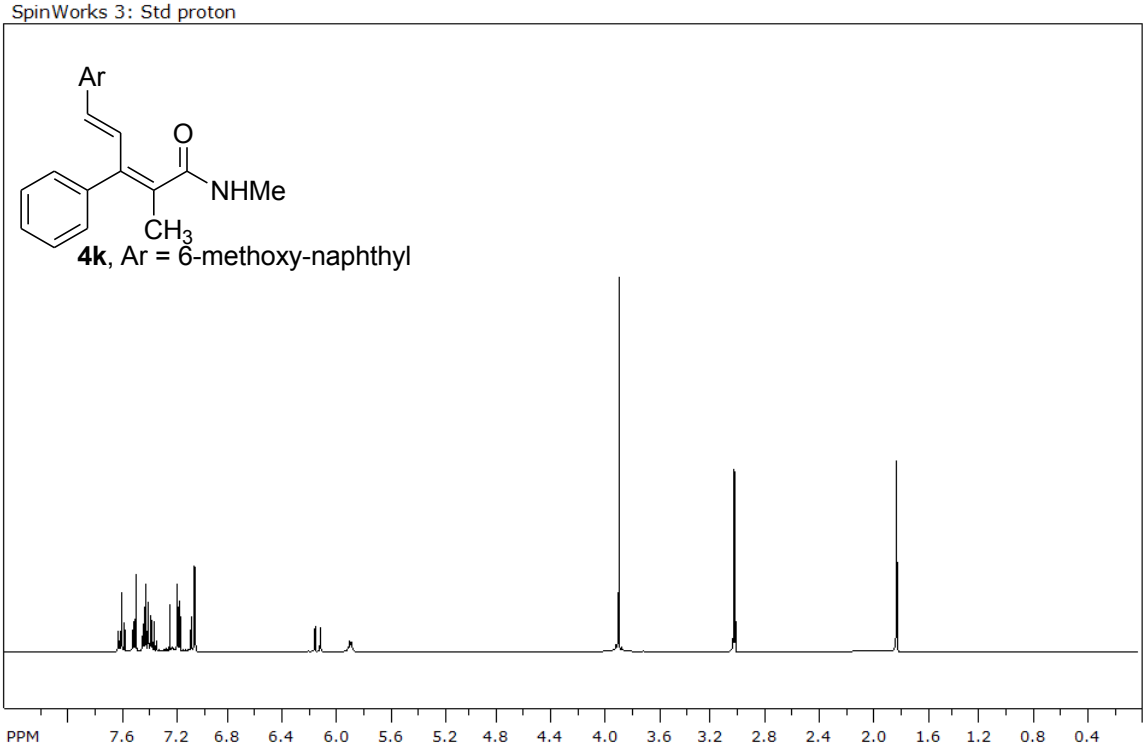

SpinWorks 3:

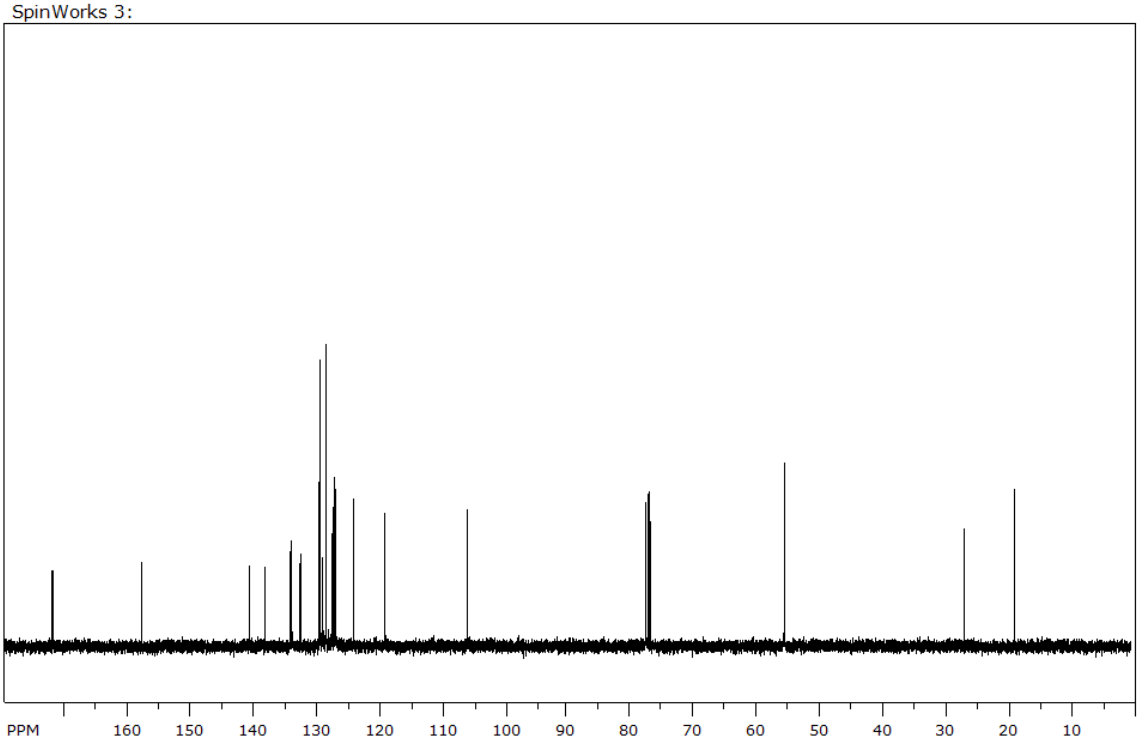

SpinWorks 3: Std proton

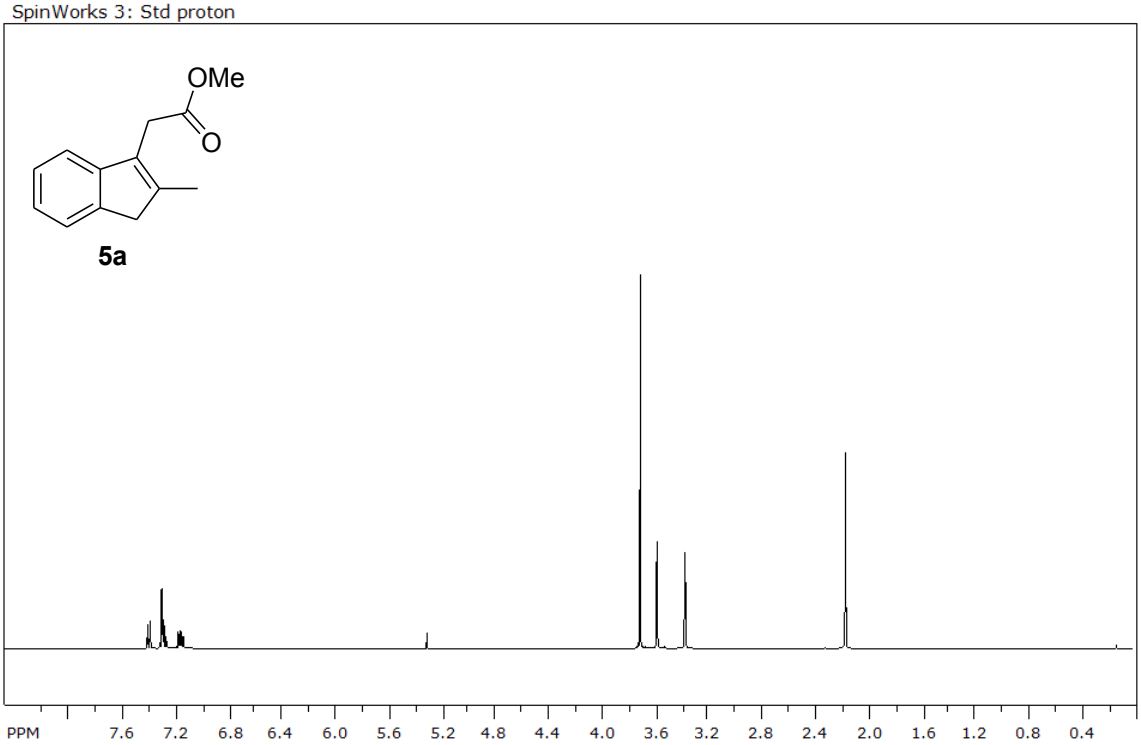

SpinWorks 3: Std carbon

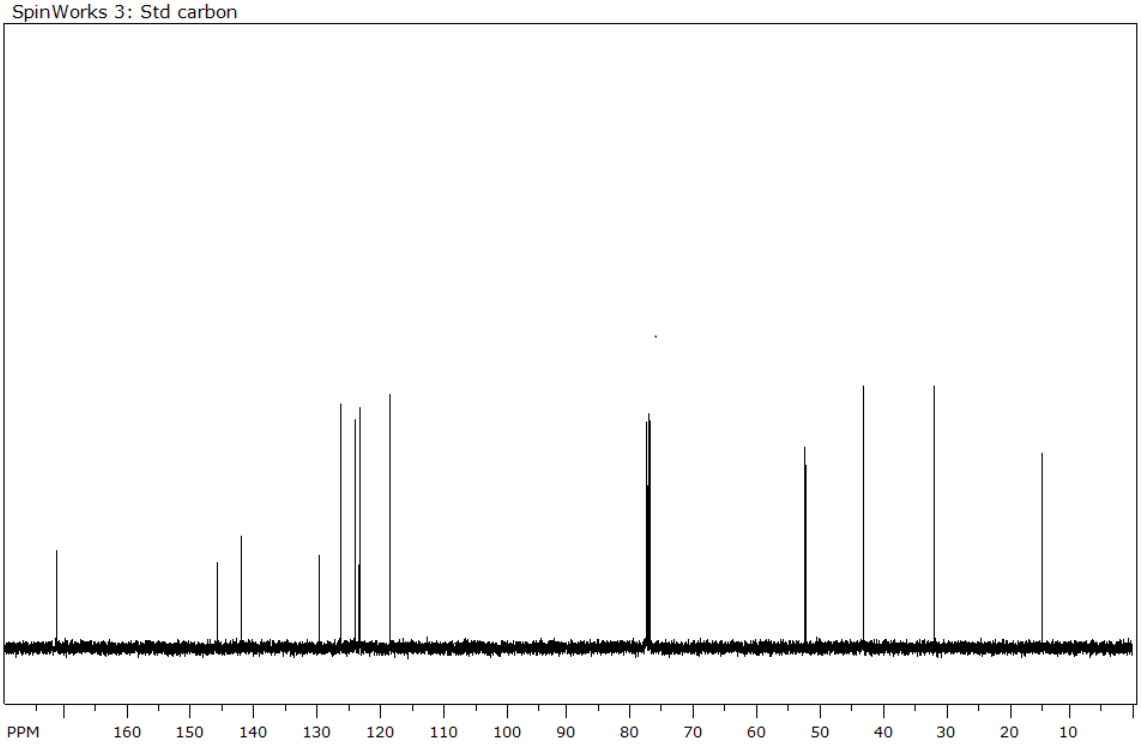

SpinWorks 3: Std proton

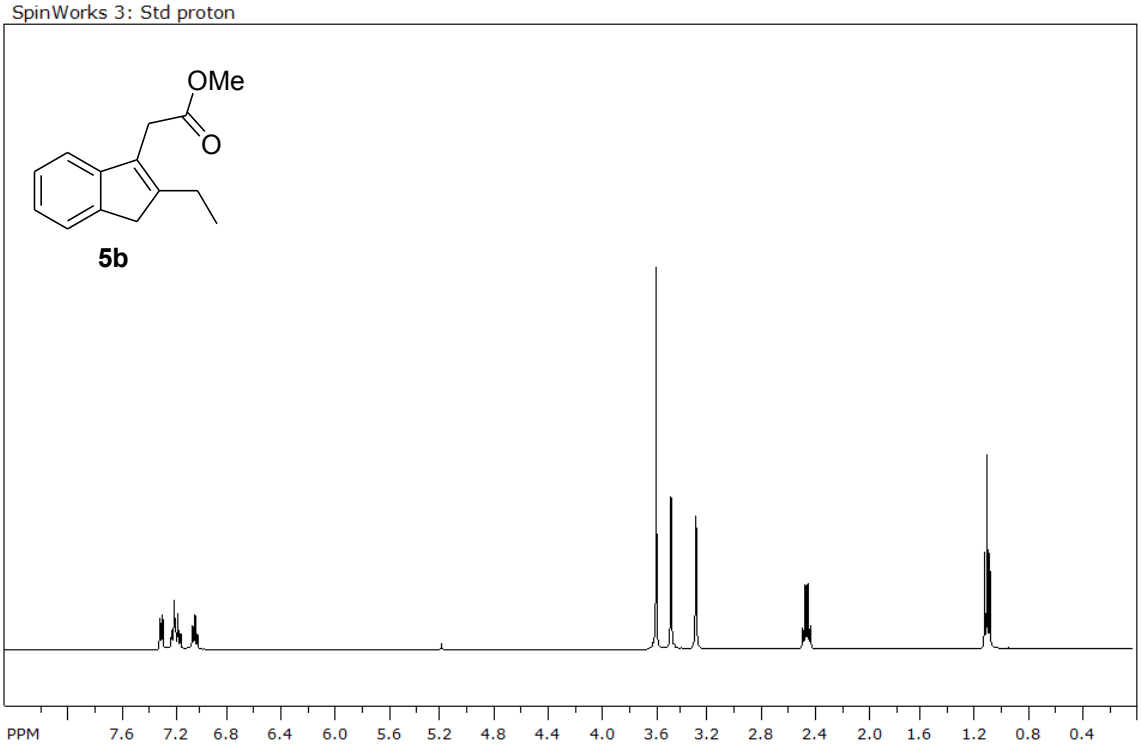

SpinWorks 3: Std carbon

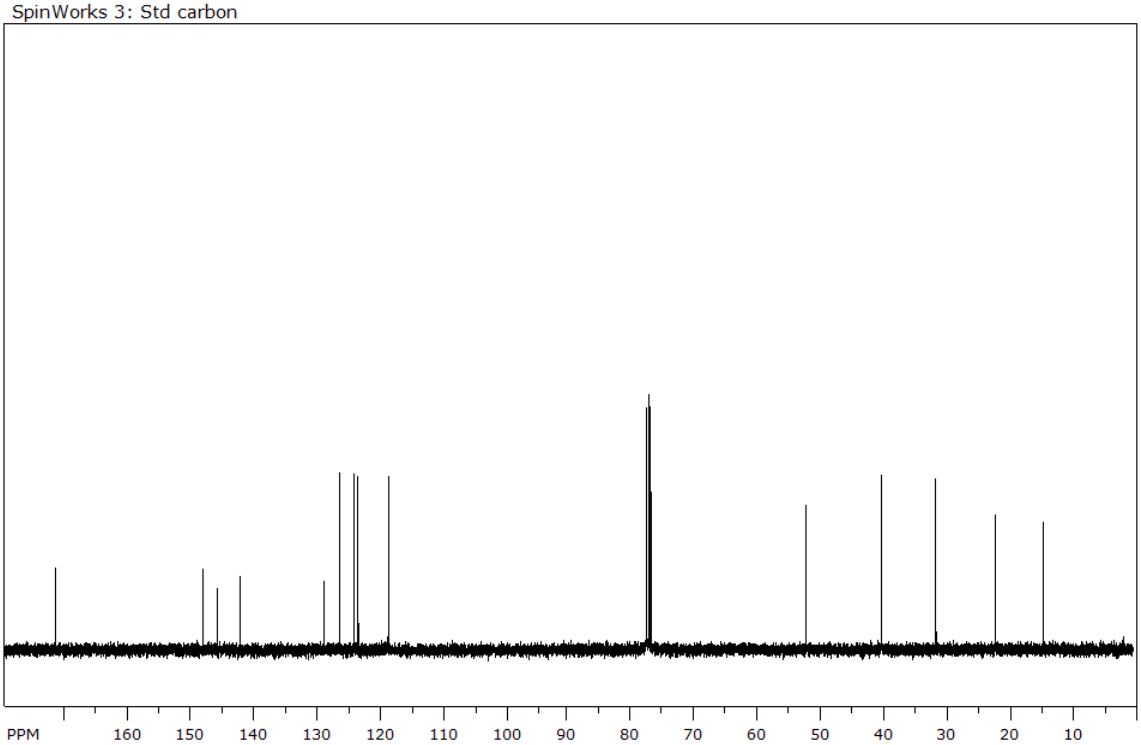

SpinWorks 3: Std proton

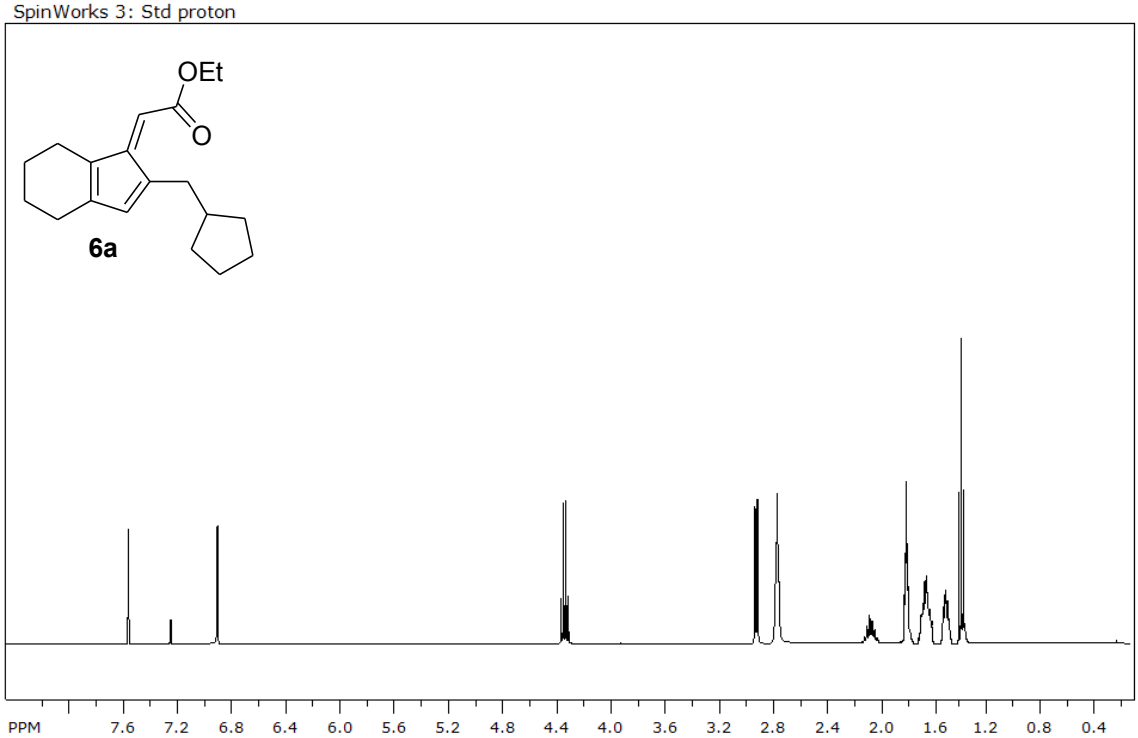

SpinWorks 3: Std carbon

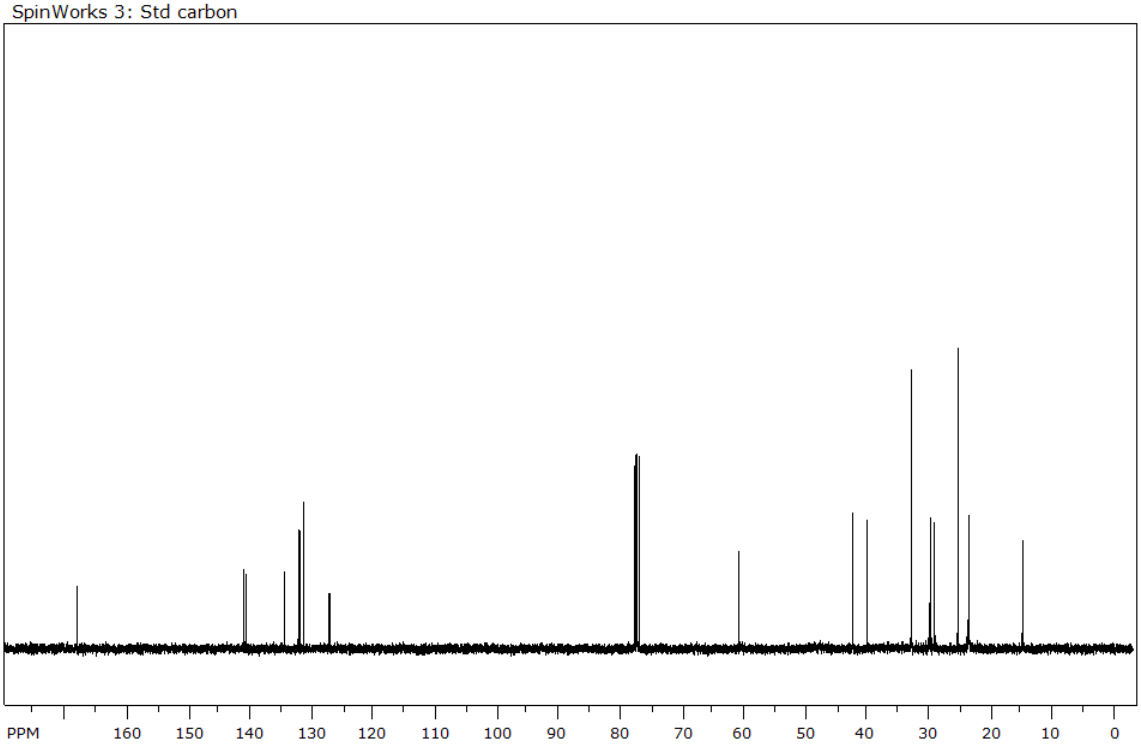

SpinWorks 3: Std proton

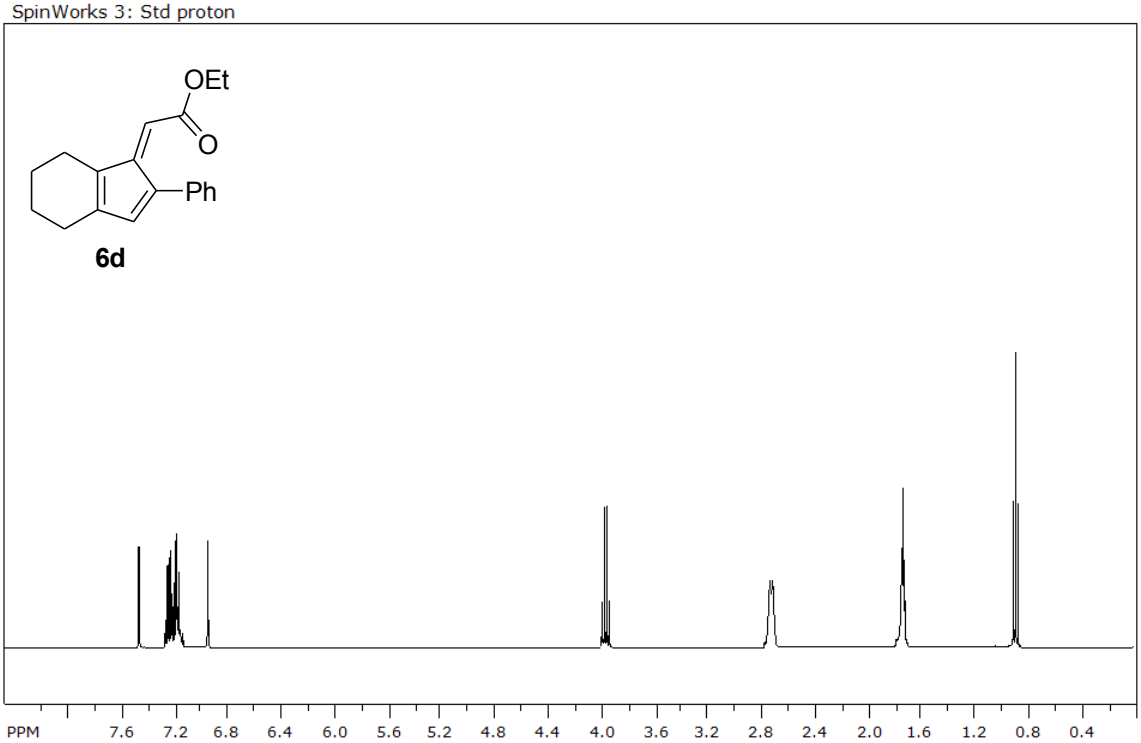

SpinWorks 3: Std carbon

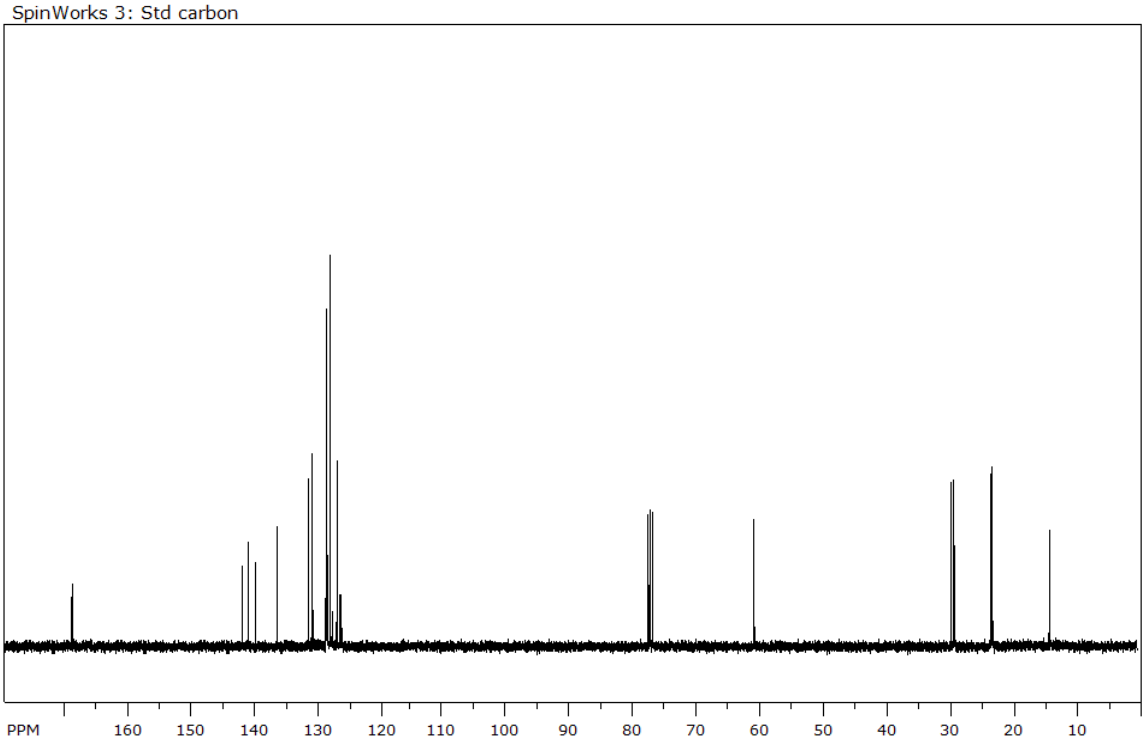

SpinWorks 3: Std proton

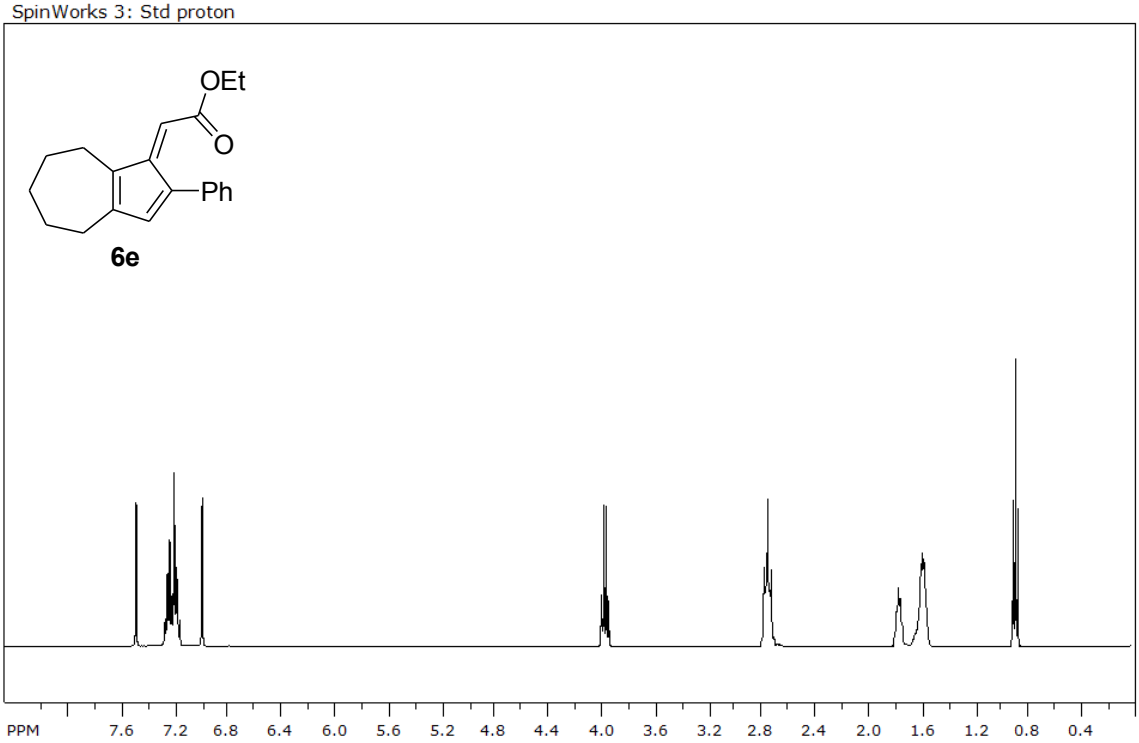

SpinWorks 3: Std carbon

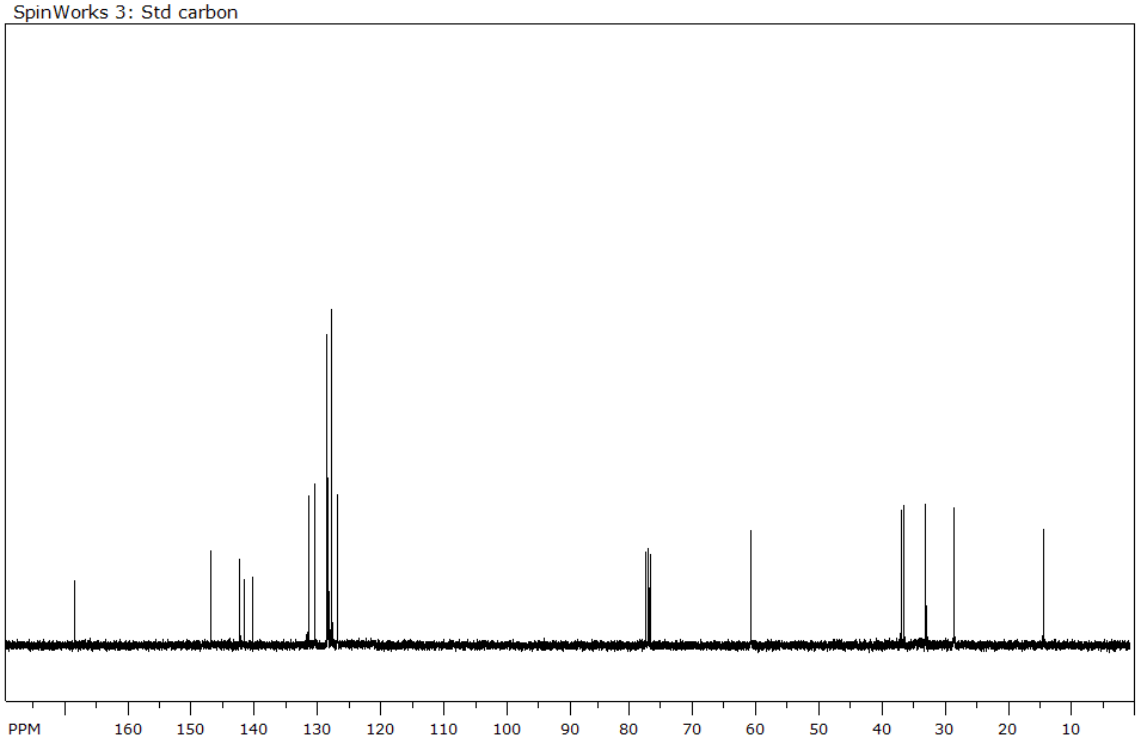

SpinWorks 3: Std proton

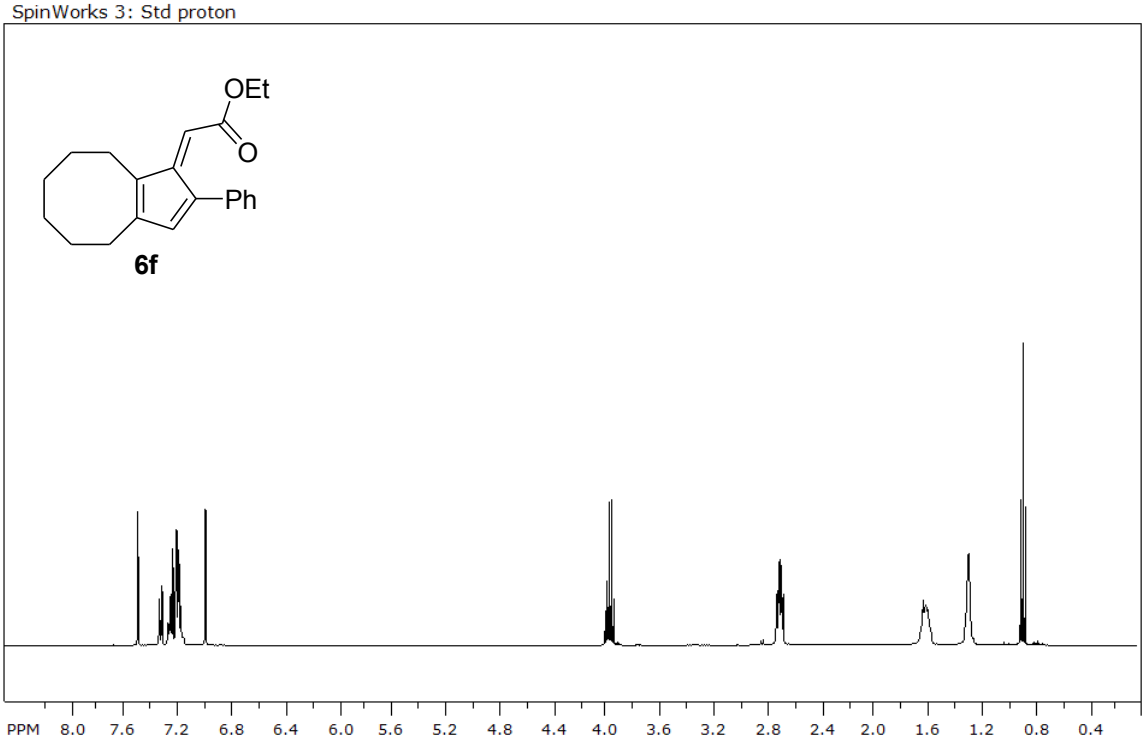

SpinWorks 3: Std carbon